The Islamic University Gaza
Higher Education Deanship
Faculty of Engineering
Department of Electrical Engineering
Program of Control Systems

الجامعة الإسلامية – غزة
عمادة الدراسات العليا
كلية الهندسة
قسم الهندسة الكهربائية
برنامج أنظمة التحكم

# تصميم وتحليل إستراتيجية تحكم مثالي لمُعوِّض التوزيع الساكن ـ شبكة الضغط المنخفض لغزة كدراسة حالة

# Design And Analysis of Optimal Based Control Strategy for D-STATCOM, Gaza Low Voltage Network - Case Study

Submitted by:

**Eng. Ahmed A. Abu Alamaren**

Supervised by:

Dr. Mahir Sabra

A Thesis Submitted to Faculty of Engineering, Islamic University of Gaza in Partial Fulfillment of the Requirements for the Degree of Master of Science

In

Electrical Engineering

1432 هـ -2011 م

بسم الله الرحمن الرحيم


الجامعة الإسلامية – غزة
The Islamic University - Gaza

عمادة الدراسات العليا
هاتف داخلي: 1150


الرقم ج س. غ/35/..... Ref
17/09/2011
التاريخ ..... Date

# نتيجة الحكم على أطروحة ماجستير

بناءً على موافقة عمادة الدراسات العليا بالجامعة الإسلامية بغزة على تشكيل لجنة الحكم على أطروحة الباحث/ أحمد علي أبو العمرين لنيل درجة الماجستير في كلية *الهندسة* قسم الهندسة الكهربائية-أنظمة التحكم وموضوعها:

**Design and Analysis of Optimal Based Control Strategy for D-STATCOM, Gaza Low Voltage Network-Case Study**

وبعد المناقشة العلنية التي تمت اليوم السبت 18 شوال 1432هـ، الموافق 2011/09/17م الساعة الثانية عشرة والنصف ظهرًا، اجتمعت لجنة الحكم على الأطروحة والمكونة من:

| | | |
|---|---|---|
| د. ماهر بدر صبرة | مشرفاً ورئيساً | ..... |
| د. حاتم علي العايدي | مناقشاً داخلياً | ..... |
| د. باسل محمود حمد | مناقشاً داخلياً | ..... |

وبعد المداولة أوصت اللجنة بمنح الباحث درجة الماجستير في كلية *الهندسة*/ قسم الهندسة الكهربائية- أنظمة التحكم.

***واللجنة إذ تمنحه هذه الدرجة فإنها توصيه بتقوى الله ولزوم طاعته وأن يسخر علمه في خدمة دينه ووطنه.***

والله ولي التوفيق،،،

عميد الدراسات العليا

أ.د. فؤاد علي العاجز


P.O. Box 108, Rimal, Gaza, Palestine fax: +970 (8) 286 0800 فاكس Tel: +970 (8) 286 0700 ص.ب. 108 الرمال، غزة، فلسطين هاتف
public@iugaza.edu.ps www.iugaza.edu.ps

# *DEDICATION*

*To my Great Parents*

*To Teaching Staff of Engineering Faculty of IUG*

*To Martyrs of Palestine, My Brothers; Ghassan,*

*Hammam, Musa'ab and Hani*

*To My Beloved Wife*

*To My Dear, Dr. Derar Abu Sisi*

*To All Whom I Love*

# ACKNOWLEDGEMENT

I address my sincere gratitude to Allah as whenever I face difficulty I pray to him to help me and he always there protecting and reconciling me.

Then, I would like to express my great appreciating to my advisor Dr. Mahir Sabra for his invaluable advices, comments and guidance for directing and completing this work. I am deeply grateful to Dr. Hatem Elaydi and Dr. Basel Hamad for accepting to be on my thesis committee and for providing many insightful discussion and comments. Thanks also, to Dr. Derar Abu Sisi who helped me in deciding the thesis topic and encouraged me in that research field.

Finally, I thank my parents, my family and my wife for their support, patience and prayers through my life.

## ملخص الدراسة

أتاحت إلكترونيات القوى وتقنيات التحكم المتقدمة معالجة مشاكل جودة القدرة الكهربائية، والتي هي بالتأكيد من القضايا ذات الاهتمام الكبير في العصر الحاضر. يتمثل بعض مشاكل جودة القدرة الكهربائية الحادة في اضطرابات النظام الكهربائي، تقلص وتضخم الجهد الكهربي، والتوافقيات في الجهد والتيار.

تتناول هذه الأطروحة أداة "مُعوّض التوزيع الساكن (D-STATCOM)" الذي يستخدم على نطاق واسع للتغلب على المشكلات المتعلقة بجودة القدرة الكهربائية. المبدأ الأساسي لهذه الأداة يتمثل في امتصاص أو توليد كمية قدرة كهربائية فعّالة وغير فعّالة قابلة للتحكم، حيث يمكن التحكم بها بواسطة وحدة تحكم لامتصاص أو توليد كمية مناسبة من القدرة من قبل هذا المعوّض. العديد من استراتيجيات التحكم مستخدمة في هذا الصدد، مثل: التحكم اللحظي بالقدرة غير الفعّالة، التحكم المباشر وغير المباشر بالتيار، طريقة المكونات المتناظرة، وإستراتيجية التحكم المزدوجة. استراتيجيات التحكم هذه تستخدم أنواعاً مختلفة من وحدات التحكم، مثل المتحكم الطردي التكاملي PI، المتحكم الضبابي، متحكم إزاحة القطب، والمتحكمات الهجينة.

هذه الأطروحة تطرح إستراتيجية تحكم لمعوض التوزيع الساكن (D-STATCOM) تعتمد على أساليب التحكم المثالي: LQR ، وبشكلٍ خاص $H_2$ و $H_\infty$ والتي لم تطبق من قبل في هذا المجال. وذلك للاستفادة من مزايا أساليب التحكم المثالي في إطار الوصول لحلول مثالية لمشاكل الجودة الكهربية، إزالة الإزعاج في الأنظمة الكهربية، وتضخيم متانة النظام الكهربي. إستراتيجية التحكم المقترحة تعتمد على التحويل الحقيقي-التخيلي (*Dq* transformation)، التزامن باستخدام دورة الطور المغلق (PLL)، والجهد الثابت القيمة (DC). إستراتيجية التحكم المثالي المقترحة سيتم تصميمها ومحاكاة أداءها مع أداة D-STATCOM لتحقيق فاعليتها.

أداة D-STATCOM باستخدام إستراتيجية التحكم المثالي المقترحة تتيح: إعادة تغطية انخفاض الجهد بشكل كامل، إزالة تشوه التوافقيات (THD) بالكامل، أفضل معامل قدرة، وأسرع استجابة، وهو ما يجعل إستراتيجية التحكم المثالي المقترحة لأداة D-STATCOM حلاً فعّالاً لمشاكل الجودة الكهربية.

إستراتيجية التحكم الجديدة هذه سيتم دراستها واختبارها على نطاق إحدى شبكات الضغط المنخفض (400V) في مدينة غزة كدراسة حالة.

# ABSTRACT

Power electronics and advanced control technologies have made it possible to solve power quality problems, which are certainly major concerning issues in the present era. System disturbances, voltage sags, swells and harmonics are few of severe power quality problems.

This thesis focuses on the Distribution Static Compensator (D-STATCOM) device, which is widely used to overcome the power quality problems. The concept of this device is absorbing or generating controllable active and reactive power, which can be controlled to absorb/generate suitable amount of power by the device. Several control strategies have been in use for controlling D-STATCOM, such as: instantaneous reactive power control, direct/ indirect current control algorithm, symmetrical component method, and double-loop control strategy. These control strategies use different types of controllers, such as PI, Fuzzy, Pole placement and hybrid controllers.

This thesis proposes a control strategy for D-STATCOM based on optimal control methods; LQR, and specially $H_2$ and $H_\infty$ methods which are not applied before in D-STATCOM control, in order to utilize the benefits of the optimal control methods to reach optimum solutions for power quality problems, disturbance rejection in power systems and maximizing system robustness. This proposed control strategy depends on *Dq* transformation, Phase-Locked Loop (PLL) synchronization and constant DC link voltage. The optimal based control strategy will be designed and simulated for D-STATCOM to verify its effectiveness. The D-STATCOM device using the proposed optimal based control strategy provides fully voltage recovery, fully Total Harmonic Distortion (THD) elimination, maximum *p.f* and faster response, which making the optimal based control strategy for D-STATCOM an effective solution for power quality problems.

The proposed control strategy will be designed, tested and analyzed on the demand of one of the low voltage (400V) networks of Gaza city as a case study.

# LIST OF CONTENTS

# LIST OF ABBREVIATIONS

| | |
|---|---|
| IEEE | Institute of Electrical and Electronics Engineers |
| rms | Root Mean Square |
| sag% | Percentage of voltage Sag |
| swell% | Percentage of voltage Swell |
| THD | Total Harmonic Distortion |
| STATCOM | Static Compensator |
| DVR | Dynamic Voltage Restorer |
| UPQC | Unified Power Quality Conditioners |
| D- STATCOM | Distribution Static Compensator |
| LQR | Linear Quadratic Regulator |
| $H_2$ | H-2 controller |
| $H_\infty$ | H-infinity controller |
| IGBT | Insulated Gate Bipolar Transistor |
| GTO | Gate Turn-Off thyristor |
| VSC | Voltage Source Converter |
| PWM | Pulse-Width Modulation |
| SPWM | Sinusoidal Pulse-Width Modulation |
| PCC | Point of Common Coupling |
| $\delta$ | Error signal |

| | |
|---|---|
| $S_{sh}$ | Complex power injection of the D-STATCOM shunt device |
| $I_{sh}$ | Current injected by the D-STATCOM shunt device |
| $f_{\text{tri}}$ | Frequency of Triangular voltage signal of PWM |
| $f_{\text{l}}$ | Frequency of reference sinusoidal control voltage of PWM |
| $\text{m}_{\text{f}}$ | Frequency modulation ratio of PWM |
| $m$ | Amplitude modulation ratio (index) of PWM |
| $\text{V}_{\text{l}}$ | Peak amplitude of the reference voltage of PWM |
| $\text{V}_{\text{tri}}$ | Peak amplitude of the triangular voltage of PWM |
| PI | Proportional-Integral Controller |
| DOV | Direct-Output-Voltage control strategy |
| PLL | Phase-Locked Loop |
| CRPWM | Current-Regulated Pulse-Width Modulation |
| $dq$ | Direct-Quadrture Transformation |
| AGC | Automatic Gain Controller |
| $V_s$ | Supply Votage |
| $\text{R}_{\text{s}}$ | Supply Resistance |
| $\text{L}_{\text{s}}$ | Supply Inductance |
| $i_s$ | Supply Currnet |
| $V_c$ | Voltage at PCC (point of the load) |
| $i_L$ | Load Currnet |
| $\text{R}_{\text{L}}$ | Load Resistance |
| $\text{L}_{\text{L}}$ | Load Inductance |

| | |
|---|---|
| $i_f$ | Currnet in L-branch of filter |
| $i_{fc}$ | Currnet in C-branch of filter |
| $R_c$ | Filter Resistance |
| $L_c$ | Filter Inductance |
| C | Shunt filter Capacitor |
| $V_{dc}$ | DC voltage of the storage device |
| $u(t)$ | System Input |
| $y(t)$ | System Output |
| $x(t)$ | System State |
| $p.f$ | Power Factor |
| $\omega$ | Angular frequency |
| VCO | Voltage-Controlled Oscillator |
| $J$ | Cost Function |
| $K$ | LQR gain |
| $H$ | Hamiltonian |
| $\lambda(t)$ | Lagrange multiplier |
| $v$ | Uncorrelated White-noise disturbance |
| $z$ | Performance vector |
| S | Apparent (Complex) Power |
| P | Real Power |
| Q | Reactive Power |

| | |
|---|---|
| $V_{\text{ph}}$ | Single-phase system voltage |
| $I$ | System current |
| $Z_{\text{L}}$ | Load Impedance |
| $K_i$ | Integral gain |
| $K_p$ | Proportional gain |
| $W_n$ | Weighting functions |
| FFT | Fast Fourier Transform tool |

# LIST OF TABLES

# LIST OF FIGURES

# 1 CHAPTER 1: INTRODUCTION

## 1.1 Background

Until recently, most electrical equipment could operate satisfactorily during expected deviations from the nominal voltage and frequency supplied by the utility. In the modern industrial facility, many electrical and electronic devices have been incorporated into the automated processes which are more sensitive to power quality variations than was equipment used in the past [1].

The term *Power Quality* has become one of the most prolific buzzword in the power industry since the late 1980s. The issue in power quality problems is not confined to only energy efficiency and environment but more importantly on quality and continuity of supply, or power quality and supply quality. Both electric utilities and end users of electric power are becoming increasingly concerned about the quality of electric power [2]. Power quality may also be defined as the degree to which both the utilization and delivery of electric power affects the performance of electrical equipment [3].

A power quality problem is defined as any power problem manifested in voltage, current, or frequency deviations that result in power failure or disoperation of customer or equipment from the perspective of customers [2]. Problems mainly include voltage sag, voltage dip, voltage swell, flicker, harmonics, and power interruption. These power quality problems may cause abnormal operations of facilities or even trip protection devices. Hence, the maintenance and improvement of electric power quality have become an important scenario today [4]. This is a very important reason for interesting in power quality which is the economic value, such that there are economic impacts on utilities, their customers, suppliers and load equipment. Recently there has been a great emphasis on revitalizing industry with more automation and more modern equipment. This usually means electronically controlled, energy-efficient equipment that is often much more sensitive to deviations in the supply voltage than were its electromechanical predecessors, in addition of the electrical disturbances and the resultant financial losses associated with these disturbances [2]. Hence, the interesting in power quality became a very urgent need in modern era.

Main power quality terminologies are defined by IEEE Standard 1159-1995 [5], as follows:

- Voltage dip: A short-term reduction in voltage of less than half a second.
- Voltage sag: A reduction of the rms voltage or current at the power frequency, with magnitude ranging from 10 – 90% of the pu value and a duration lasting for 0.5 cycle to 1 minute.
- Undervoltage: A decrease in the rms voltage to less than 90% of the pu value at the power frequency for a duration longer than 1 min. Undervoltages are usually the result of load switching (e.g., switching on a large load or switching off a capacitor bank).
- Voltage swell: An increase in the rms voltage or current at the power frequency with magnitude ranging from 110 – 180% of the pu value for durations from 0.5 cycle to 1 min.
- Overvoltage: An increase in the rms voltage greater than 110% at the power frequency for a duration longer than 1 min. Overvoltages are the result of switching events that are the opposite of the events that cause undervoltages. (e.g., switching off a large load or energizing a capacitor bank).
- Voltage 'spikes', 'impulses' or 'surges': These are terms used to describe abrupt, very brief increases in voltage value.
- Voltage transients: A temporary, undesirable voltages that appear on the power supply line. Transients are high over-voltage disturbances (up to 20KV) that last for a very short time.
- Harmonics: Any sinusoidal frequency component, which is a multiple of the fundamental frequency. Harmonic frequencies can be even or odd multiples of the sinusoidal fundamental frequency.
- Flickers: Visual irritation and introduction of many harmonic components in the supply power and their associated ill effects.

## 1.2 Main Power Quality Problems

Actually the power quality is the quality of the voltage that is being addressed in most cases. Technically, power is the rate of energy delivery and is proportional to the product of the voltage and current. It would be difficult to define the quality of this quantity in any meaningful manner. The power supply system can only control the quality of the voltage; it has no control over the currents that particular loads might draw. Therefore, its very useful to study the problems of the voltage quantity as power quality problems [2]. The most power quality problems that always occur at the distribution systems are voltage sag, voltage swell and harmonics. This thesis will concern on these power problems.

### 1.2.1 Voltage Sag/ Swell

Voltage sag and voltage swell are defined according to IEEE Standard 1159-1995 as mentioned above, and it can be described as indicated in Figure 1.1.

Thus, voltage sag and voltage swell can be characterized by their magnitude (rms value) and duration. This characterization can be specified as mentioned in Table 1.1.

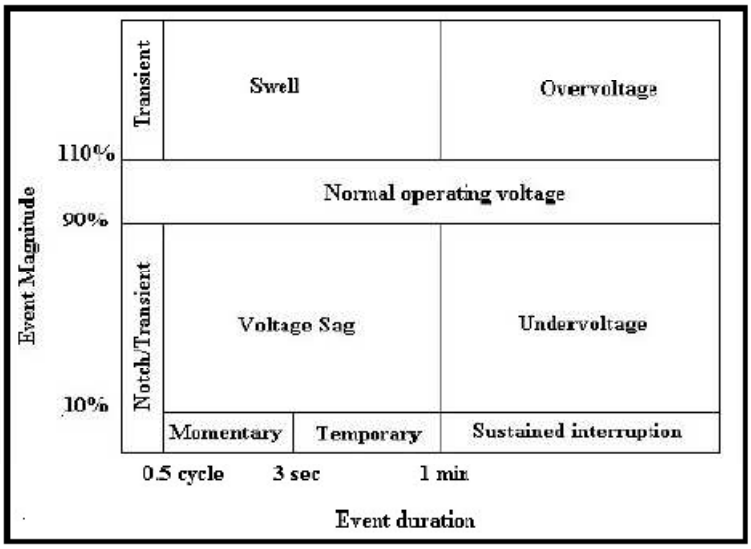


**Figure 1.1: Demarcation of the various power quality issues defined by IEEE Std. 1159-1995 [5]**

A voltage sag is by nature a three-phase phenomenon, which affects both the phase-to-ground and phase-to-phase voltages. The most common causes of over-currents

leading to voltage sags are motor starting, transformer energizing, large increase of the load (overloads) and short-circuit

**Table 1.1: Limitations of Power Quality Problems According to IEEE Std. 1159-1995**

| Disturbance | Voltage (pu) | Duration (cycle) |
|---|---|---|
| **Voltage Sag** | 0.1 – 0.9 | 0.5 – 30 |
| **Voltage Swell** | 1.1 – 1.8 | 0.5 – 30 |

faults. Capacitor energizing and switching of large loads also introduce short-duration over-currents. Voltage sag cause severe problems and economical losses; devices /process down time, effect on product quality, failure/malfunction of customer equipments and associated production, maintenance and repair costs. [7].

A very common quantity to define the voltage sag is "percentage of sag"; *sag%*, which can be calculated using equation (1.1), [8]:

$$\text{sag\%} = \frac{V_{pre\_sag} - V_{sag}}{V_{pre\_sag}} \times 100 \qquad (1.1)$$

Swells are less common than voltage sags, but also usually associated with system fault conditions. A swell can occur due to a single line-to ground fault on the system, which can also result in a temporary voltage rise on them unfaulted phases. This is especially true in ungrounded or floating ground delta systems, where the sudden change in ground reference result in a voltage rise on the ungrounded phases. Swells can also be generated by sudden load decreases. The abrupt interruption of current can generate a large voltage. Switching on a large capacitor bank can also cause a swell, though it more often causes an oscillatory transient. Like voltage sags, voltage swells cause devices /process down time, effect on product quality, failure/malfunction of customer equipments and associated production, maintenance and repair costs [2,9].

"Percentage of swell*"; swell%*, term is quantity to define the voltage swell , which can be

calculated using equation (1.2), [8]:

$$\text{swell}\% = \frac{V_{swell} - V_{pre\_swell}}{V_{pre\_swell}} \times 100 \qquad (1.2)$$

### 1.2.2 Harmonics

Harmonics are voltages or currents at frequencies that are integer multiples of the fundamental 50 Hz frequency (100 Hz, 150 Hz, 200 Hz, etc.) which combine with the fundamental voltage or current and produce a distorted waveform. Harmonic distortion exists due to the nonlinear characteristics of devices and loads so that does not draw sinusoidal current when a sinusoidal voltage is applied [4]. Most equipment only produces odd harmonics but some devices have a fluctuating power consumption, for half cycle or shorter, which then generates odd, even and interharmonic currents. The current distortion, for each device, changes due to the consumption of active power, background voltage distortion and changes in the source impedance [10].

*Total Harmonic Distortion* (THD) is the percentage measurement of the distortion resulted in voltage or current waveforms due to harmonics. To understand the THD term, let return back to the fundamentals. Any periodic signal (waveform) can be described by a series of sine and cosine functions, also called Fourier series:

$$u(t) = U_{dc} + \sum_{n=1}^{\infty} (U_{\max} \sin(nwt) + U_{\max} \cos(nwt)) \qquad (1.3)$$

Hence, when a signal passes through a non-ideal, non-linear device, additional content is added at the harmonics of the original frequencies, these content are of the multiples of the fundamental frequency $nf$, which actually destroy the signal. THD is a measurement of the extent of that distortion and is defined by equation (1.4) [10].

$$\text{THD} = \frac{\sqrt{V_2^2 + V_3^2 + V_4^2 + \ldots + V_\infty^2}}{V_1} \qquad (1.4)$$

Hence, THD is a ratio of all signal components of the multiple frequencies except the fundamental frequency, to the first signal component of the fundamental frequency.

IEEE Standard 519-1992 [11] lists the limits of the THD which should be used as system design values for the "worst case" for normal operation. Table 1.2 shows the IEEE standard values of THD.

**Table 1.2: Voltage Distortion Limits According to IEEE Std. 519-1992**

| Bus Voltage (kV) | THD (%) |
|---|---|
| 69 and below | 5.0 |
| 69 through 161 | 2.5 |
| 161 and above | 1.5 |

Fundamentally, one needs to control harmonics only when they become a problem. When a problem occurs, the basic options for controlling harmonics are [2]:

2 Reduce the harmonic currents produced by the load.

3 Add filters to either siphon the harmonic currents off the system, block the currents from entering the system, or supply the harmonic currents locally.

4 Modify the frequency response of the system by filters, inductors, or capacitors.

## 1.3 Custom Power devices as Power Quality Solutions

To overcome the power quality related problems occurring in the transmission and distribution network system, custom power devices play a major role. Custom power devices is a strategy which is normally targeted to sensitive equipped customers, and is introduced recently and designed primarily to meet the requirements of industrial and commercial customer [12]. One of the main advantages of custom power devices is ensuring a greater reliability and a better quality of power flow to the load centers in the distribution system by successfully compensating for voltage sags, dips, surges, swell, harmonic distortions, interruptions and flicker, which are the frequent problems associated with distribution lines [13].

Custom power devices overcome the major power quality problems by the way of injecting active and/or reactive power(s) into the system. The concept of custom power devices is to use solid state power electronic components or static controllers in the medium voltage distribution system aiming to supply reliable and high quality power to sensitive users. Power electronic valves are the basis of those custom power devices such as converter-based devices, which can be divided into three groups [12]:

- Series controllers (an example is Static Compensator: STATCOM),
- Shunt controllers (an example is Dynamic Voltage Restorer: DVR), and
- Combined Series-Shunt controllers (an example is Unified Power Quality Conditioner UPQC).

Among Custom power devices controllers, the shunt controllers have shown feasibility in term of cost-effectiveness in a wide range of problem-solving from transmission to distribution levels. In this regard, Static Synchronous Compensator (STATCOM) is an effective solution of power quality problems. STATCOM systems are used in distribution and transmission systems for different purposes. The STATCOM installed in distribution systems or near the loads to improve power factor and voltage regulation is called D-STATCOM. D-STATCOMs have faster response when compared with transmission STATCOMs [14].

## 1.4 Motivation

Much research confirms several advantages of D-STATCOM compared to other custom power devices, which make the motivation of concerning on D-STATCOM. These advantages include [16]:

- Size, weight, and cost reduction.
- Equality of lagging and leading output.
- Precise and continuous reactive power control with fast response.
- Possible active harmonic filter capability.

In addition, it can perform several useful tasks [22]:

- Voltage regulation and compensation of reactive power.
- Correction of power factor.
- Elimination of voltage and current harmonics.

For the above reasons, and due to the fact that the D-STATCOM is more useful for distribution networks, it is desired to utilize all the D-STATCOM dynamic characteristics, and improve its dynamic performance.

The electric utility environment has never been one of constant voltage and frequency, and thus power quality problems cannot be specified with certain limits. Hence, it is not easy to have the system which is the end result of the control process with desirable or certain constraints. Therefore, classical control methods dose not the best solutions for power quality problems. In Addition, disturbance and noise in power systems need to be faced in the base of optimal control knowledge, such that optimal control methods provides the best possible performance and reach the system which is supposed to be the best possible system of a particular type. Hence, it is interesting that the optimal control of D-STATCOM for power quality improvement be covered and demonstrated.

## 1.5 Thesis Objectives

The main objectives of this thesis are to propose and employ an optimal based control strategy which is simple and flexible compared with the other control strategies, in order to improve the D-STATCOM performance and demonstrate its behavior using optimal control methods to face the noise and disturbances inherit in D-STATCOM. The simplicity and flexibility of the proposed control strategy is due to using only one control loop and one voltage measurement are required.

$H_2$ and $H_\infty$ controllers were not applied before in D-STATCOM control. Applying optimal control methods; $H_2$ and $H_\infty$ methods into D-STATCOM within the proposed control strategy in this thesis is a new contribution in the research of D-STATCOM control

field in order to maximize system robustness and disturbance rejection in power systems which is expected as the optimum solutions of power quality problems.

LQR controller was used in previous researches for D-STATCOM as a part of hybrid controllers based on double-loop control strategy. Another important objective of the thesis is to enhance the optimal LQR controller for D-STATCOM with the simple and flexible proposed control strategy, and to apply $H_2$ and $H_\infty$ controllers within this control strategy.

In addition, it is desired to have a controller with an investigation of all of the following factors as the result of the proposed control strategy:

- Faster control response,
- Fully voltage recovery,
- Optimal THD elimination, and
- Maximum mitigation of power factor (*p.f*).

Making a tradeoff between these factors is an important aspect in various control strategies of D-STATCOM. Thus, the achievement of all these factors is a research challenge to be faced in this thesis.

The proposed control strategy based on optimal control methods will be studied and tested on a case study as a realistic power system to verify the effectiveness of the optimal based control strategy for D-STATCOM.

## 1.6 Literature Review

Depending on the power system parameter to be controlled, various control strategies have been proposed for D-STATCOM. A large volume of literature is available on D-STATCOM control.

*Liqun Xing (2003)* [16], designed and compared an optimal linear quadratic regulator (LQR) and pole assignment controller for transient dynamic performance of STATCOM. The thesis found that LQR controllers do not offer significant performance improvement to pole assignment. *Xing* stated that there are topics need further investigation and research;

one of these is using robust and optimal control methods to determine if improvements can be made in STATCOM performance, to face the noise and disturbances inherit in STATCOM.

*Cai Rong (2004)* [17], designed a Dual Vector Controller of the STATCOM, incorporating a vector voltage controller (outer loop) which controls the current through the filter to achieve proper reference output voltage of the voltage source converter (VSC), and a vector current controller (inner loop) which tracks the reference obtained by the outer control loop voltage to realize the voltage dip mitigation at load terminal; Figure 1.2, and the voltage and current control loops are indicated in Figure 1.3. The vectors are implemented by using the Clarke and Park (*dq*) transformations (explained in Section 3.1.1). The steady state error nullified by using PI controller. Phase-Locked Loop (PLL) (explained further in Section 3.1.2) is used in the controller in order to synchronize the compensating signal with the system voltage signal. The concept of these two control loops is also known as double-loop control strategy. The controller was

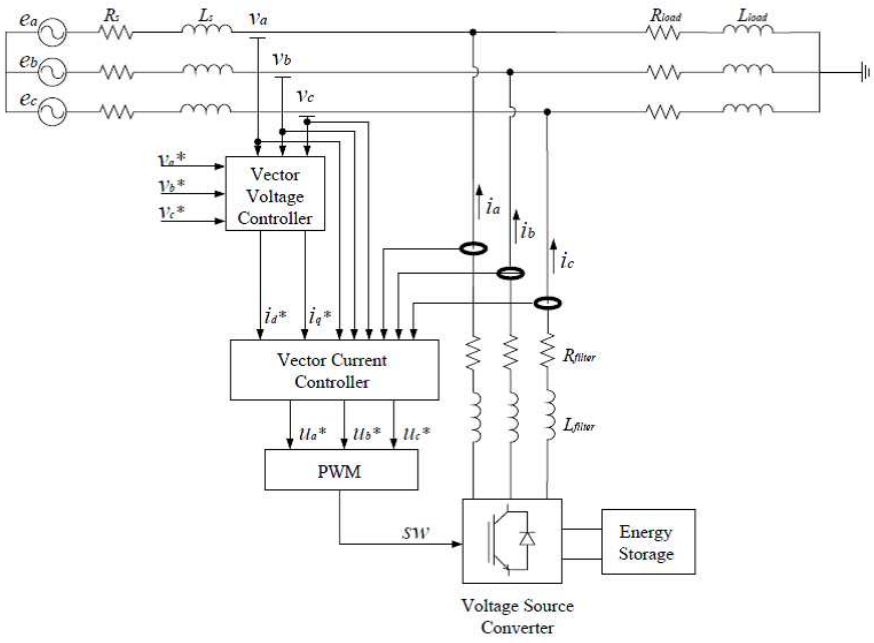


**Figure 1.2: Dual Vector Controller scheme of [17]**

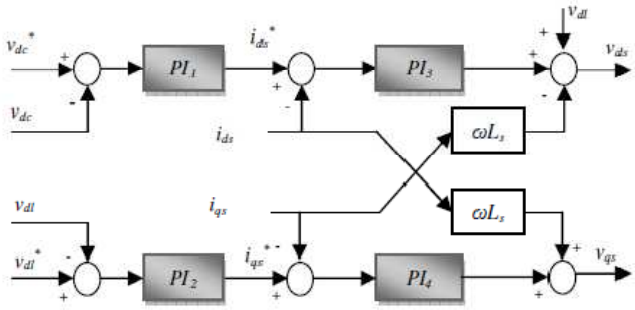


**Figure 1.3: Schematic configuration of double-loop control strategy [15]**

verified both in 400V system and 10kV system for the different load characteristics. Results demonstrated that there were small oscillations in *dq* component of the shunt compensation current due to the switching ripple of the VSC. *Rong* stated that his proposed dual vector controller is sensitive to the variation of the system parameters. Results of *Rong*'s thesis showed also that the shunt compensation current, active and reactive power decrease as the source impedance increases for the same sag magnitude, and the STATCOM injects less shunt compensation current, active and reactive power into the power system if the device is installed closer to the sensitive load. That is meaning that larger shunt compensation current is required if the fault is closer to the STATCOM. Thus, the STATCOM cannot be used to protect from faults at the same bus.

*N. Mariun, S. Aizam, H. Hizam and N. Abd Wahab (2005)* [20], designed a pole placement controller for D-STATCOM in mitigation of three-phase fault.

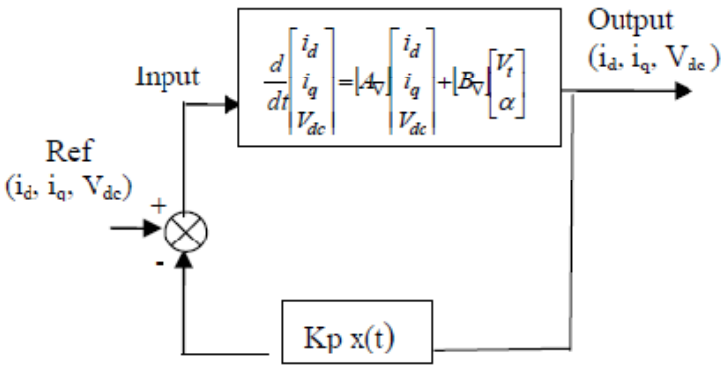


**Figure 1.4: Pole placement control scheme of [20]**

The pole placement method was structured by shifting the existing poles to the new locations of poles at the real-imaginary axes for better response. Hence, the steady-state model of the system was needed in order to achieve the pole placement and implement the control scheme indicated in Figure 1.4. This type of controller was able to control the amount of injected current or voltage or both from the D-STATCOM inverters. The simulation was done on an 11 kV distribution system. It was showed that the amount of injected current during fault period is very high (about 20 times the rated load current). This very high amount of injected current during fault which make the control strategy unpractical to be applied.

*A. H. Norouzi & A. M. Sharaf (2005)* [21], proposed a new Automatic Gain Controller (AGC) STATCOM, to reduce the voltage regulator gain and therefore ensure the stable operation of the STATCOM under various load conditions. The block diagram of the AGC is indicated in Figure 1.5. This proposed control strategy used also *dq* transformations to produce reference and compensated components, and used PLL for synchronization. The simulation was done on an 230 kV system, and it was shown that the voltage regulator is stabilized after a few oscillations.

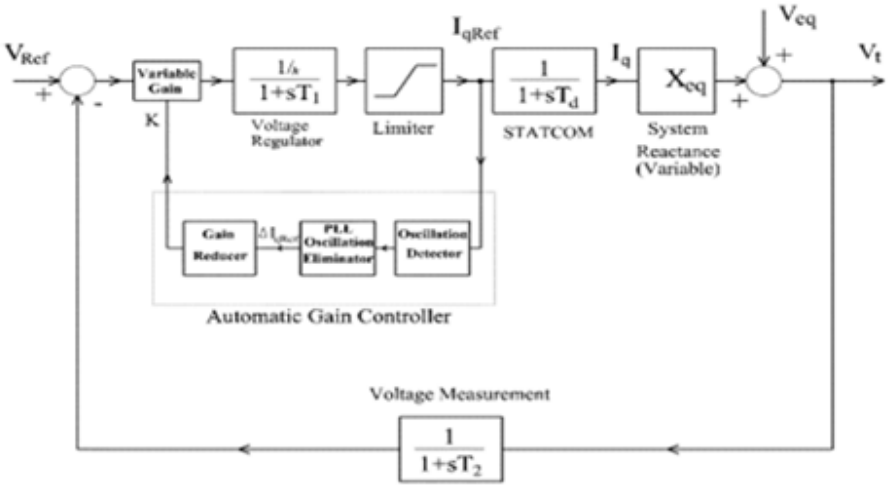


**Figure 1.5: AGC control scheme of [21]**

This AGC control strategy is a powerful tool to ensure stable operation of the STATCOM as the power system conditions may change at any time. However, *Norouzi* and *Sharaf*

stated that the AGC did not guarantee the optimum gain to obtain the fastest response of the STATCOM for a weak power system due to the fact that the optimum gain is a function of the power system strength which varied as the loads were switched in or out of the power system or to generator and transmission line outages.

*S.V Kumar & S. Nagaraju (2007)* [22], used a PI controller to process the error signal which was obtained directly by comparing the reference voltage with the measured voltage at the load point in the *abc* frame form. The generated angle produced by the PI controller was fed to the sinusoidal pulse width modulation (SPWM) (explained in Section 2.5) based control scheme to control the electronic valves of the VSC. The simulation was applied to 13 kV, 50 Hz system with different sizes of DC storage device, and the voltage sag was fully recovered. This control strategy is the simplest and the most common control algorithm for D-STATCOM and other custom power devices, and it can be described as direct control method. It is clear that this control strategy requires only voltage measurements in the *abc* frame form, but although it works well for sag/ swell compensation, it cannot be applied for other control strategies which use other than PI controller, such as: Fuzzy, LQR, AGC, etc. Also, the tuning of PI parameters has to be done empirically or by trial and error method.

*Srinivas, B. Singh, A. Chandra and K. Al-Haddad (2008)* [23], proposed fuzzy, PI and hybrid fuzzy-PI controllers for STATCOM, to utilize the advantages of both fuzzy and PI controllers. The control algorithm was based on the double-loop control strategy; the desired (reference) reactive current produced by fuzzy controller, while the DC link voltage was controlled by PI controller. The desired (reference) reactive current was processed again by the hybrid controller which acts as a fuzzy logic controller when it is far from the reference value, and acts as a PI controller when it is near to the reference value. A similar hybrid controller was also used for the AC terminal voltage controller. The simulation was done on an 132 kV system. It was showed that the total harmonic distortion (THD) of the STATCOM current is high and above the IEEE standard.

*Wei-Neng Chang & Kuan-Dih Yeh (2009*) [4], derived a compensation scheme with the symmetrical components method; Figure 1.7. The needed compensation currents were

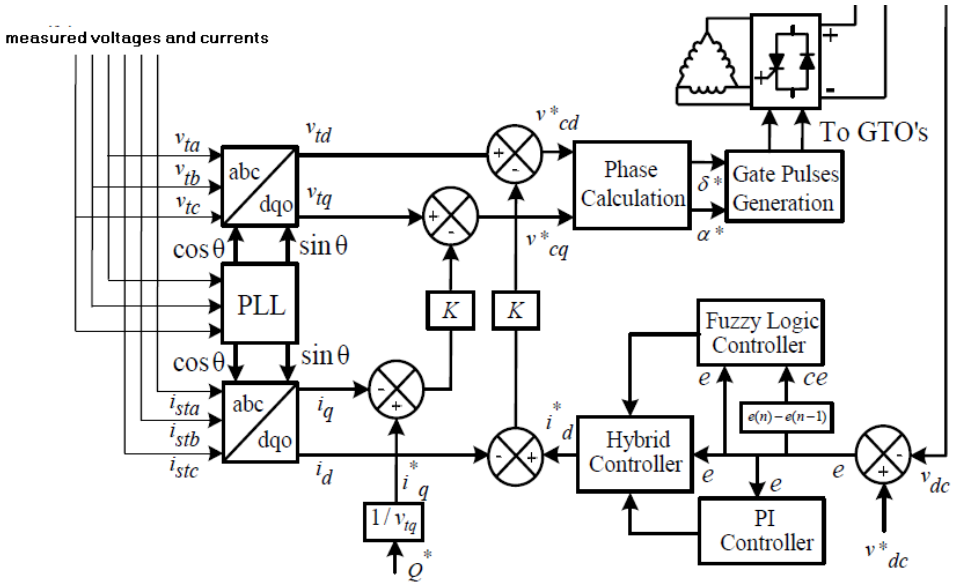


**Figure 1.6: Hybrid fuzzy-PI controllers of [23]**

generated using current-regulated PWM (CRPWM) inverter and controlled by PI controller which process the deference of the measured DC voltage side and the desired DC voltage. PLL scheme was used to synchronize the switching to the system voltage and lock to the phase at fundamental frequency to generate the PWM triangular carrier signals. The simulation was applied to 220 V, 60 Hz system.

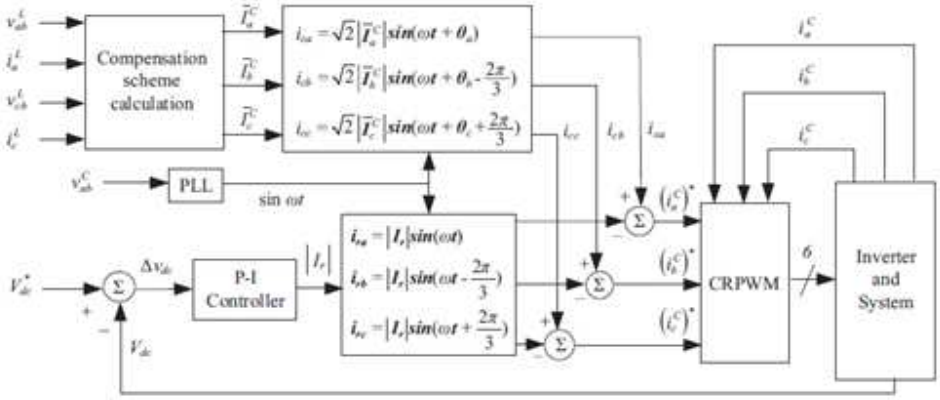


**Figure 1.7: Compensation scheme of [4] with symmetrical components method**

*Suchismita A. Chatterjee & K. D. Joshi (2010)* [15], investigated and implemented the Fuzzy-PI control of DSTATCOM based on the double-loop control strategy. A fuzzy

adjuster was added to tune the parameters of the PI controllers. The simulation was done on an 230 kV system. Although the fuzzy controllers can effectively improve the dynamic performance of the system, but this control strategy still classified as double-loop control strategy which has four PI controllers as showed in Figure 1.3, and as mentioned above, tuning of these PI parameters has to be done empirically or by trial and error method which is time consuming.

*A. Ajami & N.Taheri (2011)* [24], designed a hybrid Fuzzy/LQR control method for STATCOM based on double-loop control strategy. The PI controllers involved in this algorithm, Figure 1.3, was replaced by the Fuzzy controller and followed by the LQR controller to produce the final compensating signal which fed to SPWM pulse generation scheme. The LQR determines the feedback gain matrix that minimized the cost function and derived the states to zero. The simulation was done on an 22 kV system, and it was showed that the hybrid Fuzzy/LQR strategy acted well than the conventional PI method.

## 1.7 System Case Study

The local low voltage networks in Gaza Strip is combined of step down 22/0.4 kV, 630 KVA or 400 KVA transformers feed various loads. Gaza electrical utility suffer from several power quality problems, and therefore it is a good case study to verify the optimal based control strategy.

One of Gaza low voltage networks is chosen as a case study to apply and test the D-STATCOM device and analyze its behavior for power quality improvements. The choice was on Southern Al-Zaitoon Neighborhood low voltage network indicated in *Annex A*. The reason for choosing this network is that it is one of the most modern networks built by Gaza electricity distribution company (GEDCo.) and it has simple plan to be modeled for simulation and study purposes. The load of this network is rated at 410 KVA with 0.92 *p.f* [25]. Power and load calculations for this network are extracted in Chapter 3.

The system model for this network was built using "SimPowerSystems" toolbox in MATLAB environment as illustrated in Figure 1.8.

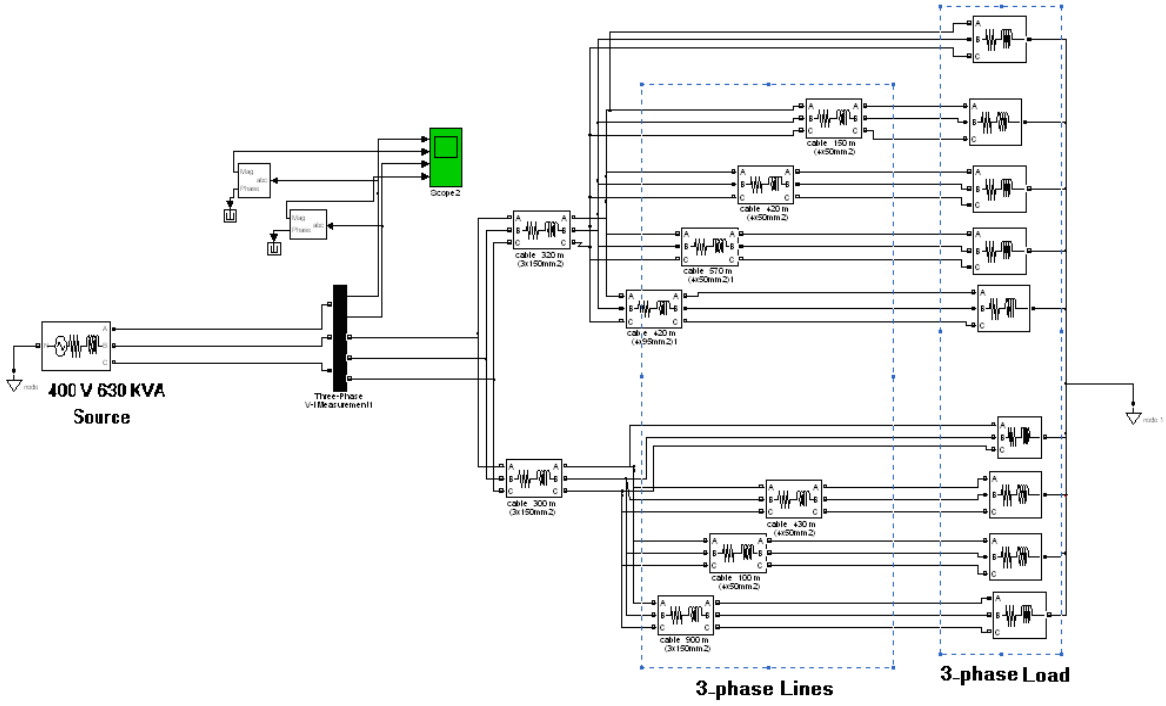


**Figure 1.8: Simulated model of Southern Al-Zaitoon Neighborhood low voltage network**

The network is simulated using 400V voltage source representing the step down 22/0.4 kV, 630 KVA transformer and using the internal parameters of the transformer as the internal parameters of the voltage source, that is to deal with the network as an isolated network. Customer subscriptions are simulated as load blocks, and the distribution lines are simulated by its resistance R and inductive reactance L values representing its real lengths. *Annex A* contain all parameters needed for the simulation.

## 1.8 Thesis Organization

In this thesis, Chapter 2 gives an overview of D-STATCOM, its control and modeling. A D-STATCOM circuit is analyzed and the mathematical model to represent its dynamic characteristics is also presented. In Chapter 3, an optimal based control strategy for D-STATCOM is proposed using conventional PI controller, and optimal control methods; LQR, $H_2$ and $H_\infty$ controllers. In Chapter 4, simulation of D-STATCOM applied to the local utility of Gaza with the proposed control strategy using different control methods (PI, LQR, $H_2$ and $H_\infty$) is presented, and then, analysis and comparison of these

different control methods are made to find out the most suitable for D-STATCOM.

Chapter 5 concludes the most important attained results and suggested different research topics for future work.

# 2 CHAPTER 2: D-STATCOM CONFIGURATION, CONTROL AND MODELLING

## 2.1 Overview of D-STATCOM device

A distribution Static Synchronous Compensator (D-STATCOM) is a medium power systems (up to 5 MVA) and is installed in distribution systems or near the loads to improve power factor and voltage regulation. It can also use high switching frequencies. The insulated gate bipolar transistor (IGBT), high voltage IGBT (HV IGBT) and gate turn-off thyristor (GTO) are the candidate power semiconductors for D-STATCOMs [14].

The concept of STATCOM was disclosed by Gyugyi in 1976. In 1995, the first 100 MVA STATCOM was installed at the Sullivan substation of Tennessee Valley Authority in northeastern Tennessee, United States. This unit is mainly used to regulate 161 kV bus during the daily load cycle to reduce the operation of the tap changer. In 1996, the National Grid Company of England and Wales designed a dynamic reactive compensation equipment with inclusion of a STATCOM of 150 MVA range [16,21].

Confidence in the STATCOM principle has now grown sufficiently for some utilities to consider them for normal commercial service. Japan (Nagoya), United States, England and Australia (QLD) also use STATCOM in practice [16].

**Figure 2.1: Voltage Source Converter Based STATCOM**

A D-STATCOM consists of Voltage Source Converter (VSC), a DC energy storage device,

a capacitor, and a coupling transformer to connect the D-STATCOM through it in shunt to the distribution network [17].

## 2.2 D-STATCOM Parts

- Voltage Source Converter (VSC) is the core component of the D-STATCOM. VSC is a power electronic device that converts the direct (DC) voltage to alternating (AC) voltage, and combined by six transistors, usually IGBT or GTO types, such that the six transistors form a single level converter (see Figure 2.2). A D-STATCOM can be built by single or multilevel VSCs. The converted AC voltage is injected into the power system and introduces a voltage difference between the VSC and the point of connection with the power system. This voltage difference results in proper current that is injected into the power system. Active and reactive power can be injected independently in the power system.

- Energy storage: The purpose of energy storage is to maintain the DC side voltage of VSC. It can be capacitor or DC source, e.g. battery. Traditional STATCOM only has DC capacitor, thus, only reactive power can be injected to the power system by STATCOM, whereas both active and reactive power can be injected to the power system by STATCOM if DC source is used.

- Filter: As the Pulse-Width Modulation (PWM) technique is used in VSC, the output voltage of VSC has switching ripple, which bring harmonics into the current injected to the power system. These harmonics will affect the voltage quality of the power system. Therefore, a relatively small reactor is installed between VSC and the point of the system which the D-STATCOM is connected, to filter those harmonics in the current. The filter can be L-filter LC-filter and LCL-filter.

Additional important part for the D-STATCOM is the controller. The controller executes the calculation of the correct output voltage of VSC, which leads to proper shunt compensation current [26]. The control process affect usually on the "trigger pulse" showed in Figure 2.2.

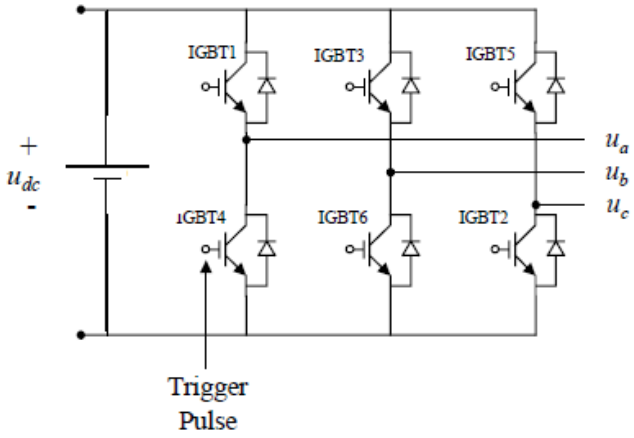


**Figure 2.2: VSC based on IGBT valves [25]**

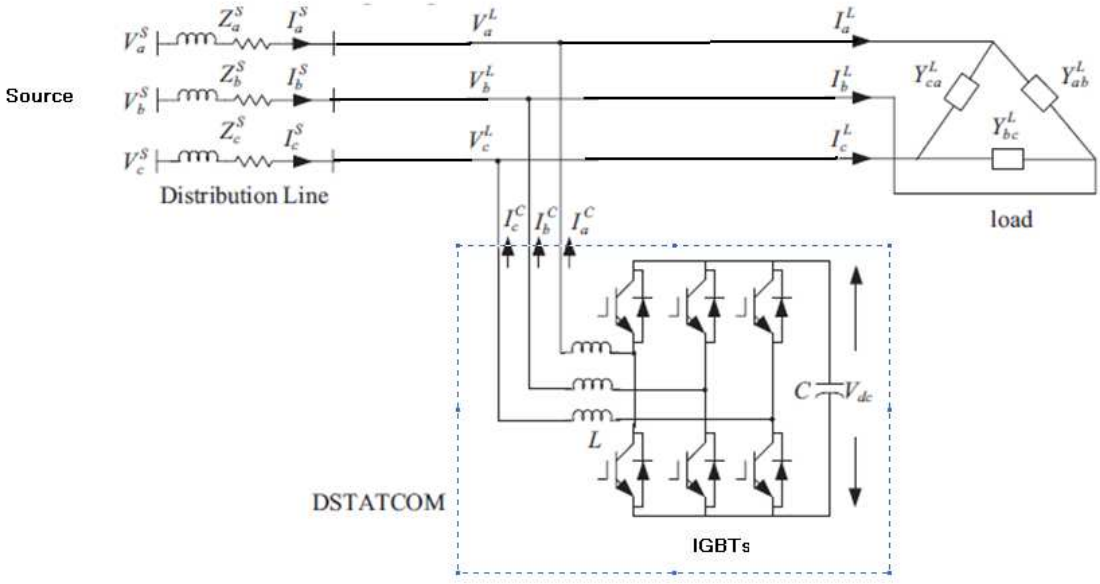


**Figure 2.3: Basic configuration of D-STSTCOM device [4]**

## 2.3 D-STATCOM Operation

The basic VSC based D-STATCOM operating principle is to control current flow by generation and absorption of controllable active/ reactive power for compensating voltage variation and unbalance active and reactive power, this is by adding current in parallel with the load bus to offset the sag. Therefore the D-STATCOM can be treated as

a voltage-controlled source. The VSC converts the DC voltage across the DC storage device into a set of three-phase AC output voltages. These voltages are synchronized with the main network voltage and coupled with the AC system through the reactance of the coupling transformer which can be combined with the reactance of an L-filter [17], as shown in Figure 2.3. Suitable adjustment of the phase and magnitude of the D-STATCOM output voltages allows effective control of active and reactive power exchanges (absorption or generation) between the D-STATCOM and the AC system, which can be controlled traditionally by a PI controller [12,22].

Operation modes of the D-STATCOM is illustrated in Figure 2.4.

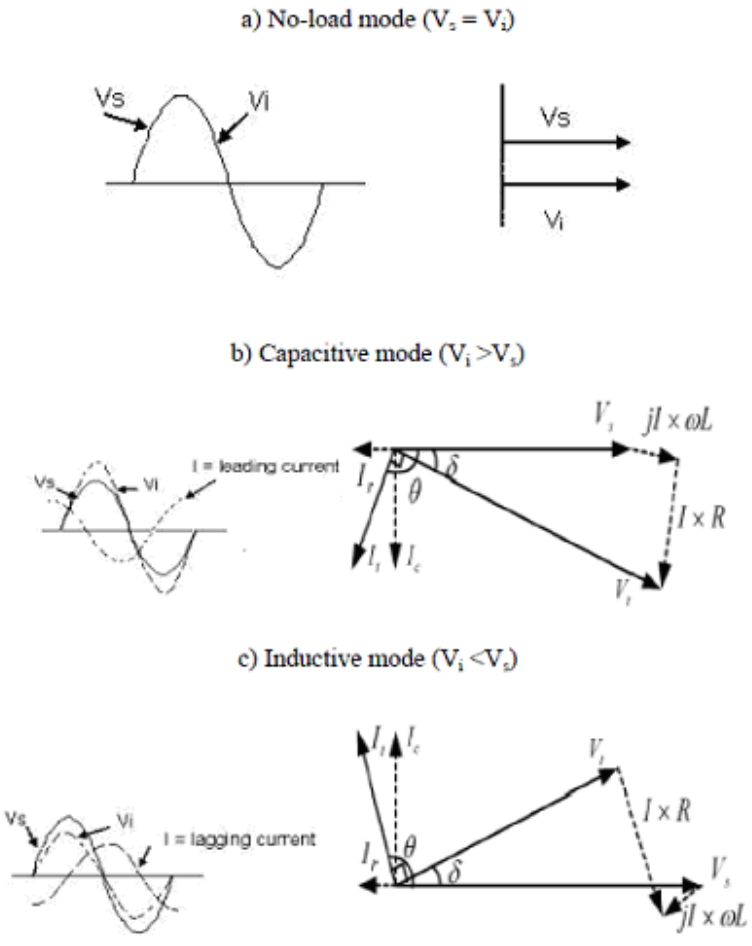


**Figure 2.4: Operation modes of D-STATCOM [8]**

Referring to Figure 2.3, if the voltage $V^L$ at the point of common coupling with the load (PCC) and the source voltage $V^s$ are equal, the reactive power exchange is zero and the D-STATCOM does not generate or absorb reactive power. When $V^L$ is greater than $V^s$, the D-STATCOM shows an inductive reactance connected at its terminal and the current $I^c$ flows through the reactance from the D-STATCOM to the AC system, and the device generates capacitive reactive power. If $V^s$ is greater than $V^L$, the D-STATCOM shows the system as a capacitive reactance, and the current flows from the AC system to the D-STATCOM, resulting in the device absorbing inductive reactive power [8].

## 2.4 D-STATCOM Control Concept

As illustrated in the previous section, the output voltage of D-STATCOM is controlled in such a way that the phase angle between the inverter voltage and the line voltage $\delta$ is dynamically adjusted so that the D-STATCOM generates or absorbs the desired reactive power at PCC point [8]. Hence, the phase angle control between the voltage of PCC and the source voltage is the main principle of D-STATCOM control. The aim of such control scheme is to maintain constant voltage magnitude at the point of the load under system disturbances [22]. Figure 2.5 shows the control concept of D-STATCOM.

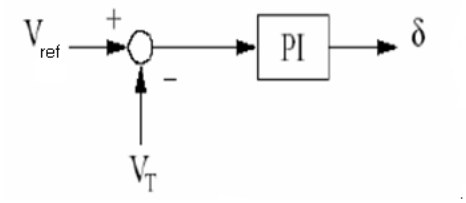


**Figure 2.5: Direct PI control for D-STATCOM**

The controller input is an error signal obtained from difference of the reference rms voltage and the rms value of the terminal voltage measured. The controller processes the error signal and generates the required angle to drive the error to zero, i.e., the load rms voltage is brought back to the reference voltage. Such error is processed traditionally by a PI controller, or by any other controllers. The output angle $\delta$ is provided to the Sinusoidal Pulse Width Modulation (SPWM) signal generator. The generated SPWM signal is fed to

the VSC of the D-STATCOM to pulse the IGBT gates; Figure 2.6.

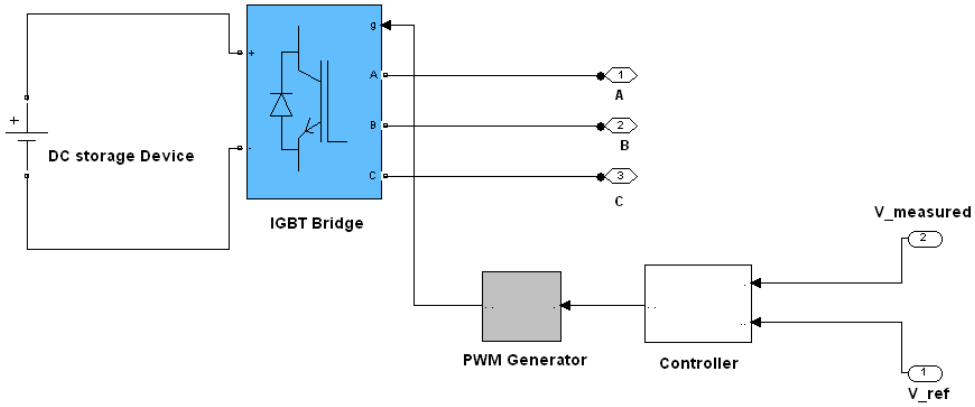


**Figure 2.6: PWM based generation pulses**

Complex power injection of the D-STATCOM can be expressed as,

$$S_{sh} = V_L I_{sh}^{*} \tag{2.1}$$

$$I_{sh} = I_L - I_s = I_L - \frac{V_s - V_L}{Z_s} \tag{2.2}$$

## 2.5 Sinusoidal Pulse Width Modulation SPWM Technique

Sinusoidal Pulse Width Modulation (SPWM) technique is used to control the fundamental component of the line-to-line converter voltage. Three-phase converter voltages are obtained by comparing the same triangular voltage of $f_{\text{tri}}$ frequency with three reference sinusoidal control voltages of $f_1$ frequency as shown in Figure 2.7.

The frequency of the triangular voltage (carrier frequency $f_{\text{tri}}$) determines the converter switching frequency and the frequency of the control voltages $f_1$ determines the fundamental frequency of the converter voltage (modulating frequency). Hence, modulating frequency is equal to supply frequency in D-STATCOM.

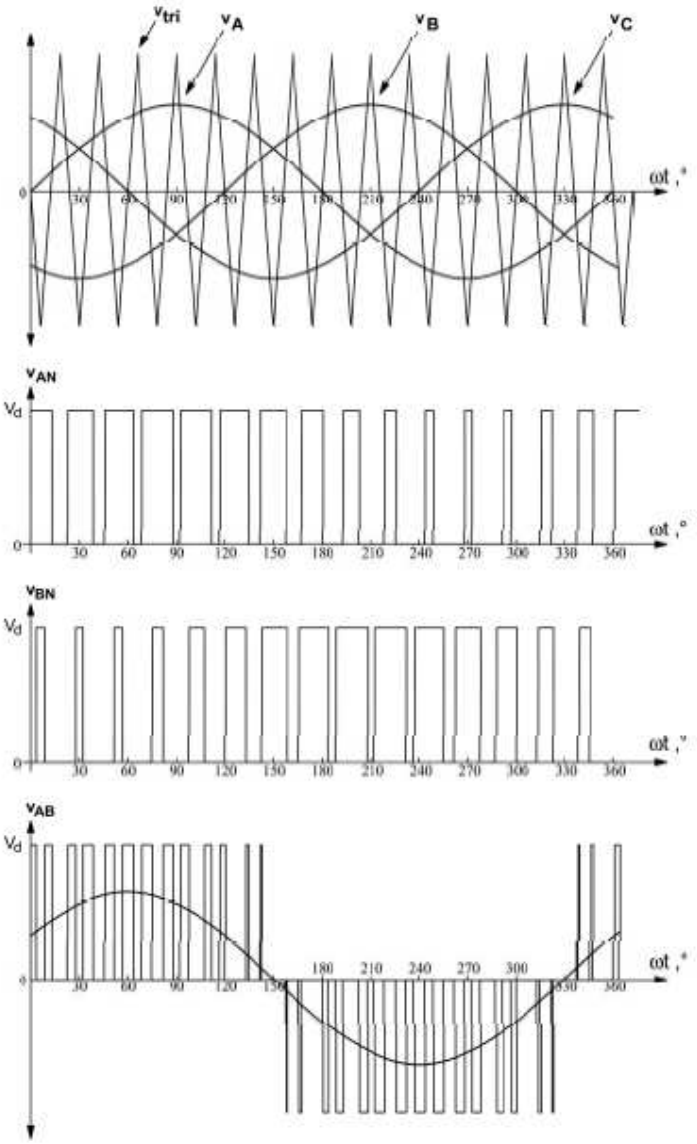


**Figure 2.7 SPWM Technique for three phase voltages [14]**

Frequency modulation ratio $m_f$ is defined as :

$$m_f = \frac{f_{tri}}{f_1} \tag{2.3}$$

$m_f$ must be chosen as an odd integer to form an odd and half wave symmetric converter line-to-neutral voltage. Therefore, even harmonics are eliminated. Moreover, $m_f$ is chosen

as a multiple of 3 in order to eliminate the harmonics at $m_f$ and odd multiples of $m_f$ in the converter line-to-line voltages. Harmonics in the converter voltages appear as sidebands, centered around the switching frequency and its multiples. This is true for all values of amplitude modulation ratio (*m*) in the linear range [14,27].

In this thesis the fundamental frequency of the converter voltage (modulating frequency $f_1$) is 50 Hz which is the power system frequency, and the carrier frequency ($f_{tri}$) is chosen as 2500 Hz, hence $m_f$ ratio of equation (2.3) is 5. This $m_f$ ratio is a good and proper ratio for the D-STATCOM converter in order to produce smooth conversion of the DC voltage into AC voltage according to Figure 2.7, and to provide better harmonics elimination.

The control parameters for SPWM are the modulation index (*m*) and phase shift angle $\delta$. Amplitude modulation (*m*) ratio is defined as :

$$m = \frac{V_1}{V_{tri}} \tag{2.4}$$

where

$V_1$ peak amplitude of the reference voltage

$V_{tri}$ peak amplitude of the triangular voltage

The magnitude of the triangular voltage is kept constant and the amplitude of the control voltage is allowed to vary. Linear range of SPWM is defined for $0 \leq m \leq 1$. These control parameters of SPWM; modulation index *m* and phase shift angle $\delta$, are fed from the D-STATCOM controller, to produce the compensated control signal from the SPWM as a switching pattern of the IGBT gates of the D-STATCOM inverter (VSC).

SPWM techniques present i) cost effective, efficient and more compact systems, ii) nearly sinusoidal input/output waveforms, and iii) superior control characteristics that can be used for D-STATCOM control [28].

## 2.6 D-STATCOM System Modeling

### 2.6.1 Background

Henceforth, the term *D-STATCOM system* will be used to express the D-STATCOM device connected to the studied system of the local low voltage utility of Gaza.

For the proposed control strategy of the thesis, based on optimal control, the state-space model of the D-STATCOM system circuit must be introduced. State-space model is an important part of designing optimal controllers; LQR, $H_2$ and $H_\infty$, which will be further explained in Chapter 3. State-space model is important also to test the step response of the system with the PI and optimal controllers. This is the objective of this section.

Several aspects are assumed in formulation the equations that describe the D-STATCOM system according to analysis and control strategy used by the designer, and the states, inputs and outputs chosen to be manipulated by the controller. For example, [15,17,20] obtain the state-space representation in *dq* stationary frame with four, three and five states respectively, and [29-32] obtain the state-space representation in *abc* stationary frame with four states to represent the D-STATCOM system.

Due to its simplicity and clarity of describing the D-STATCOM system, the choice is to adopt the equivalent circuit that used in [29,32] and shown in Figure 2.9, to represent the D-STATCOM system, and to be used in the proposed controller in this thesis.

### 2.6.2 Derivation of The System State-Space Model

As mentioned in Section 2.1, the D-STATCOM as a shunt compensator is connected to a three-phase grid connected system through a coupling transformer. The rating of this transformer is comparable with the source of the low voltage network which is the case study of the thesis. That is unreasonable and high cost requirement. The coupling transformer can be represented by its leakage inductance added to an L-filter or LC-filter inductance [13,14,16,17,24] which together work the same role of voltage coupling and signal filtering.

Returning back to Figure 2.3, and combining the LC-filter to the connection branch of

D-STATCOM to the main system, The D-STATCOM system can be represented as shown in Figure 2.8.

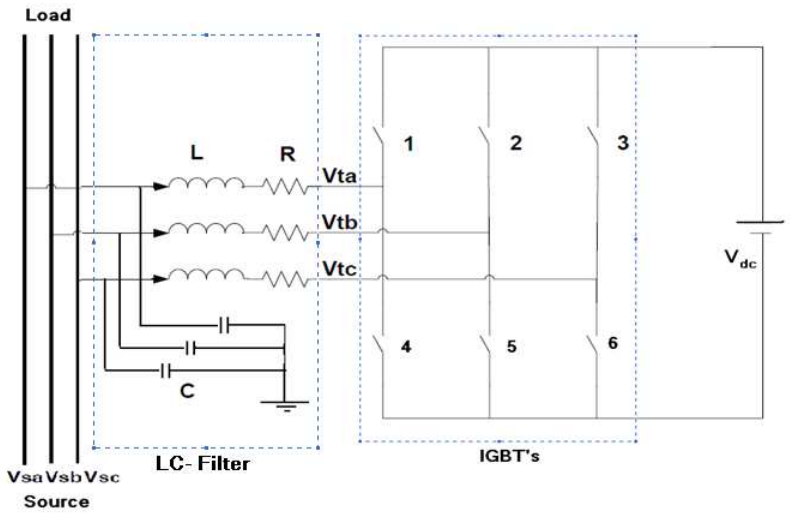


**Figure 2.8: Basic configuration of D-STSTCOM system with LC-filter**

This configuration may be represented per phase basis as shown in Figure 2.9.

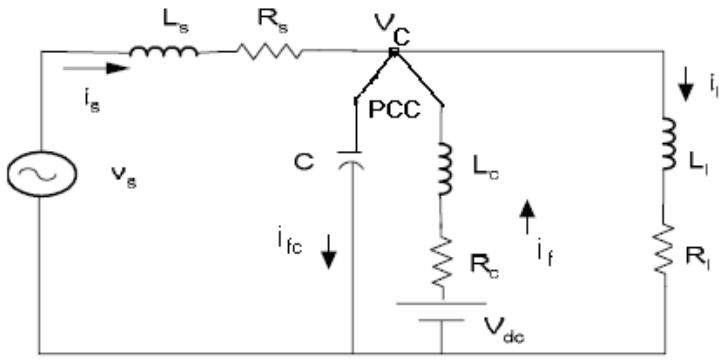


**Figure 2.9: Single-phase circuit of D-STSTCOM system**

where,

$V_s$ supply votage
$R_s$ supply resistance
$L_s$ supply inductance

$i_s$ supply currnet
$V_c$ voltage at load point
$i_L$ load currnet
$R_L$ Load resistance
$L_L$ Load inductance
$i_f$ currnet in L-branch of filter
$i_{fc}$ currnet in C-branch of filter
$R_c$ filter resistance (includes coupling transformer losses)
$L_c$ filter inductance (includes leakage inductance of coupling transformer)
C shunt filter capacitor
$V_{dc}$ DC voltage of the storage device

Referring to Figure 2.9, the following equations can be written to express the system:

$$V_s = L_s \frac{di_s}{dt} + i_s R_s + V_c \quad (2.5)$$

$$V_c = -L_c \frac{di_f}{dt} - i_f R_c + V_{dc} \quad (2.6)$$

$$V_c = L_L \frac{di_L}{dt} + i_L R_L \quad (2.7)$$

$$i_{fc} = C \frac{dV_c}{dt} \quad (2.8)$$

The filter capacitor C is connected to the PCC to provide a path for the harmonic currents generated due to switching, while the main branch of the compensated current is the L-branch with its compensated current $i_f$ . Hence, it is correct to express $i_{fc}$ as:

$$i_{fc} = i_f + i_s - i_L \quad (2.9)$$

that is from the currents relation of PCC node:

$$i_f + i_s = i_{fc} + i_L \quad (2.10)$$

then, by substituting equation (2.9) in equation (2.8) we get:

$$i_f + i_s - i_L = C \frac{dV_c}{dt} \quad (2.11)$$

Equations (2.5), (2.6), (2.7) and (2.11) can be rewritten as:

$$\frac{di_s}{dt} = \frac{V_s}{L_s} - \frac{i_s}{L_s} R_s - \frac{V_c}{L_s} \tag{2.12}$$

$$\frac{di_f}{dt} = \frac{V_{dc}}{L_c} - \frac{i_f}{L_c} R_c - \frac{V_c}{L_c} \tag{2.13}$$

$$\frac{di_L}{dt} = \frac{V_c}{L_L} - \frac{i_L}{L_L} R_L \tag{2.14}$$

$$\frac{dV_c}{dt} = \frac{i_s + i_f - i_L}{C} \tag{2.15}$$

As mentioned previously, the assumption of system input, output and states is differ from design to another according to analysis and control strategy used. This also the case for [29,32] although using the same system circuit configuration and equations.

The proposed control strategy in this thesis is applied with constant DC link voltage to detect the voltage sag/ swell caused in the voltage source $V_s$ and process the error signal to produce controlled voltage signal to compensate the sag/ swell at the PCC point. This controlled signal is $V_c$ voltage. Hence, $V_s$ will be considered as the system input $u$, while $V_c$ will be considered as the system output $y$. The $V_{dc}$ term in equation (2.13) is a constant term, which can be ignored in state-space representation. The states will be chosen as: source current $i_s$, compensated current $i_f$, load current $i_l$ and the PCC voltage $V_c$. Thus, $x_1 = i_s$, $x_2 = i_f$, $x_3 = i_L$, $x_4 = V_c$ and $y = x_4$.

Therefore, the differential equations (2.12)-(2.15) can be expressed by linear continuous time system, or state-space model of the form:

$$\dot{x} = Ax + Bu$$
$$y = Cx + Du$$

where,

$$u = V_s,$$
$$y = x_4 = V_c \tag{2.16}$$

the state variables are:

$$\begin{bmatrix} x_1 \\ x_2 \\ x_3 \\ x_4 \end{bmatrix} = \begin{bmatrix} i_s \\ i_f \\ i_L \\ V_c \end{bmatrix} \tag{2.17}$$

and the state-space model can be given in equation (3.14).

$$\begin{bmatrix} \dot{x}_1 \\ \dot{x}_2 \\ \dot{x}_3 \\ \dot{x}_4 \end{bmatrix} = \begin{bmatrix} -\mathrm{R_s}/\mathrm{L_s} & 0 & 0 & -1/\mathrm{L_s} \\ 0 & -\mathrm{R_c}/\mathrm{L_c} & 0 & -1/\mathrm{L_c} \\ 0 & 0 & -\mathrm{R_L}/\mathrm{L_L} & 1/\mathrm{L_L} \\ 1/C & 1/C & -1/C & 0 \end{bmatrix} \begin{bmatrix} x_1 \\ x_2 \\ x_3 \\ x_4 \end{bmatrix} + \begin{bmatrix} 1/L_s \\ 0 \\ 0 \\ 0 \end{bmatrix} u \tag{2.18}$$

$$y = \begin{bmatrix} 0 & 0 & 0 & 1 \end{bmatrix} \begin{bmatrix} x_1 \\ x_2 \\ x_3 \\ x_4 \end{bmatrix}$$

# 3 CHAPTER 3: THE PROPOSED CONTROL STRATEGY FOR D-STATCOM

## 3.1 Introduction

The dynamic performance of the D-STATCOM is important since the load will not maintain the normal operation if it is exposed to voltage sag/ swell. Although design and implementation of the conventional control methods are simple, they do not yield an optimal control system and it result with some difficulties and undesired results as showed in the literature review (Section 1.6).

The key factors for testing and comparing controller performance of D-STATCOM device are:

- Magnitude of sag/ swell voltage after controlling process; sag/swell % of equations (1.1) and (1.2).
- Resultant total harmonic distortion of the voltage signal; THD of equation (1.5).
- The total power factor of the electrical network; *p.f.*
- Conventional response criteria's of controllers, such that settling time, max. overshoot and steady-state error.

The first two factors, sag/swell % and THD, must be decreased by the controller as minimum as possible and within the IEEE standards (Tables 1.1 and 1.2), while the third factor, *p.f,* must result with the highest value closed to one (100%). That is with faster controller response. Hence, the best controller must yield:

- min. sag/ swell %
- min. THD
- *max. p.f*
- faster and best response.

In order to meet these requirements, an optimal based control strategy of D-STATCOM

with constant DC link is presented in this Chapter, and step response will be tested for D-STATCOM system.

### 3.1.1 *DQ* Rotating Transformation

It is common practical in power system application to transform three-phase AC dynamics (voltages and currents) into orthogonal components in a rotating reference frame. *dq* transformation is a very common transformation for power systems, and the major control strategies depend on that transformation [13-20]. The use of *dq* transformation for D-STATCOM control open the field for other control methods strategies than the traditional one to be applied and utilized for the D-STATCOM applications. The components are referred to the direct or real '*d*', quadrture or reactive '*q*' and zero *'0'* components, those that lead to useful work in power systems. From the power system theory we get the real and reactive components relative to a rotating reference frame with angular frequency $\omega$ ( $\omega = 2\pi f$ ) as showed in Figure 3.1.

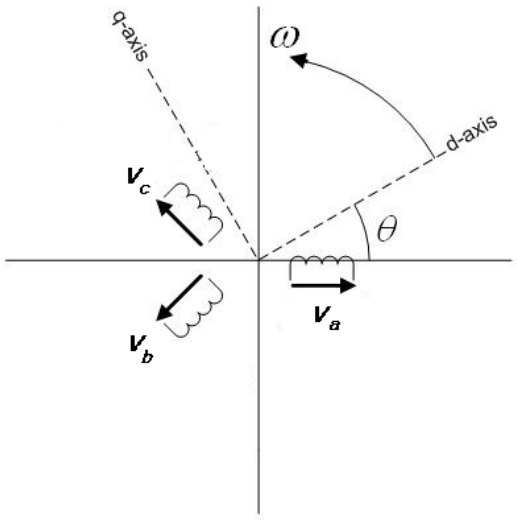


**Figure 3.1: *dq* reference frame**

The two axes are called the direct or *d*-axis, and the quadrature or *q*-axis. The *q*-axis is at an angle of $90^{\circ}$ to (in quadrature with) the direct *d* axis. They follow the trajectory of the voltage vector by the angular speed of $\omega$ and maintaining the $90^{\circ}$ between each other. The

three components *d,q,0* can be calculated from the three-phase *abc* stationary coordinate system by the following transformation [26]:

$$\begin{bmatrix} V_d \\ V_q \\ V_0 \end{bmatrix} = T \begin{bmatrix} V_a \\ V_b \\ V_c \end{bmatrix} \tag{3.1}$$

$$T = \frac{2}{3}\begin{bmatrix} \cos(\omega t) & \cos(\omega t - \frac{2}{3}\pi) & \cos(\omega t + \frac{2}{3}\pi) \\ -\sin(\omega t - \frac{2}{3}\pi) & -\sin(\omega t - \frac{2}{3}\pi) & -\sin(\omega t + \frac{2}{3}\pi) \\ 1/2 & 1/2 & 1/2 \end{bmatrix} \tag{3.2}$$

and the inverse transformation can be evaluated as [25]:

$$\begin{bmatrix} V_a \\ V_b \\ V_c \end{bmatrix} = T^{-1} \begin{bmatrix} V_d \\ V_q \\ V_0 \end{bmatrix} \tag{3.3}$$

$$T^{-1} = \frac{2}{3}\begin{bmatrix} \cos(\omega t) & \sin(\omega t) & 1 \\ \cos(\omega t - \frac{2}{3}\pi) & \sin(\omega t - \frac{2}{3}\pi) & 1 \\ \cos(\omega t + \frac{2}{3}\pi) & \sin(\omega t + \frac{2}{3}\pi) & 1 \end{bmatrix} \tag{3.4}$$

Such transformation is accomplished for the *abc* voltage or current wave forms, the controller of the proposed control process is applied to the resultant real '*d*' and reactive '*q*' components instead of the *abc* signal itself.

The benefits of such arrangement are: the control problem is greatly simplified because the system variables become DC values under balanced condition; multiple control variables are decoupled so that the use of classic control method is possible, and even more physical meaning for each control variable can be acquired [24]. The *dq* method gives the sag depth and phase shift information with start and end times. In the balanced condition *d* component is equal to system voltage, and *q* and *0* components are zero [33]. Then the

controlled *dq* components are retransformed to the original three-phase *abc* stationary coordinate system which will contain all dynamic signal information after control.

### 3.1.2 Synchronization Scheme

A very impressive part of the proposed control strategy of D-STATCOM is a Phase-Locked Loop (PLL). The Phase-Locked Loop (PLL) is a feedback control system includes voltage-controlled oscillator (VCO), phase detector and low pass filter; Figure 3.2. Its purpose is to track the frequency and phase of the input signal [34], hence the PLL synchronizes the converter AC output voltage with the main AC system voltage.

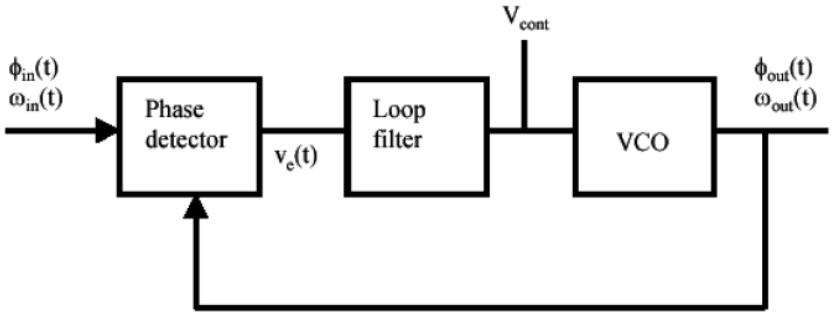


**Figure 3.2: Configuration of PLL scheme [33]**

## 3.2 Methodology of the Proposed Control Strategy

Basing on the main control concept of D-STATCOM; Figure 2.5, only one control loop of the measured voltage will be used. Using more than one control loop as [15-19,23,24] is more complex and time consuming, and requires several voltages and currents measurements.

### 3.2.1 Controlled Signal Components

As mentioned in the analysis of the previous researches (Section 1.6), *dq* transformation of the voltage and current signals makes the ability for other control methods and strategies to be applied other than the traditional PI control method. Hence, the use of the *dq* transformation of the measured voltage signal is a main part of the proposed control strategy. To show the effect of the *dq* components, simulation of D-STATCOM system of Figure 1.9 is presented. The simulation was performed for 1.0 sec. with applied voltage sag of 22.5% for the time duration of 0.2-0.4 sec, and 15.0% voltage swell for the time duration

of 0.6-0.8 sec. Figure 3.3 shows the resultant three-phase load voltages, and the corresponding $V_d$ and $V_q$ response.

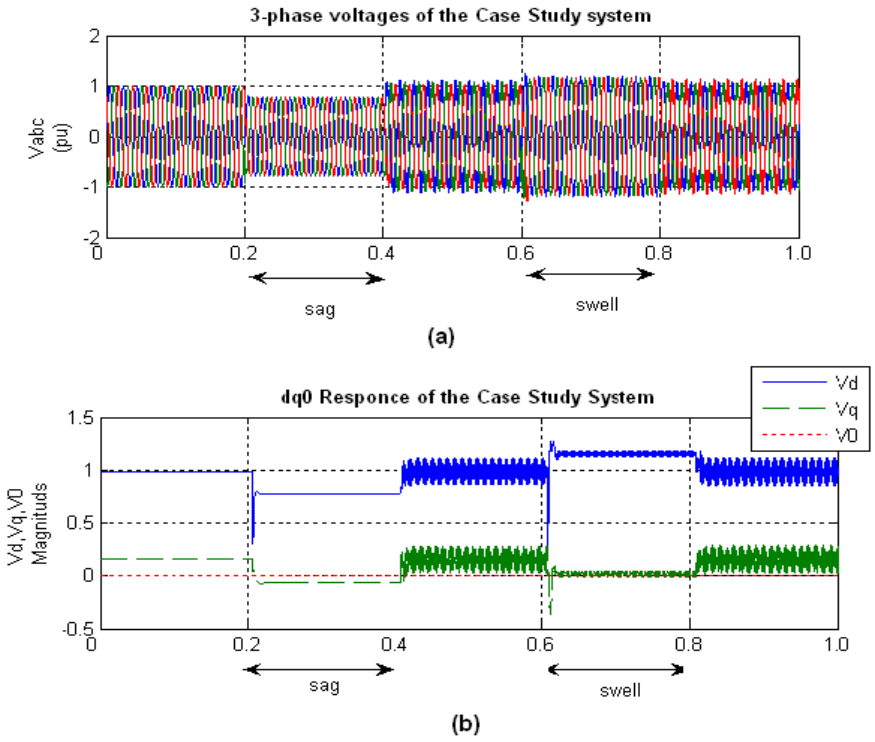


**Figure 3.3: Simulation the case study system voltages during sag and swell situations; (a) 3-phase voltages. (b) $V_{dq0}$ components**

It is clear from Figure 3.3 (b), that $V_d$ component represents the main 3-phase voltage information which is affected by any change of the original signal. It has 0.985 pu rated value, 0.7725 value pu during sag duration and 1.155 pu value during swell duration, while $V_q$ component has some distortion (0.155 pu rated value and -0.066 during sag duration) with value $\neq 0$ unlike the expected behavior.

Hence, it can be concluded that for system control purpose, only $V_d$ and $V_q$ need to be controlled;

- Controlling $V_d$ by adjusting it to 1.0 pu value, and
- Controlling $V_q$ by adjusting it to 0.0 pu value.

This is a new control scheme compared with the present researches which can be classified into: controlling the *abc* stationary voltage form as [7,8,12,21,22,32], or controlling only $V_d$ component with and without controlling $V_{dc}$ as [14-19,23,24].

### 3.2.2 Phase-Locked Loop (PLL) Scheme

There are two choices to use the phase-locked loop (PLL) technique for synchronization purpose. The first is derivation of the frequency and phase shift information dynamically from the controlled system and feed it to the retransformation pattern of the controlled signal from the *dq* frame to *abc* frame to track the main system voltages, and this is the used PLL scheme in [2,3,10-12, 15,17,18,20,28]. The second is extraction a fixed 50 Hz, $0^{\circ}$ phase shift values for the retransformation pattern of the controlled signal. This PLL scheme is used for pole placement control strategy of [24], but it was applied for current components instead of voltage components.

By applying the two choices for the studied D-STATCOM system, it was found that the second choice is better for sag/ swell compensation due to its ideal extracted information and behavior that complete the control process by returning the system to its ideal frequency and phase shift situation which may be affected by any undesired actions, while the first choice requires additional internal control loop with its PI parameters tuning, to control the frequency and phase shift system information, and it has a great effect on the dynamic operation of the device and a new auxiliary regulator is needed to enhance the dynamic performance. This fixed PLL scheme will be illustrated in Figure 3.4.

### 3.2.3 DC Storage Device

The DC storage device is an effective part the D-STATCOM. It is considered as the voltage source to compensate the voltage during sag/ swell conditions. Using a DC capacitor as a DC storage device is a common control strategy which has been used in [4,8,15,16, 18-21,23, 26,28,32]. The role of that capacitor is to be charged and recharged during power exchange process. This strategy requires more control loops to control the DC voltage across the capacitor and to control the power exchange, which is also more complex and may be affected by some voltage deviations and slow response time.

Traditional D-STATCOM only has DC capacitor; thus, only reactive power can be injected to the power system by D-STATCOM. Whereas both active and reactive power can be injected to the power system by D-STATCOM if constant DC source is used as in [12,14,17,22] with faster step response. This is also a result of applying the two DC storage schemes on the studied D-STATCOM system. Thus, constant DC link voltage scheme is adopted in the proposed control strategy.

### 3.2.4 Optimal Control

Due to the weakness of researches of the robust and optimal control methods for D-STATCOM to improve its performance, the interest in this thesis is concerned on optimal control methods for D-STATCOM, such that applying LQR, $H_2$ and $H_\infty$ controllers in addition of the PI controller to control the $V_d$ and $V_q$ components separately, that is in order to utilize the benefits of the optimal control methods to reach optimum solutions of power quality problems. The system which is the end result of an optimal design is supposed to be the best possible system of a particular type and provides the best possible performance with respect to given measure of performance by mean of the *cost function*. Optimal controllers will be explained further and designed in Section 3.4.

## 3.3 Algorithm of the Proposed Control Strategy

Now, the proposed control strategy is ready to be presented as the following algorithm, and showed in Figure 3.4:

- The AC three phase voltages at the PCC point is measured and transformed into *dq* reference frame.
- The $V_d$ and $V_q$ components are processed by separated, but similar two controllers to derive the compensating *dq* components. $V_d$ component is compared with the 1.0 pu reference value and the $V_q$ component is compared with the 0.0 pu reference value, to maintain the non disturbance voltage signal.
- The resultant $V_d$ and $V_q$ controlled components are combined with the $V_0$ component (of '0' value) and then retransformed to the original three-phase *abc* stationary

coordinate system using virtual PLL fixed at 50 Hz frequency and $0^{\circ}$ phase shift, which result with ideal synchronized voltage signal with the main network voltage.

- The resultant $V_{abc}$ voltage signal is fed to the SPWM pattern to produce a switching pulses of the IGBT's gates of the D-STATCOM inverter.
- The two separated controllers for the $V_d$ and $V_q$ components will be: conventional PI controller, and optimal controllers; LQR, $H_2$ and $H_\infty$.

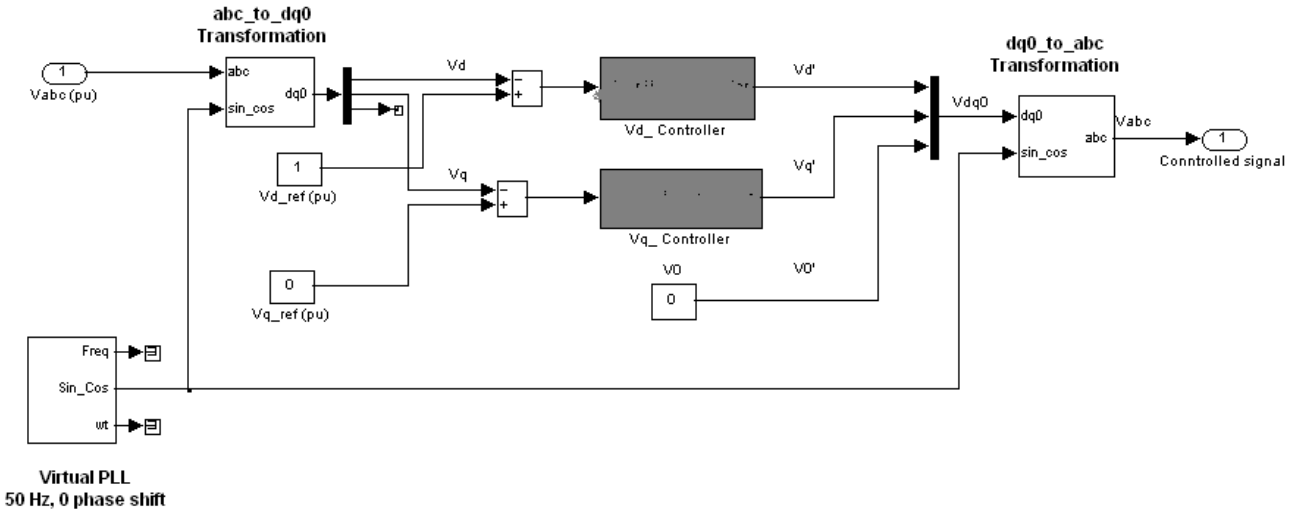


**Figure 3.4: Configuration of the proposed control strategy**

## 3.4 Design of Optimal Controllers

### 3.4.1 Background

In the main, the primary aim of the designer using classical control design methods is to stabilize a plant, and to obtain a certain transient response, bandwidth, steady state error, and so on. Optimal control is one particular branch of modern control (since 1960's), as opposed to classical, that sets out to provide analytical designs of a specially appealing type. The system which is the end result of an optimal design is not supposed merely to be stable, or satisfy any one of the desirable constraints associated with classical control, but it is supposed to be the best possible system of a particular type [35].

An optimal control is characterized by the specification of a *cost function* that combines all the variable performance specifications. This cost function is a real, scalar-valued function of the system that can be minimized to obtain the single best controller, such that superior performance is indicated by a smaller numerical value. Linear Quadratic Regulator (LQR), $H_2$ controller and H-infinity $(H_\infty)$ optimization problem are solutions of optimal control problem [36].

### 3.4.2 Linear Quadratic Regulator (LQR)

The *regulator problem* is providing a plant input or applying a control to take the plant from a nonzero state to the zero state. This problem may typically occur where the plant is subjected to unwanted disturbances that perturb its output [35].

Consider a system represented as:

$$\begin{aligned} \dot{x}(t) &= Ax(t) + Bu(t) \\ y(t) &= Cx(t) + Du(t) \end{aligned} \tag{3.5}$$

The *regulator problem* is to achieve a *control law* so that an input *u(t)* is required to be an instantaneous function of the plant state *x(t)*. Linear Quadratic Regulator (LQR) is a control scheme that provides the best possible performance with respect to given measure of performance, which is the cost function. LQR is produced by the minimization of the cost function; *J*, where the state equation of the plant is linear and the cost function is quadratic [35].

The nature of this function may be permitted to vary with time,

$$u(t) = -Kx(t) \tag{3.6}$$

The natural formulation of a cost for the system is given directly in terms of states and inputs, rather than inputs and outputs. Thus, a cost function $J$ is defined as [37]:

$$J = \frac{1}{2}x(t_f)^T Q(t_f)x(t_f) + \frac{1}{2}\int_{t_0}^{t_f}\left[x(t)^T Qx(t) + u(t)^T Ru(t)\right]dt \tag{3.7}$$

where *Q* and *R* are real positive-definite and positive-semidefinite matrices, respectively,

for all *t*, which can always be taken as symmetric. The optimal control problem posed in equation (3.7) is a constrained optimization problem. This optimal control problem can be converted to unconstrained optimization problem by the application of *Lagrange multiplier* in the following form [36]:

$$J_L = \frac{1}{2}x(t_f)^T Q(t_f)x(t_f) + \int_{t_0}^{t_f} \{\frac{1}{2}x(t)^T Qx(t) + \frac{1}{2}u(t)^T Ru(t) + \lambda^T\left[Ax(t) + Bu(t) - \dot{x}(t)\right]\} dt \tag{3.8}$$

where $\lambda(t)$ is the family of Lagrange multipliers, one at each point. The optimal control is found by forming the *Hamiltonian system* as [36]:

$$H = \frac{1}{2}\left[x(t)^T Qx(t) + u(t)^T Ru(t)\right] + \lambda^T(t)\left[Ax(t) + Bu(t)\right] \tag{3.9 a}$$

$$\frac{\partial H}{\partial u} = 0;\ u(t) = -R^{-1}B^T\lambda(t) \tag{3.9 b}$$

$$\dot{\lambda}(t) = -\left(\frac{\partial H}{\partial u}\right)^T = -Qx(t) - A^T\lambda(t) \tag{3.9 c}$$

$$\dot{x}(t) = Ax(t) - BR^{-1}B^T\lambda(t) \tag{3.9 d}$$

where $H$ is the Hamiltonian, and $u(t)$ of equation (3.9 b) is the optimal control. Substituting equation (3.9 b) into equation (3.9 d) and combining the resulting equation with equation (3.9 c) into a single state equation yields the *Hamiltonian system* of equation (3.10):

$$\begin{bmatrix}\dot{x}(t)\\ \dot{\lambda}(t)\end{bmatrix} = \begin{bmatrix}A & -BR^{-1}B^T\\ -Q & -A^T\end{bmatrix}\begin{bmatrix}x(t)\\ \lambda(t)\end{bmatrix} \tag{3.10}$$

Now, let $\lambda(t) = Px(t)$, then:

$$\dot{\lambda}(t) = \dot{P}x(t) + P\dot{x}(t) \tag{3.11}$$

Substituting $\dot{\lambda}(t)$ and $\dot{x}(t)$ from equations (3.9 c) and (3.9 d), respectively, into equation (3.11) yields:

$$-\dot{P} = A^T P + PA - PBR^{-1}B^T P + Q \tag{3.12}$$

which called *Algebric Ricatti Equation*. The *Ricatti Equation* has only final conditions and can, therefore, be solved for *P(t)* backward in time using any numerical integration method with boundary condition: $P(t_f) = Q(t_f)$, and the solution *P(t)* is a unique positive definite solution matrix that minimizes the cost function [36].

The optimal control can be found by finding this unique solution matrix and substituting it into equation (3.9 b) to have the *optimal control law*:

$$u(t) = -R^{-1}B^T Px(t) \tag{3.13}$$

where $-R^{-1}B^T P = K$ is the LQR gain matrix of the *control law* (3.6). A suitable choice of the *Q* and *R* matrices leads to the computation of the LQR gain *K* [35].

As mentioned in Section 1.6, the LQR can be applied to design the control law of error of system states. Thus, the LQR *control law* will be:

$$u(t) = -K(t)\left[x(t) - x_{ref}(t)\right] \tag{3.14}$$

Linear Quadratic Regulator (LQR) is an optimal control method and is also a pole placement method. LQR achieve the optimal tradeoff between the use of control effort, the magnitude and the speed of response [24].

The major limitations of the LQR are: the test conditions are limited to initial conditions and no disturbance inputs, and the entire state must be measured [36].

### 3.4.3 H - Optimal Control

The LQR can be posed as 2-norm optimization problem due to the formulation of the cost function to be minimized [36]. In general, 2-norm of a stable transfer function *G* can be defined as:

$$\|G\|_2 = \left( \int_{-\infty}^{\infty} |G(j\omega)|^2 \, d\omega \right)^{\frac{1}{2}} \tag{3.15}$$

LQR is an optimal control problem of minimizing the 2-norm of the closed-loop system

when the plant is appropriately defined and within the limitation of that the entire state must be measured. In many applications, some states are unmeasurable, and in addition, no measurement is ever exact. The $H_2$ controller is an optimal controller that utilizes partial state information and noisy information. The $H_2$ controller estimates the system state, which then used in the LQR. Hence, the $H_2$ controller is basically a *regulator*, and the $H_2$ controller is designed to reject white-noise disturbance inputs [36].

**Formulation of $H_2$ control Problem**

Consider a standard feedback design diagram of Figure 3.5, which can be described by the system dynamics (3.16).

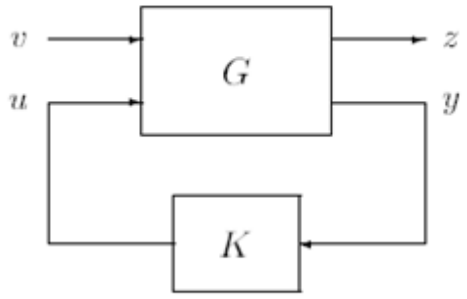


**Figure 3.5: Standard feedback control system**

$$\begin{aligned} \dot{x}(t) &= Ax(t) + B_1 v(t) + B_2 u(t) \\ z(t) &= C_1 x(t) + D_{12} u(t) \\ y(t) &= C_2 x(t) + D_{21} v(t) \end{aligned} \tag{3.16}$$

where $v$ is a vector of uncorrelated white-noise disturbances with unit intensity, $u$ is the control input vector, $z$ is the performance vector, and $y$ is the measurement vector. The task is to find a state space controller $K$, such that the feedback interconnection of $G$ and $K$ is well-posed, defines a stable state space model $F(G,K)$, and minimizes the $H_2$ norm of $F(G,K)$ described as [38]:

$$J_2(K) = \left\| F(G,K) \right\|_2^2 \tag{3.17}$$

The stable state space model $F(G,K)$ is:

$$\begin{aligned} \dot{x_c}(t) &= A_c x(t) + B_c u(t) \\ y_c(t) &= C_c x(t) \end{aligned} \tag{3.18}$$

Recall the cost function of LQR (equation (3.7)) which is also a 2-norm optimization problem. It is appropriate to introduce the time-domain characterization of the cost (3.17):

$$J_2(K) = \int_0^\infty z(t)^T z(t)\, dt \tag{3.19}$$

It is easy to see that the cost functions (3.7) and (3.19) are equivalent, because the positive (semi) defnite matrices $Q$ and $R$ can always be factorized as [38]:

$$Q = (Q^{1/2})^T Q^{1/2}, \quad R = (R^{1/2})^T R^{1/2} \tag{3.20}$$

Defining the matrices [38]:

$$C_1 = \begin{bmatrix} Q^{1/2} \\ 0 \end{bmatrix}, \quad D_{12} = \begin{bmatrix} 0 \\ R^{1/2} \end{bmatrix} \tag{3.21}$$

it follows from equation (3.16) that:

$$\begin{aligned} z^T(t) z(t) &= (C_1 x(t) + D_{12} u(t))^T (C_1 x(t) + D_{12} u(t)) \\ &= x^T(t) Q x(t) + u^T(t) R u(t) \end{aligned} \tag{3.22}$$

and the costs (3.19) and (3.7) are thus equivalent [38].

The solution of $H_2$ control problem follow the same procedures of the solution of control LQR problem, but by applying the control gain into the estimation of the states, such that the cost (3.19) is minimized by the static state-feedback controller [36,38]:

$$u(t) = K_2 \hat{x}(t) \tag{3.23}$$

where $\hat{x}(t)$ is the state estimation, and $K_2$ can be represented as:

$$K_2 = -(D_{12}{}^T D_{12})^{-1} B_2^T P_H \tag{3.24}$$

where $P_H$ is the unique symmetric positive definite solution to the *Algebraic Riccati equation* [38]:

$$A^T P_H + P_H A - P_H B_2 (D_{12}{}^T D_{12})^{-1} B_2^T P_H + C_2{}^T C_2 = 0 \tag{3.25}$$

**The optimal state-estimation problem**

Consider the system:

$$\begin{aligned} \dot{x}(t) &= Ax(t) + B_1 y(t) \\ z(t) &= C_1 x(t) \\ y(t) &= C_2 x(t) + D_{21} y(t) \end{aligned} \tag{3.26}$$

Notice that in the estimation problem, we need not consider the input $u(t)$. A stable causal state estimators $F$ that the state estimate is determined from the measured output $y$ according to: $\hat{x}(s) = F(s)y(s)$. In the $H_2$ optimal estimation problem, the problem is to construct an estimator, such that its $H_2$-cost:

$$J_e(F) = \int_0^\infty \left[x(t) - \hat{x}(t)\right]^T C_1^T C_1^T \left[x(t) - \hat{x}(t)\right] dt \tag{3.27}$$

is minimized [38]. The solution of the optimal state estimation problem is given as:

$$\dot{\hat{x}}(t) = A\hat{x}(t) + L\left[y(t) - C_2\hat{x}(t)\right] \tag{3.28}$$

where

$$L = SC_2^T (D_{21}{}^T D_{21})^{-1} \tag{3.29}$$

and $S$ is the unique symmetric positive definite solution to the *Algebraic Riccati equation* [38]:

$$A^T S + SA - SC_2^T (D_{21}{}^T D_{21})^{-1} C_2^T S + B_1 B_1^T = 0 \tag{3.30}$$

### $H_2$ optimal controller

Combining the optimal state-feedback problem (3.23) and the optimal state-estimation problem (3.28), then the controller *u(t) = K y(t)* which minimizes the $H_2$ cost (3.19) is given by the equation [38]:

$$\begin{aligned} \dot{\hat{x}}(t) &= \left(A + B_2 K_2\right)\hat{x}(t) + L\left[y(t) - C_2\hat{x}(t)\right] \\ u(t) &= K_2(t)\hat{x}(t) \end{aligned} \tag{3.31}$$

### 3.4.4 $H_\infty$ Optimal Control

The 2-norm optimization problem can also be posed using the system $\infty$–norm as a cost function. The $\infty$–norm is the worst case gain of the system and therefore provides a good match to engineering specifications, which are typically given in terms of bounds on errors and controls. The $\infty$–norm of a stable transfer function *G* can be defined as:

$$\|G\|_\infty = \sup_\omega |G(j\omega)| \tag{3.32}$$

### Formulation of $H_\infty$ control Problem

Recall again the standard feedback design diagram of Figure 3.5, equation (3.16). The standard task of $H_\infty$ optimal problem is to find a state space controller $K$, such that the feedback interconnection of *G* and *K* is well-posed, defines a stable state space model *F*(*G*,*K*), and minimizes the $H_\infty$-norm of *F*(*G*,*K*) described as [39]:

$$J_\infty(K) = \|F(G,K)\|_\infty^2 \tag{3.33}$$

The direct minimization of the cost $J_\infty(K)$ turns out to be a very hard problem, and it is therefore not feasible to tackle it directly. Instead, it is much easier to construct conditions which state whether there exists a stabilizing controller which achieves the $H_\infty$-norm bound:

$$J_\infty(K) < \gamma \tag{3.34}$$

for a given $\gamma > 0$, and then checking the achievability of the performance bound (3.34) for various values of $\gamma$ (for any degree of accuracy) by iteration procedures [39].

The $H_\infty$ performance measure can be characterized in terms of the worst-case gain in terms of 2-norm as [39]:

$$J_\infty(K) = \sup\left\{\frac{\|z\|_2}{\|v\|_2}\right\},\ v \neq 0 \tag{3.35}$$

The performance bound (3.34) is thus equivalent to:

$$\frac{\|z\|_2}{\|v\|_2} < \gamma \ \text{ or } \ J_\infty = \|z\|_2^2 - \gamma^2 \|v\|_2^2 < 0 \tag{3.36}$$

which is equivalent to:

$$J_\infty = \int_0^\infty [z^T(t)z(t) - \gamma^2 v^T(t)v(t)]\, dt < 0,\ \ v \neq 0 \tag{3.37}$$

Similar to $H_2$ control problem, The problem of finding a controller $u = Ky$ such that the cost $J_\infty$ is minimized, and it will be solved in two stages: the first is solving a problem with complete state information, and the second stage consists of an associated worst-case estimation problem. A combination of the two stages provides the solution of the original $H_\infty$ control problem.

**The $H_\infty$ optimal state-feedback problem**

A controller that achieves the bound (3.37) is given by the static state-feedback controller [39]:

$$u(t) = K_\infty x(t) \tag{3.38}$$

$$K_\infty = -(D_{12}{}^T D_{12})^{-1} B_2^T X_\infty \tag{3.39}$$

where $X_\infty$ is the unique symmetric positive semidefinite solution to the *Algebraic Riccati equation* [39]:

$$A^T X_\infty + X_\infty A - X_\infty B_2 (D_{12}{}^T D_{12})^{-1} B_2^T X_\infty + \gamma^{-2} X_\infty B_1 B_1^T X_\infty + C_2{}^T C_2 = 0 \tag{3.40}$$

Now, define the signals [39]:

$$\begin{aligned}\tilde{z}(t) &= (D_{12}{}^{T} D_{12})^{1/2} u(t) + (D_{12}{}^{T} D_{12})^{1/2} B_2^T X_\infty x(t) \\ \tilde{v}(t) &= v(t) - \gamma^{-2} B_1^T X_\infty x(t)\end{aligned} \tag{3.41}$$

Then we have:

$$\tilde{J}_\infty = \|\tilde{z}\|_2^2 - \gamma^2 \|\tilde{v}\|_2^2 < 0 \quad \text{or} \quad J_\infty = \|\tilde{z}\|_2^2 - \gamma^2 \|\tilde{v}\|_2^2 < 0 \tag{3.42}$$

which is equivalent to inequality (3.37). Introducing the signals $\tilde{z}(t)$ and $\tilde{v}(t)$ into the system equations (3.16) gives:

$$\begin{aligned}\dot{x}(t) &= \tilde{A}x(t) + \tilde{B}_1\tilde{v}(t) + \tilde{B}_2 u(t) \\ \tilde{z}(t) &= \tilde{C}_1 x(t) + \tilde{D}_{12} u(t) \\ y(t) &= \tilde{C}_2 x(t) + \tilde{D}_{21}\tilde{v}(t)\end{aligned} \tag{3.43}$$

where

$$\begin{aligned}\tilde{A} &= A + \gamma^{-2} B_1 B_1^T X_\infty \\ \tilde{B}_1 &= B_1 \\ \tilde{B}_2 &= B_2 \\ \tilde{C}_1 &= (D_{12}{}^{T} D_{12})^{-1/2} B_2^T X_\infty \\ \tilde{C}_2 &= C_2 + \gamma^{-2} D_{21} B_1^T X_\infty \\ \tilde{D}_{12} &= (D_{12}{}^{T} D_{12})^{1/2} \\ \tilde{D}_{21} &= D_{21}\end{aligned} \tag{3.44}$$

Notice that in the state-feedback case the output $\tilde{z}$ can be made equal to zero by the controller (3.38).

**The $H_\infty$ optimal estimation problem**

Similar to $H_2$ control problem, the $H_\infty$-optimal control problem is transformed to an equivalent $H_\infty$-optimal estimation problem. Consider a stable causal state estimator $F$ of the output $z$ based on the measured output $y$ according to: $\hat{z}(s) = F(s)y(s)$. In the $H_\infty$ optimal estimation problem, we define the $H_\infty$-norm of the transfer function from the

disturbance *v* to the estimation error $z - \hat{z}$ [39],

$$J_\infty(F) = \sup\left\{\frac{\|z - \hat{z}\|_2}{\|v\|_2}\right\},\ v \neq 0 \tag{3.45}$$

and consider the existence of an estimator which achieves the bound:

$$J_\infty(F) < \gamma \ \text{ or } \ J'_\infty = \|z - \hat{z}\|_2^2 - \gamma^2 \|v\|_2^2 < 0 \tag{3.46}$$

The solution of the $H_\infty$-optimal estimation problem can be characterized as [39]:

$$\begin{aligned} \dot{\hat{x}}(t) &= A\hat{x}(t) + L_\infty\left[y(t) - C_2\hat{x}(t)\right] \\ \hat{z}(t) &= C_1\hat{x}(t) \end{aligned} \tag{3.47}$$

where

$$L_\infty = YC_2^T(D_{21}{}^T D_{21})^{-1} \tag{3.48}$$

And $Y$ is the unique symmetric positive definite solution to the *Algebraic Riccati equation* [39]:

$$A^T Y + YA - YC_2^T(D_{21}{}^T D_{21})^{-1}C_2 Y + \gamma^{-2} Y C_1 C_1^T Y + B_1 B_1^T = 0 \tag{3.49}$$

In contrast to the $H_2$-optimal estimator, the $H_\infty$-optimal estimator also depends on the output *z* which is estimated.

**The $H_\infty$ optimal controller**

Combining the optimal state-feedback problem (control law (3.38) applied into the transformed system (3.43) ) and the optimal state-estimation problem (3.47), then the $H_\infty$ optimal estimate of the output $\tilde{z}$ of the transformed system (3.43) ; $\hat{\tilde{z}}$ can be written as [39]:

$$\begin{aligned} \dot{\hat{x}}(t) &= \tilde{A}\hat{x}(t) + \tilde{B}_2 u(t) + L_Z\left[y(t) - \tilde{C}_2\hat{x}(t)\right] \\ u(t) &= K_\infty \hat{x}(t) \end{aligned} \tag{3.50}$$

where

$$L_Z = Z\tilde{C}_2^T(\tilde{D}_{21}{}^T \tilde{D}_{21})^{-1}, \tag{3.51}$$

$K_\infty$ is defined as (3.39), and $Z$ is the unique symmetric positive definite solution to the *Algebraic Riccati equation* [39]:

$$\tilde{A}^T Z + Z\tilde{A} - Z\tilde{C}_2^T (\tilde{D}_{21}{}^T \tilde{D}_{21})^{-1} \tilde{C}_2 Z + \gamma^{-2} Z\tilde{C}_1 \tilde{C}_1^T Z + \tilde{B}_1 \tilde{B}_1^T = 0 \qquad (3.52)$$

## 3.5 Step Response of D-STATCOM System

The state-space model of D-STATCOM system was presented in Chapter 2; equation (2.18). To verify the performance of the D-STATCOM with the new controllers, a step response is presented using the state-space model to test its characteristics and performance

using different parameters for each controller, and then the best parameters of the controllers will be used to simulate the real D-STATCOM system and show the results in Chapter 4. Step response and simulations will be executed using Simulink toolbox in MATLAB environment.

First, system parameters will be calculated and presented in Section 3.5.1, and then the step response and the results will be showed in Section 3.5.2.

### 3.5.1 System Parameters

Referring to state-space model of the D-STATCOM system of equation (2.18), the needed system parameters to be calculated and determined are:

$R_s$ supply resistance
$L_s$ supply inductance
$R_L$ Load resistance
$L_L$ Load inductance
$R_c$ filter resistance
$L_c$ filter inductance
$C$ shunt filter capacitor

Calculations and methodology of extracting all of such parameters are presented in this section.

#### 3.5.1.1 Source Parameters

The parameters of the source can be calculated from the data available in *Annex A*, as:

$R_s = 0.254\ \Omega,\ L_s = 0.808$ mH

### 3.5.1.2 Load/ Power Calculations

For different load conditions, the single-phase load data of the studied system can be summarized as indicated in Table 3.1 [40].

**Table 3.1: Summarized Single-phase Load Data of The Studied System [40]**

| Load Status | Current $I$ (A) | $V_{ph}$ (V) | *p.f* |
|---|---|---|---|
| **Rated** | 593 | 230 | 0.92 |
| **Max.** | 905 | | |
| **Min.** | 110 | | |

The following equations are used to extract load resistance $R_L$ and load inductance $L_L$ of the single-phase circuit for the rated, maximum and minimum load conditions of the studied system as listed in Table 3.2.

Active power $P\ (W) = 3|V_{ph}||I\ |\cos\phi$ (3.16)

where $V_{ph}$ is single-phase voltage (phase to neutral)
$\cos\phi$ is the system $p.f$.

apparent power $|S|\ (VA) = 3|V_{ph}||I\ |$ (3.17)

reactive power $Q\ (VAR) = 3|V_{ph}||I\ |\sin\phi$ (3.18)

load impedance per phase $Z_L(\Omega) = \dfrac{|V_{ph}|}{|I|}\ \underline{\phi}$ (3.19)

load resistance per phase $R_L(\Omega) = Re\{Z_L\}$ (3.20)

load inducyance per phase $L_L(H) = Im\{Z_L\}/2\pi f$ (3.21)

**Table 3.2: Results of Load/ Power Calculation For The Studied System**

| Load Status | Real Power P (KW) | Reactive Power Q (KVAR) | Apparent Power S (KVA) | load resistance per phase $R_L$ (Ω) | load inductance per phase $L_L$ (mH) |
|---|---|---|---|---|---|
| **Rated** | 376.44 | 160.36 | 410 | 0.357 | 0.484 |
| **Max.** | 574.50 | 243.53 | 625 | 0.234 | 0.317 |
| **Min.** | 69.83 | 29.60 | 76 | 1.92 | 2.608 |

### 3.5.1.3 Filter Parameters

As mentioned in Section 2.2, a filter is one of D-STATCOM parts that is useful to filter those harmonics in the current due to the switching ripple caused by the PWM technique, and this filter can be L-filter or LC-filter (Figure 2.8).

The experiments on D-STATCOM system were began with the simplest type; L-filter with relatively comparable values with the L-filter used by *Cai Rong* (2004) [17]. That is because the applied system in his thesis is an 400V system which is similar with the studied system in this thesis. The used L-filter parameters by *Rong*'s thesis were: $R = 0.0248\ \Omega,\ L = 2\ mH$. These values have been applied first for the D-STATCOM system, and the values are then tuned by trial and error to reach the best L-filter parameters for the D-STATCOM system according to the simulation results. Then a capacitor C was added in order to eliminate the remaining switching harmonics with simple tuning.

Hence, the resultant LC-filter parameters are: $R_c = 0.010\ \Omega,\ L_c = 2.5$ mH and $C = 60\mu F$.

### 3.5.1.4 Summery of System Parameters

Finally, the parameters of the D-STATCOM system which complete the D-STSTCOM system circuit of Figure 2.9, and hence, D-STSTCOM system state-space model of equation (2.18), can be summarized as shown in Table 3.3.

Thus, the simulation of D-STATCOM system will be implemented for the studied system with three load conditions; rated, maximum and minimum load to verify the D-STATCOM performance for the studied system during various load conditions.

**Table 3.3: D-STATCOM System Parameters**

| Parameter | value |
|---|---|
| $R_s$ | 0.254 Ω |
| $L_s$ | 0.808 mH |
| $R_L$ | 0.357, 0.234, 1.92 Ω |
| $L_L$ | 0.484, 0.317, 2.608 mH |
| $R_c$ | 0.010 Ω |
| $L_c$ | 2.5 mH |
| C | 60 $\mu$F |

The state-space models will be yield with the following state-space matrices.

**System 1; Rated Load:**

$$A = \begin{bmatrix} -31.43 & 0 & 0 & -1237.62 \\ 0 & -4 & 0 & -400 \\ 0 & 0 & -736.62 & 2057.6 \\ 16666.67 & 16666.67 & -16666.67 & 0 \end{bmatrix}, B = \begin{bmatrix} 1237.62 \\ 0 \\ 0 \\ 0 \end{bmatrix}$$

$$C = \begin{bmatrix} 0 & 0 & 0 & 1 \end{bmatrix}, D = [0] \tag{3.22}$$

**System 2; Max. Load:**

$$A = \begin{bmatrix} -31.43 & 0 & 0 & -1237.62 \\ 0 & -4 & 0 & -400 \\ 0 & 0 & -738.99 & 3144.7 \\ 16666.67 & 16666.67 & -16666.67 & 0 \end{bmatrix}, B = \begin{bmatrix} 1237.62 \\ 0 \\ 0 \\ 0 \end{bmatrix}$$

$$C = \begin{bmatrix} 0 & 0 & 0 & 1 \end{bmatrix}, D = [0] \tag{3.23}$$

**System 3; Min. Load:**

$$A = \begin{bmatrix} -31.43 & 0 & 0 & -1237.62 \\ 0 & -4 & 0 & -400 \\ 0 & 0 & -736.196 & 383.43 \\ 16666.67 & 16666.67 & -16666.67 & 0 \end{bmatrix}, B = \begin{bmatrix} 1237.62 \\ 0 \\ 0 \\ 0 \end{bmatrix} \quad (3.24)$$

$$C = \begin{bmatrix} 0 & 0 & 0 & 1 \end{bmatrix}, D = [0]$$

The difference between the systems is only in $A(3,3)$ and $A(3,4)$ elements, which contain the $R_L$ and $L_L$ components.

### 3.5.2 Step Response Results

The step response now is performed for the three load condition systems (3.22, 3.23 and 3.24), by applying PI, LQR, $H_2$ and $H_\infty$ controllers for each system. Closed-loop control for D-STATCOM is showed in Figure 3.6, where the "controller" block represents the PI, LQR, $H_2$ and $H_\infty$ controllers separately.

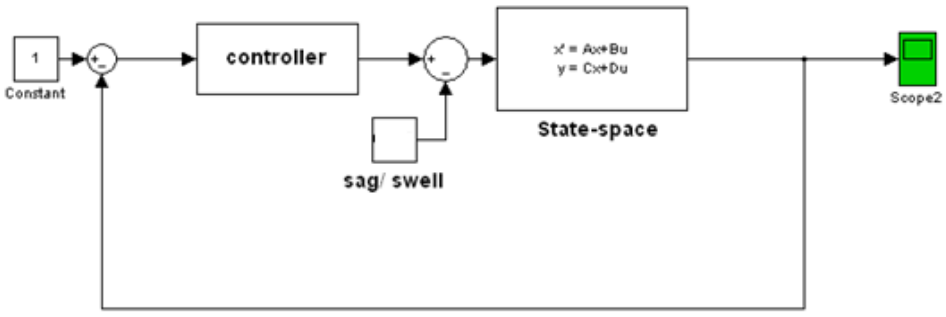


**Figure 3.6: Closed-loop control system for D-STATCOM**

The step response is tested during the following conditions:

- The input is 1.0 step value represent 1.0 pu voltage source to be tracked by the controller.

- The voltage sag will be represented by the added disturbance value of -0.225 to simulate a voltage sag of 22.5% decreasing below the 1.0 pu value.

- The voltage swell will be represented by the added disturbance value of 0.15 to simulate a voltage swell of 15.0% increasing above the 1.0 pu value.

- The settling time as one of the step response characteristics is considered as the time required for the step response to settle to within 5.0% of its final value.

The voltage sag condition of the value 22.5% is a situation of the system due to 3-phase to ground fault through $0.3\,\Omega$ resistance which result with faulted current > 900A. This faulted current value is closed to the rated current of the source transformer of the network which can't be exceeded. Thus a 22.5% voltage sag is adopted as a tested voltage sag condition representing the worst case sag condition for the studied network.

The voltage swell condition of the value 15.0% is a situation of the system due to connecting a 200 KVAR capacitive load as a test situation to produce the voltage swell. This 200 KVAR capacitive load is a very large value compared with the normal loads that can be connected and consumed within the studied network.

#### 3.5.2.1 Response of PI Controller

In order to reach the best parameters for PI controller, several experiments of PI parameters will be applied on System 1; Rated Load (system equation 3.22) as a reference system, and then the best parameters resulted is adopted for the other systems.

**Step Response For system 1 (Rated Load):**

The step response is tested initially using PI parameters: $K_i = 0.002, K_p = 50$, which resulted with the step response of Figures 3.7 and 3.8 for sag and swell compensations, respectively. The PI parameters were tuned by trial and error manner until reaching the best response showed in the Figures with $K_i = 0.2, K_p = 200$.

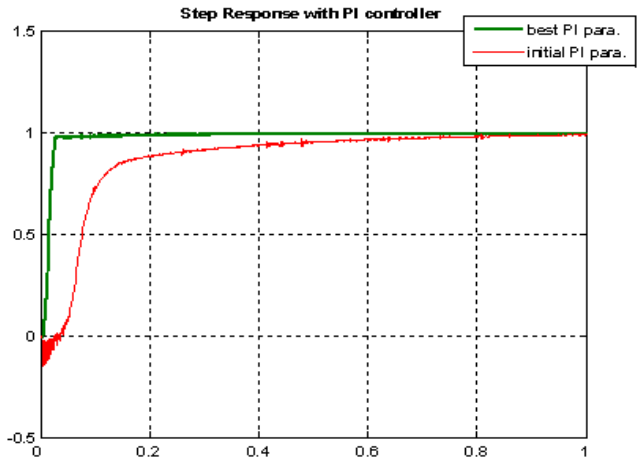


**Figure 3.7: System Step Response of PI controller during sag condition for system 1**

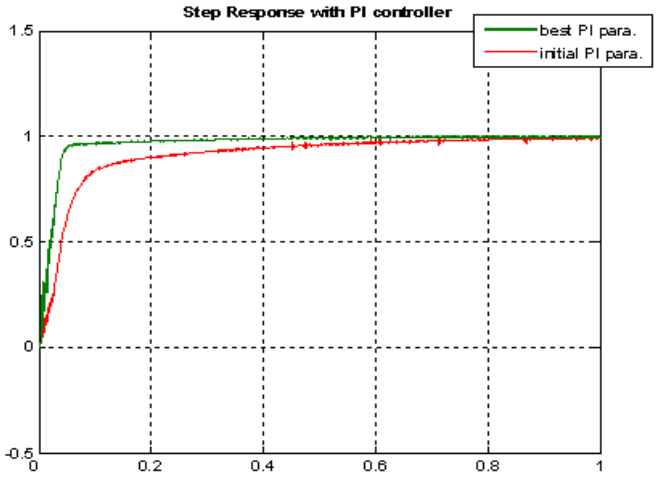


**(a)**

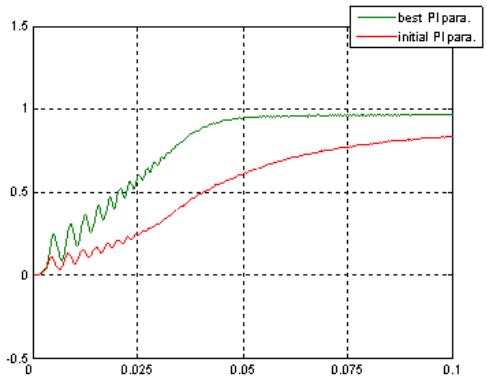


**(b)**

**Figure 3.8: (a) System Step Response of PI controller during swell condition for system 1**
**(b) An oscillation on step response- zoomed view**

It is clear that the PI parameters of $K_i = 0.2, K_p = 200$ had the best performance for sag compensation with no overshoot, no steady state error, and 0.5 sec settling time. Although thus parameters had an oscillation during swell compensation; Figure 3.8 (b), but it had faster response compared to other parameter response with 0.6 sec settling time, and the other had 1.2 sec settling time. Hence, these PI parameters will be used for simulations of systems 2 and 3.

**Step Response For system 2 (Max. Load) and system 3 (Min. Load):**

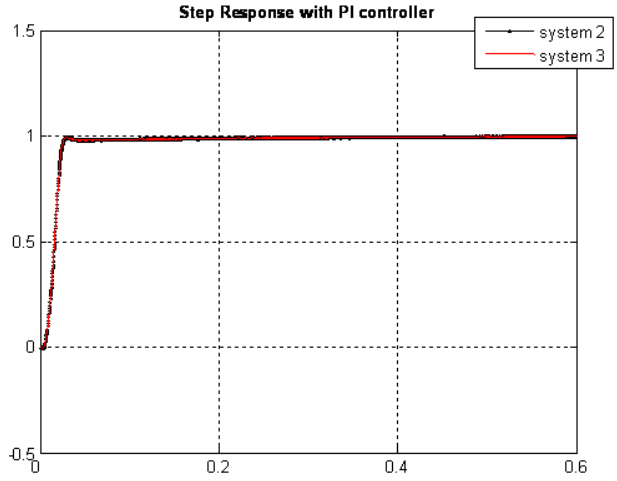


**Figure 3.9: System Step Response of PI controller during sag condition for systems 2,3.**

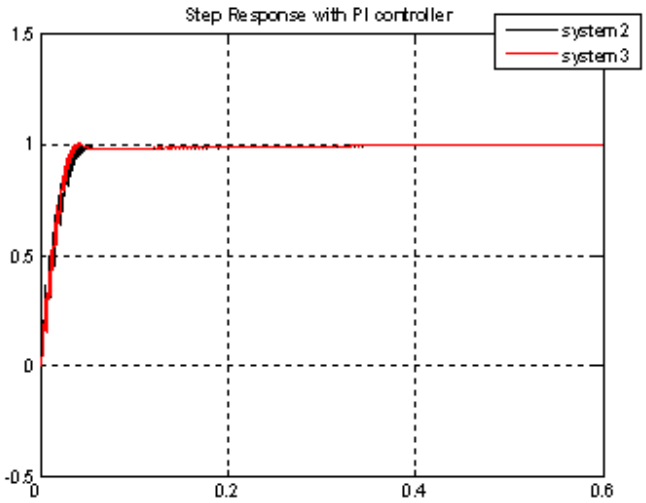


**Figure 3.10: System Step Response of PI controller during swell condition for systems 2,3.**

Figures 3.9 and 3.10 show the resultant response of the systems 2 and 3 (max. and min. load) for sag and swell compensations, respectively, by applying $K_i = 0.2, K_p = 200$ parameters. The two systems has same response (the two signals are over-riding each other) with 0.7 settling time during sag compensation 0.65 sec settling time and an oscillation during swell compensation.

#### 3.5.2.2 Response of PI/LQR Controller

The LQR controller is used to improve the PI controller response. The key features of LQR design is choosing the weighting matrices $Q$ and $R$. The LQR gain $K$ (equation (3.9)) is applied to the error of the system states. It is expected that applying the LQR control law (3.11) to the error of system states that processed by a PI controller will improve the performance of the controlling process. Thus, the controller is named as PI/LQR controller.

The selection of $Q$ and $R$ is weakly connected to the performance specifications, and a certain amount of trial and error is required with an interactive simulation before a satisfactory design results. For the D-STATCOM system $Q$ is $4 \times 4$ matrix and $R$ is $1 \times 1$ matrix, and since $Q$ and $R$ are symmetric, so there are 8 distinct elements in $Q$ and 1 element in $R$ for a total of 9 distinct elements need to be selected. Also, the matrix $Q$ and $R$ should satisfy the positive definitions. One practical method is to set $Q$ and $R$ to be diagonal matrix such that only five elements need to be decided.

The value of the elements in $Q$ and $R$ is related to its contribution to the cost function $J$ of equation (3.7). The two variables (states) that are most important to be controlled are the load current $i_L$, and the voltage at PCC; $v_c$, which are the third and fourth state variables of the state-space model (2.18). The weighting $Q$ matrix reflects the importance of those states, so it will be selected as a diagonal matrix with 0 elements except the diagonal elements.

**Design of PI/LQR Controller**

The PI controller with the adopted PI parameters; $K_i = 0.2, K_p = 200$, will be applied and followed by the LQR gain. The LQR for D-TATCOM system is designed for different values of $Q$ and $R$ using a MATLAB code indicated in *Annex B*. Several experiments of

$Q$ and $R$ parameters will be applied on System 1; Rated Load as a reference system, and then the best parameters resulted is adopted for the other systems. Only the corresponding elements of the resultant LQR gain $K$ for the two states $v_c$ and $i_L$ are used in the controller.

**Step Response For system 1 (Rated Load):**

First, the $Q$ matrix is selected as diag$\{Q\}$= [0, 0, 200, 10] and $R$ = [1] which used by *A. Shukla, A. Ghosh, and A. Joshi* (2007) [29]. The response showed that it is needed to pay more cost weight to $v_c$ as the most important state in order to satisfy the requirement. Thus the $Q$ and $R$ matrices were modified by trial and error manner until reaching the best response with diag$\{Q\}$= [0, 0, 2000, 100], $R$ = [100] and the resultant $K_{3,4}$ = [-0.746, 0.756] which are the LQR gain of $v_c$ and $i_L$ states.

The resultant response is showed in Figures 3.11 and 3.12 for sag and swell compensations, respectively. It is clear that the LQR parameters of diag$\{Q\}$ = [0, 0, 2000, 100], $R$ = [100], and resultant $K_{3,4}$ = [-0.746, 0.756] had the best performance for sag compensation with 12.0% overshoot, no steady state error, and 0.6 sec settling time. The main contribution of LQR controller is clearing the oscillation occurred during swell compensation occurred with alone PI controller (Figure 3.8 (b)). These parameters will be used for simulations of systems 2 and 3.

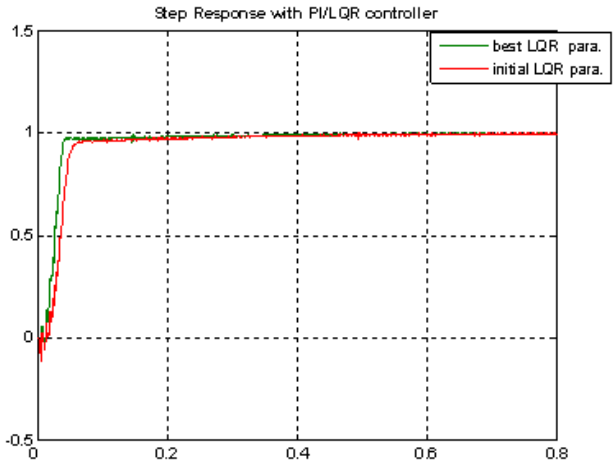


**Figure 3.11: System Step Response of PI/LQR controller during sag condition for system 1**

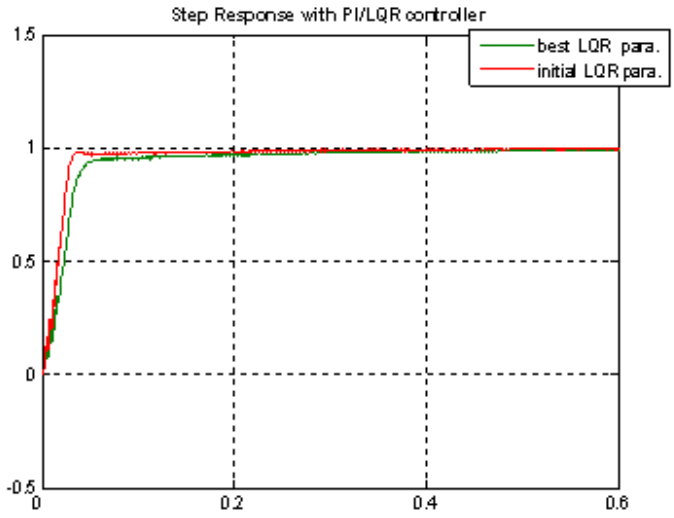


**Figure 3.12: System Step Response of PI/LQR controller during swell condition for system 1**

### Step Response For system 2 (Max. Load) and system 3 (Min. Load):

The resultant response for the two systems are showed in Figures 3.13 and 3.14 for sag and swell compensations, respectively, by applying diag$\{Q\}$ = [0, 0, 2000, 100] and $R$ = [100] parameters. The resultant $K_{3,4}$ gain are: [-0.846, 0.359] for system 2, and [-1.127, 0.958] for system 3.

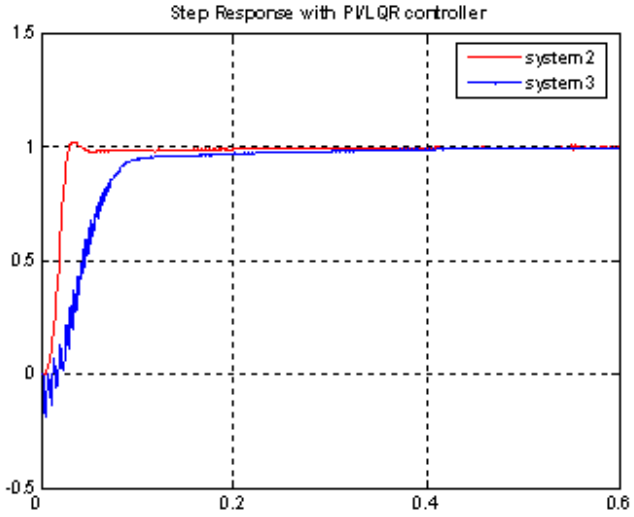


**Figure 3.13: System Step Response of PI/LQR controller during sag condition for systems 2,3.**

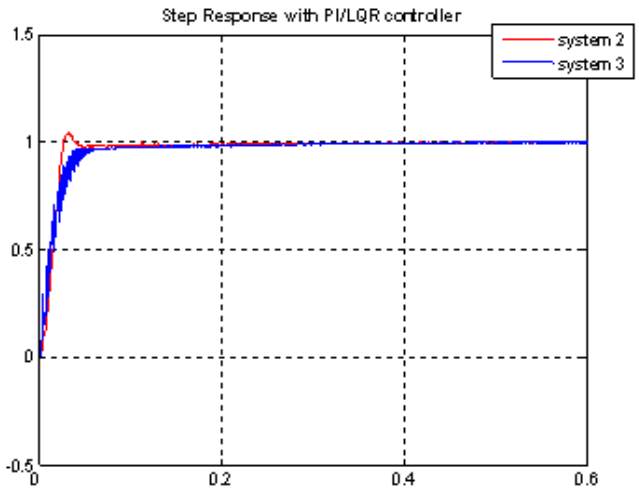


**Figure 3.14: System Step Response of PI/LQR controller during swell condition for systems 2,3**

As showed in the previous Figures, system 2 (max. load) has the better response for sag and swell compensations than system 3 (min. load). System 2 had 0.75 sec settling time, 7.3% overshoot for sag compensation, and 0.65 sec settling time, 7.3% overshoot for swell compensation, while system 3 had 1.05 sec settling time, 28.5% overshoot for sag compensation, 0.96 settling time, and no overshoot for swell compensation.

#### 3.5.2.3 Response of $H_2$ Controller

**Design of $H_2$ Controller**

Designing the $H_2$ controller in MATLAB environment requires a set of models that have different values parameters to be added to the original system, and then to be augmented in order to provide good performance of $H_2$ controller for the system with greater robustness. In the proposed control strategy of D-TATCOM system, the number of models is three, and the $H_2$ performance will be tested for several models to reach the best performance.

The models that will be chosen and added to the original system will be represented by its transfer functions as weighting functions; $W_1$, $W_2$ and $W_3$.These weighting functions are used to design the $H_2$ controller using a MATLAB code indicated in *Annex B*.

Several experiments of $W_1$, $W_2$ and $W_3$ parameters will be applied on System 1; Rated Load as a reference system, and then the best parameters resulted is adopted for the other systems.

**Step Response For system 1 (Rated Load):**

A very useful choice of the weighting functions for $H_2$ controller is [41]:

$$W_1 = \frac{0.03s^2 + 0.05s}{0.5s^2 + 1.5s + 10}$$
$$W_2 = \frac{0.5s + 1}{10s + 1}$$
$$W_3 = 0.1$$

which was applied and tested for D-STATCOM system, and resulted with the step response showed in Figure 3.15 for sag and swell compensations. It had weak response; 40% overshoot and 3.0 sec settling time.

The three weighting functions; $W_1$, $W_2$ and $W_3$ were modified by trial and error manner until reaching the best response of $H_2$ controller showed in the Figure 3.15 with:

$$W_1' = \frac{0.03s^2 + 0.05s}{0.05s^2 + 15s + 10}$$
$$W_2' = \frac{5s + 10}{10s + 10}$$
$$W_3' = 1$$

which had 0.025 sec settling time and no overshoot. These best weighting functions will be the case for step response of systems 2 and 3.

**Step Response For system 2 (Max. Load) and system 3 (Min. Load):**

The result response for the two systems is showed in Figures 3.16 for sag and swell compensations, respectively, by applying the values of weighting functions as:

$$W_1' = \frac{0.03s^2 + 0.05s}{0.05s^2 + 15s + 10}$$
$$W_2' = \frac{5s + 10}{10s + 10}$$
$$W_3' = 1$$

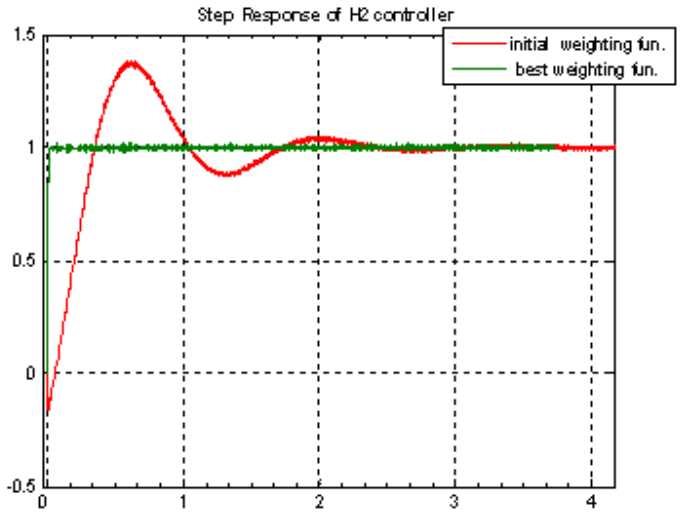


**Figure 3.15: System Step Response of $H_2$ controller during sag and swell conditions for system 1**

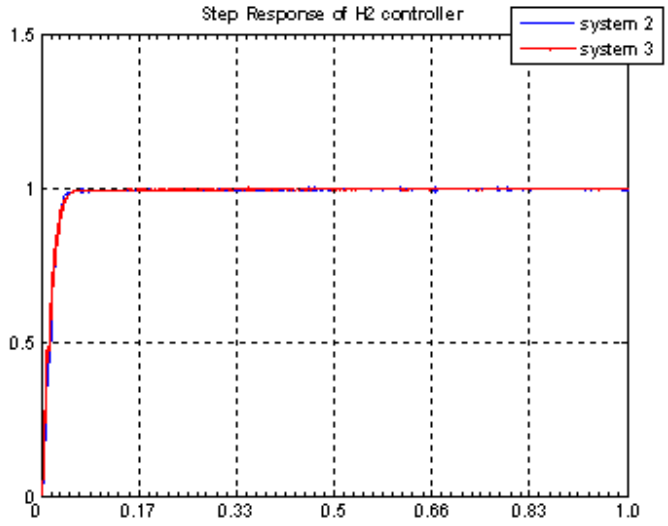


**Figure 3.16: System Step Response of $H_2$ controller during sag and swell conditions for systems 2,3**

As shown in Figure 3.16, systems 2 and 3 had the same response for sag and swell compensations (the two signals are over-riding each other) with 0.03 sec settling time and no overshoot.

#### 3.5.2.4 Response of $H_\infty$ Controller

**Design of $H_\infty$ Controller**

Similar to $H_2$ controller, a set of models that have different values parameters is added to the original system to be augmented to provide good performance of $H_\infty$ controller in order to guarantee the system robustness. The models that will be added are three also, and the $H_\infty$ performance will be tested for several models to reach the best performance.

The weighting functions (models); $W_1$, $W_2$ and $W_3$ are used to design the $H_\infty$ controller using a MATLAB code indicated in *Annex B***.** Several experiments of $W_1$, $W_2$ and $W_3$ parameters will be applied on System 1; Rated Load as a reference system, and then the best parameters resulted is adopted for the other systems.

**Step Response For system 1 (Rated Load):**

A very useful choice of the weighting functions for $H_\infty$ controller is [41]:

$$W_1 = \frac{0.3s^2 + 0.5s}{0.05s^2 + 15s}$$
$$W_2 = \frac{0.5s + 1}{10s + 1}$$
$$W_3 = 0.01$$

which was applied and tested for D-STATCOM system, and resulted with the step response showed in Figure 3.18 for sag and swell compensations. It had weak response; 14% overshoot, 1.0 sec settling time and 3.0% steady-state error.

The three weighting functions; $W_1$, $W_2$ and $W_3$ were modified by trial and error manner until reaching the best response of $H_\infty$ controller showed in the Figure 3.17 with:

$$W_1' = \frac{0.03s^2 + 0.05s}{0.05s^2 + 15s}$$
$$W_2' = \frac{5s + 10}{10s + 10}$$
$$W_3' = 1$$

which had 0.02 sec settling time and no overshoot. These best weighting functions will be the case for step response of systems 2 and 3.

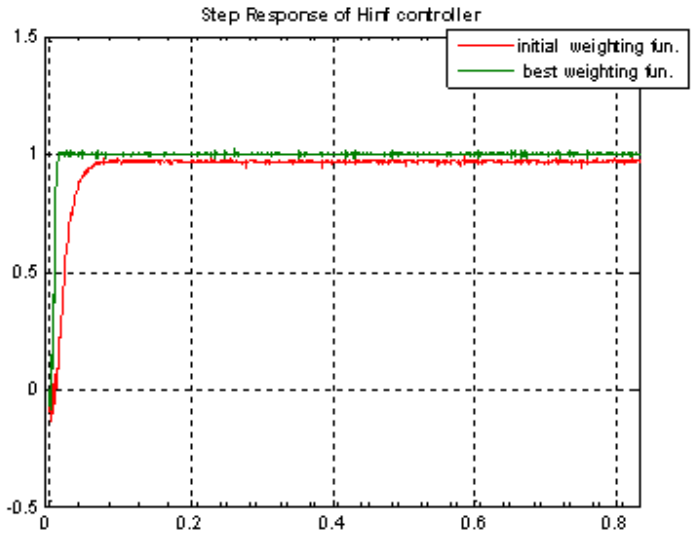


**Figure 3.17: System Step Response of $H_\infty$ controller during sag and swell conditions for system 1.**

**Step Response For system 2 (Max. Load) and system 3 (Min. Load):**

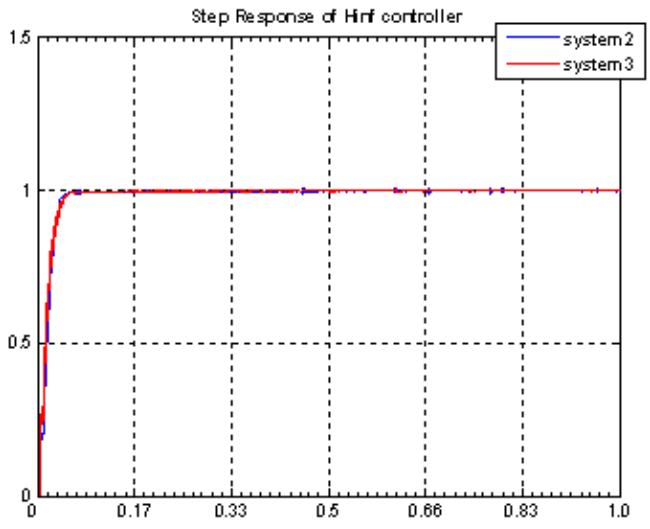


**Figure 3.18: System Step Response of $H_\infty$ controller during sag and swell conditions for systems 2,3**

The resultant response for the two systems is showed by applying the values of weighting functions as:

$$W_1' = \frac{0.03s^2 + 0.05s}{0.05s^2 + 15s}$$
$$W_2' = \frac{5s + 10}{10s + 10}$$
$$W_3' = 1$$

As shown in Figure 3.18 for sag and swell compensations, respectively, systems 2 and 3 has same response for sag and swell compensations (the two signals are over-riding each other) with 0.02 sec settling time, and no overshoot.

#### 3.5.2.5 Summery of Results

The step response results for all cases can be summarized as shown in Tables 3.4 and 3.5 for sag and swell compensations, respectively, using the best parameters of different controllers adopted as:

- **PI gains:** $K_i = 0.2,\ K_p = 200$
- **LQR matrices :** $\text{diag}\{Q\}$ = [0, 0, 2000, 100] , $R$ = [100] and resultant $K_{3,4}$ = [-0.4493, 0.5572]
- $H_2$ **weighting functions:**

$$W_1 = \frac{0.03s^2 + 0.05s}{0.05s^2 + 15s + 10}$$
$$W_2 = \frac{5s + 10}{10s + 10}$$
$$W_3 = 1$$

- $H_\infty$ **weighting functions:**

$$W_1 = \frac{0.03s^2 + 0.05s}{0.05s^2 + 15s}$$
$$W_2 = \frac{5s + 10}{10s + 10}$$
$$W_3 = 1$$

**Table 3.4: Step Response Results For Sag Compensation**

| Performance | Controllers | | | | | | | | | | | |
|---|---|---|---|---|---|---|---|---|---|---|---|---|
| | PI | | | PI /LQR | | | $H_2$ | | | $H_\infty$ | | |
| | Rated Load | Max. Load | Min. Load | Rated Load | Max. Load | Min. Load | Rated Load | Max. Load | Min. Load | Rated Load | Max. Load | Min. Load |
| **Max. Overshoot (%)** | **0.0** | **0.0** | **0.0** | **1.0** | **7.3** | **28.5** | **0.0** | **0.0** | **0.0** | **0.0** | **0.0** | **0.0** |
| **Settling Time (sec)** | **0.50** | **0.70** | **0.70** | **0.6** | **0.75** | **1.05** | **0.025** | **0.03** | **0.03** | **0.02** | **0.02** | **0.02** |
| **S.S error (%)** | No S.S. error | | | | | | | | | | | |

**Table 3.5: Step Response Results For Swell Compensation**

| Performance | Controllers | | | | | | | | | | | |
|---|---|---|---|---|---|---|---|---|---|---|---|---|
| | PI | | | PI /LQR | | | $H_2$ | | | $H_\infty$ | | |
| | Rated Load | Max. Load | Min. Load | Rated Load | Max. Load | Min. Load | Rated Load | Max. Load | Min. Load | Rated Load | Max. Load | Min. Load |
| **Max. Overshoot (%)** | **0.0** | **0.0** | **0.0** | **1.0** | **7.3** | **0.0** | **0.0** | **0.0** | **0.0** | **0.0** | **0.0** | **0.0** |
| **Settling Time (sec)** | **0.5** | **0.65** | **0.65** | **0.7** | **0.65** | **0.96** | **0.025** | **0.03** | **0.03** | **0.02** | **0.02** | **0.02** |
| **S.S error (%)** | No S.S. error | | | | | | | | | | | |

## 3.6 Conclusion

In general, the four controllers PI, PI/LQR, $H_2$ and $H_\infty$ controllers applied to D-STATCOM system have good performance for sag and swell compensations tasks. That is a result of the response for various load conditions covered overall system situations; rated, maximum and minimum load, with relatively small deviations between the

performances of the three system conditions. The typical results of each controller for sag and swell compensations ensure that the proposed optimal based control strategy will do well with various power quality problems.

Although the PI/LQR controller has some transient overshoot, it has an advantage of clearing the oscillation occurred in swell compensation performance of PI controller. The performance of PI/LQR controller differ for the three system conditions, but it has good performance for the three systems, which will be ensured by the real simulation in Chapter 4.

Its clear that the $H_2$ and $H_\infty$ controllers has better response compared with the others, and the $H_\infty$ controller is the best one for both sag and swell compensations. It is important to conclude that the good and careful selection of the weighting functions for $H_2$ and $H_\infty$ controllers is the optimality key for those controllers, such that hasty or wrong selecting of these weighting functions may result with weak performance as shown in Figures 3.15 and 3.18. Good selection of weighting functions is related to the system dynamics and expected disturbances, and also related to the experience of the controlling process.

# 4 CHAPTER 4: SIMULATION OF D-STATCOM SYSTEM USING THE OPTIMAL BASED CONTROL STRATEGY

The proposed control strategy based on optimal control methods for D-STATCOM have been explained in Chapter 3, and its algorithm presented in Section 3.3. Simulation of D-STATCOM system with the proposed control strategy is presented in this chapter to show the behavior of the designed controllers and results control process. The simulation will be tested for sag and swell compensation, and for harmonic distortion mitigation as the main power quality problems to be solved by the proposed control strategy. The simulation will be tested for various forms of sag conditions; single-phase, double–phase and three–phase faults, and during various load conditions.

Simulink model have been built for D-STATCOM system using "SimPowerSystems" toolbox in MATLAB environment to represent the real power system with real D-STATCOM device. MATLAB environment provide rich and useful tools for all needed power elements, conditions and measurements to simulate the real situations.

The simulation will be first performed for the studied system at rated load under sag and swell conditions without any control to show the effect of the sag/ swell situations. Then the simulation will be implemented for the D-STATCOM system under same problems with applying the proposed control strategy using PI, PI/LQR, $H_2$ and $H_\infty$ controllers, with the adopted parameters for each controller summarized in Section 3.5.2.5. Finally, comparisons and discussion will be presented to illustrate the advantages and benefits of the proposed control strategy.

## 4.1 Simulation model

The simulated model of the studied system (Al-Zaitoon Neighborhood-Gaza low voltage network) is shown in Figure 1.9. The model of D-STATCOM connected to the system with its control is shown in Figures 4.1 and 4.2. All system parameters have been listed in Table 3.3.

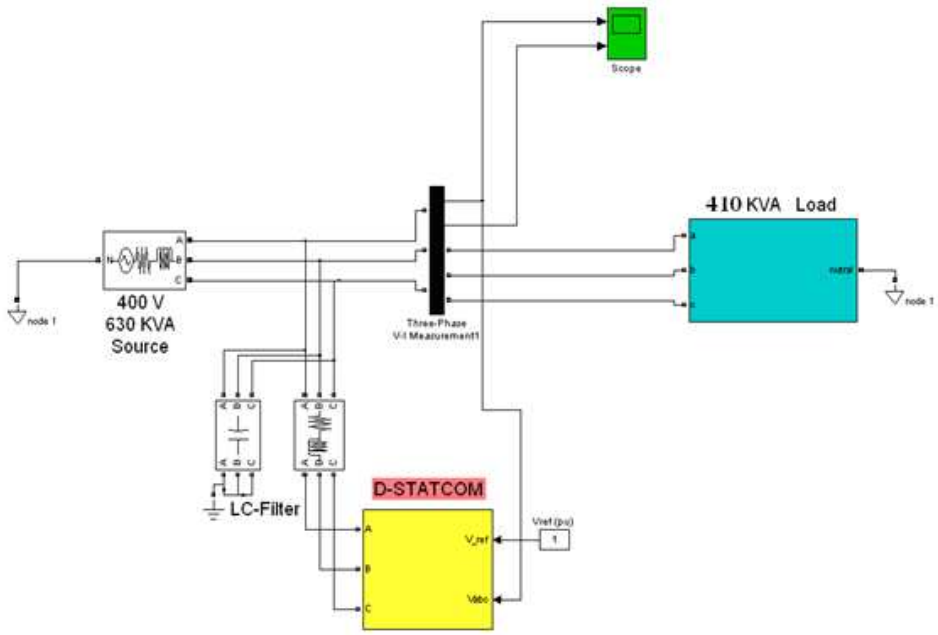


**Figure 4.1: Simulated model of D-STATCOM system (rated load)**

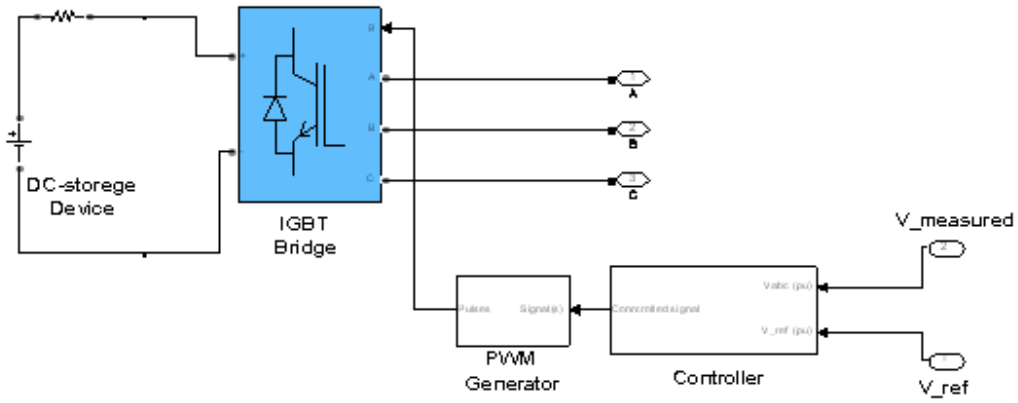


**Figure 4.2: D-STATCOM device and its control**

The simulation will be executed for time duration of 1.0 sec with applied voltage sag of 22.5% for the time duration of 0.2-0.4 sec, and 15.0% voltage swell for the time duration of 0.6-0.8 sec. The simulation results of the studied system without control is presented in Figure 4.3 that show the effect of sag and swell situations.

As mentioned in Section 3.5.2, the voltage sag condition is made by 3-phase to ground fault with faulted current < 900 A which closed to the maximum source current, and the voltage swell condition is made by connecting a 200 KVAR capacitive load, which is very high value compared with the normal loads that can be connected and consumed within the studied network. These 3-phase fault and capacitive load conditions are applied at the point nearest to the source, therefore, these conditions are considered as the worst case sag/ swell conditions that can be occurred on the studied system.

For comparison purposes, the performance factors for the controller of D-STATCOM device are:

- sag/ swell %
- THD
- *p.f*
- Max. overshoot

The simulation results of the studied system under sag/ swell conditions without D-STATCOM control is showed in Figure 4.3.

The simulation show the voltage magnitude variations during sag/ swell situations, and the resultant $V_d$ and $V_q$ response. The resultant Total harmonic distortion (THD) of the voltage signal is computed as 8.83% which exceed the IEEE standard (Table 1.2). THD is computed using Fast Fourier Transform (FFT) tool of MATLAB for up to 60th harmonic order, which yield with Figure 4.4.

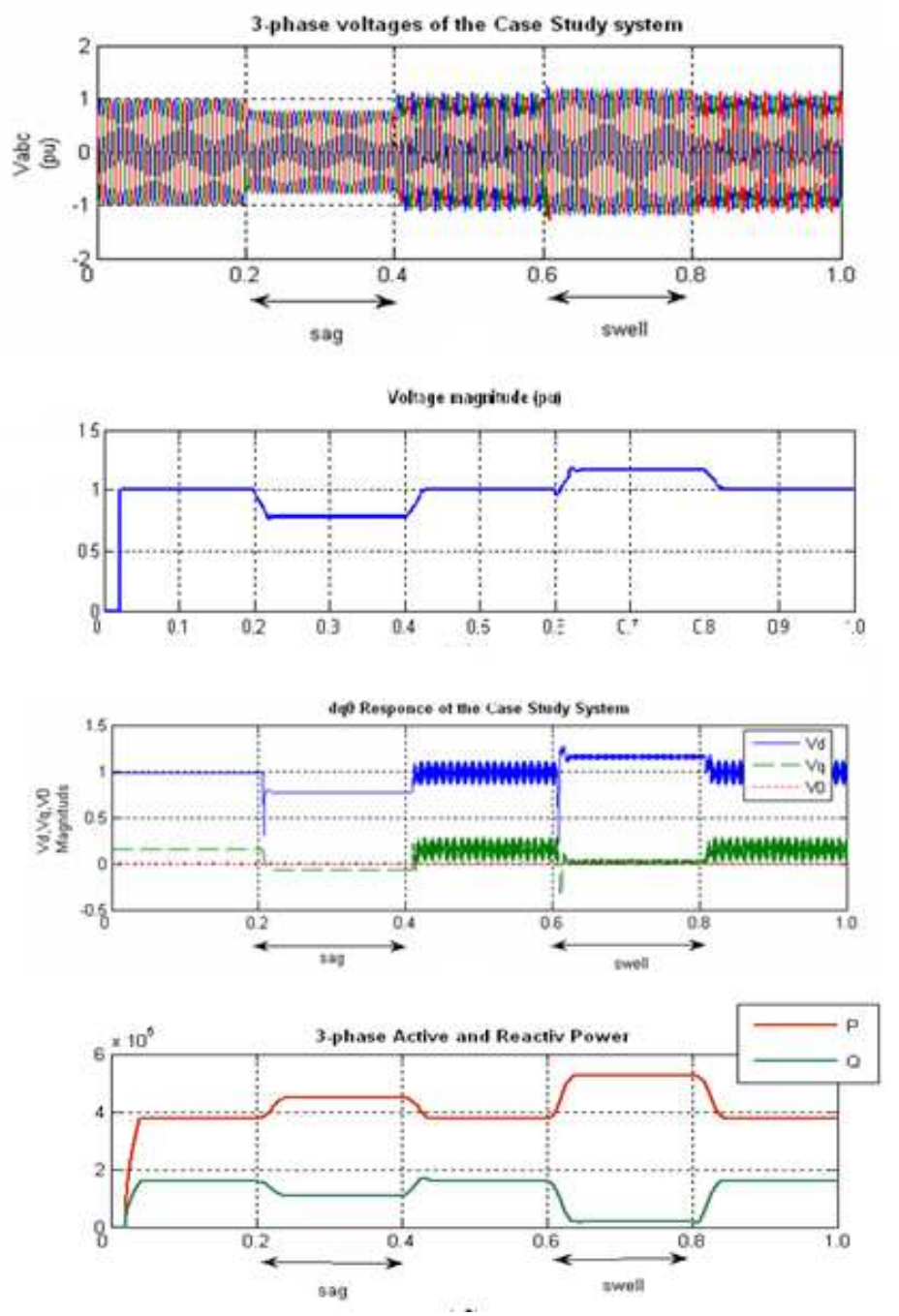


**Figure 4.3: Simulation of the studied system during sag and swell situations without control**

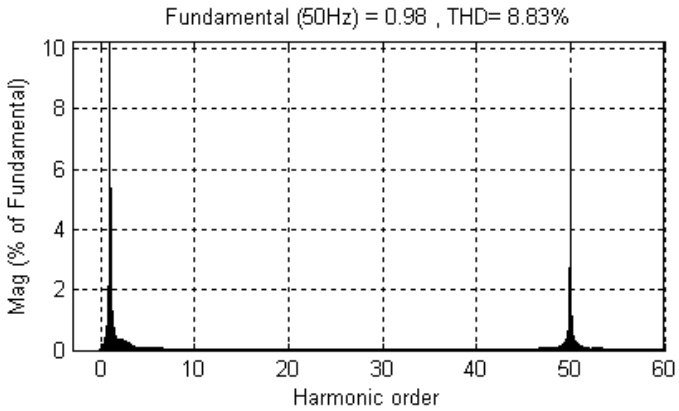


**Figure 4.4: Harmonics of the studied system during sag and swell situations without control**

**Table 4.1: Results of System Simulation without Control**

| Key Factors | value |
|---|---|
| Voltage during Sag (pu) | 0.775 |
| Voltage during Swell (pu) | 1.156 |
| THD (%) | 8.83 |
| *p.f* | 0.92 |

## 4.2 Simulation of PI Controller

The proposed control strategy depends on constant DC link voltage (Section 3.2.3). Size of the DC storage device is a quantity related to the applied system and the size of the sag voltage to be compensated. Experimenting the different sizes of DC storage device for the studied system under the sag/ swell compensation was made and simulated. The experiments yield a 700V DC storage device as the best choice for the studied system.

In general, using more size DC storage device is useful to recover more sag size but may result with unmitigated harmonic distortion, and using less size DC storage device, such that 600V and 650V DC storage device doesn't recover the desired sag size. Hence, careful

selection of the suitable DC storage device is an important role for success D-STATCOM control process.

Performing PI control for D-STATCOM system for different conditions yields the following results and figures.

### 4.2.1 System 1; Rated Load

Figure 4.5 shows the effect of controlling *d* and *q* components of the voltage signal. $V_d$ is fixed at 1.0 pu value and $V_q$ is fixed at 0.0 pu value which is the desired behavior, and that reflects the effectiveness of the proposed control strategy. The controlling (compensation) process can be understood according to

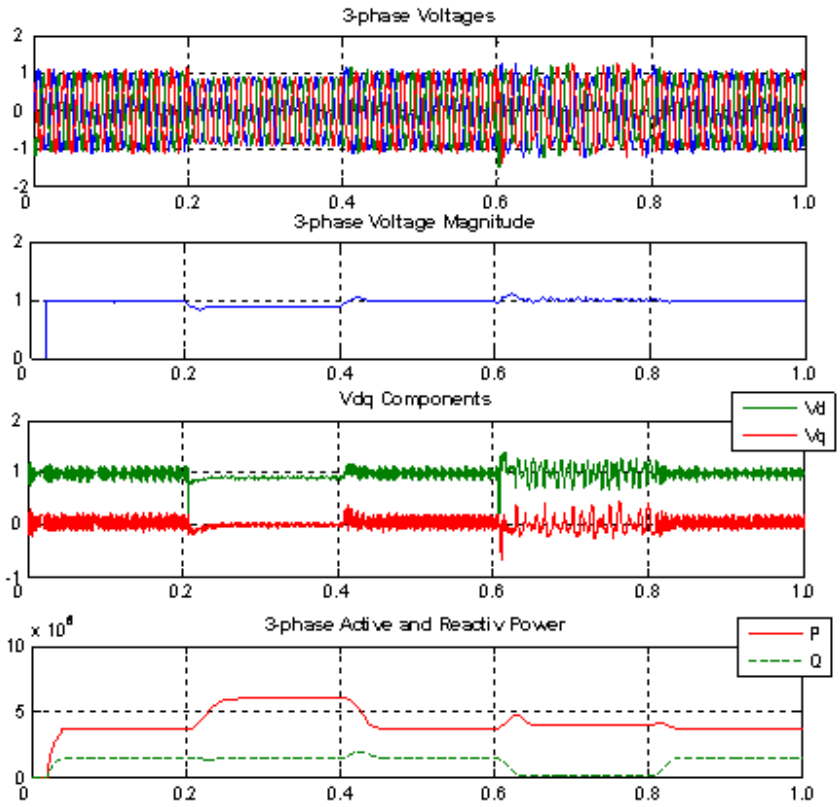


**Figure 4.5: Simulation results of D-STATCOM, PI control for system 1**

the compensation currents wave form in Figure 4.6, such that the compensation currents are injected dynamically to the main system according to the compensation process. As a result, the voltage sag was compensated to 0.9 pu value (10% sag), and the THD was

mitigated to 3.87%; Figure 4.7, and although theses values meet the IEEE standards, but it still need to be more mitigated. To attenuate harmonics, generally, harmonic filters are placed at the point of the load as mentioned in Section 1.2.2. Harmonic filter is a combination of RLC circuit elements that tuned to eliminate the most harmonic orders causes distortion on the signal.

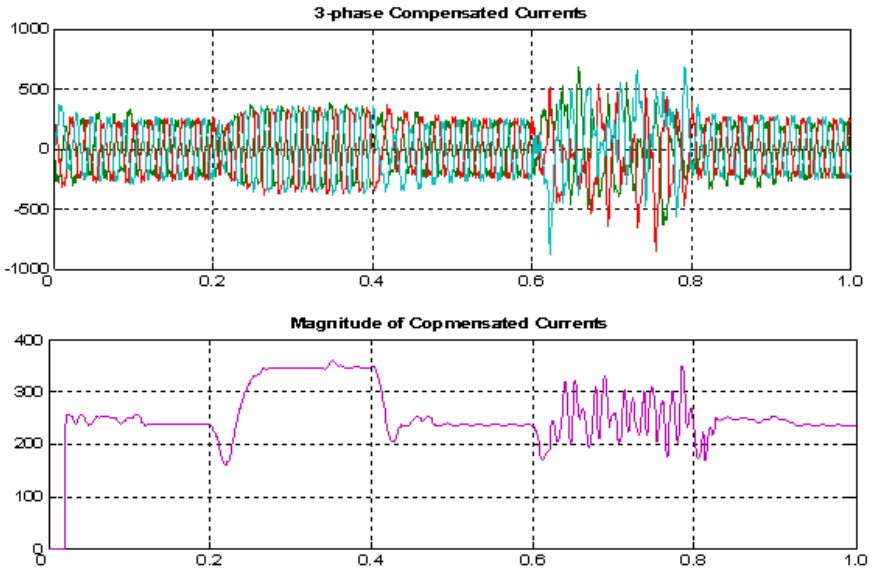


**Figure 4.6: Compensated currents with PI controller, system 1**

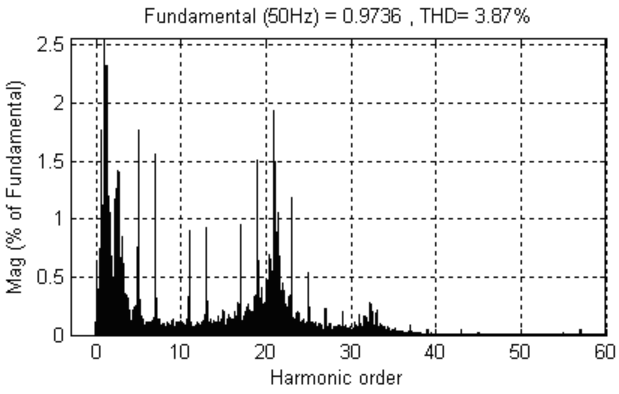


**Figure 4.7: Harmonics of PI control without harmonic filters**

Harmonic filters is added to the D-STATCOM system as shown in Figure 4.8, and it has been tuned to eliminate 5th, 7th and 11th harmonic orders, which is the best harmonic

tuning trials. The results now is mitigated to 0.93 pu voltage value during sag (only 7.0% sag) and 1.05% THD; Figure 4.9. Comparing the THD in Figures 4.7 and 4.9 shows the useful effect of harmonic filters that well eliminate unwanted harmonics.

In order to recover more sag level, the use of 750V and 800V DC was tested, but it result with unmitigated harmonic distortion, therefore, a 700V DC storage device is the best choice for D-STATCOM with PI controller, with acceptable resultant compensated sag level (7.0% sag).

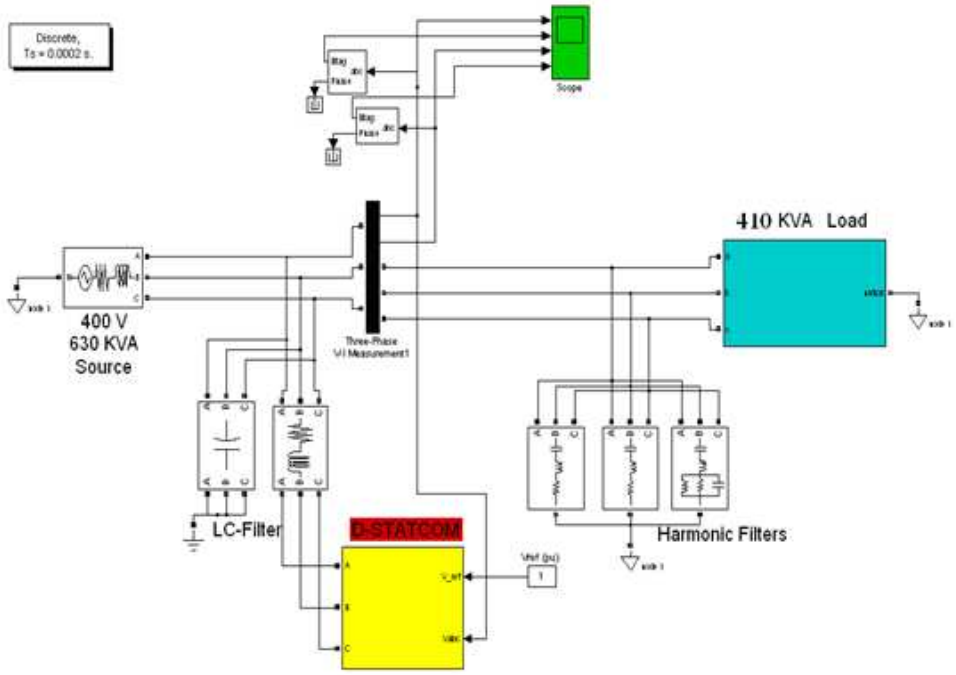


**Figure 4.8: Simulated model of D-STATCOM system with added Harmonic filters**

The swell problem was compensated to 1.0 pu voltage value but with clear oscillation, which is equivalent to the oscillation of the step response of Figure 3.8. Therefore, it is expected that the PI/LQR controller will mitigate thus oscillation.

The resultant power factor *p.f* after control process can be determined easily using the active and reactive power values (Figure 4.5), and it was obtained as 0.975 which is perfect result of power factor mitigation using this proposed control strategy for D-STATCOM. Small overshoot can be observed for small time duration during start and end of sag

compensation with 3% and 10%, respectively, and these overshoot values doesn't exceed the IEEE limits.

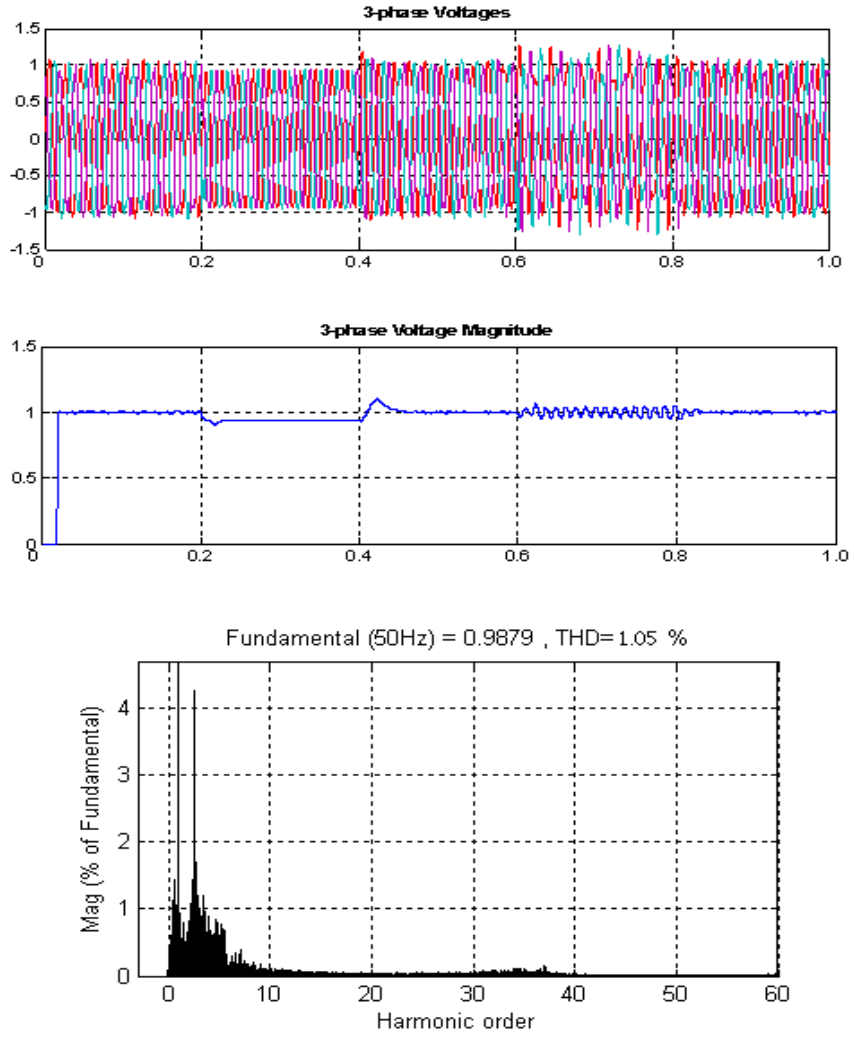


**Figure 4.9: Simulation results of D-STATCOM, PI control with added Harmonic Filters, system 1**

As mentioned previously, the above simulation is tested according to three–phase to ground fault which is the worst case faults on power systems. Single and double–phase to ground faults are more frequently power problems. It will be tested also, and the results is presented in Figures 4.10 and 4.11 for single-phase and double–phase faults, respectively, to show the effect of the D-STATCOM control to face these problems.

Single-phase fault has relatively no effect on the power system with presence of the D-STATCOM with easy fully recovery the sag occurred. Double–phase fault was successfully recovered by the D-STATCOM from 12.0% to 0.0% sag, but with swelling occurred on the unfaulted phase (phase c) but within the IEEE limits, which indicated by the zoomed view-Figure 4.11 (b), The compensated currents is clearly injected as the need of compensation process for the proper phase as shown in Figures 4.10 and 4.11.

Therefore, the results of PI control for rated load system can be summarized as shown in Table 4.2 for the case of three–phase fault for comparison purposes.

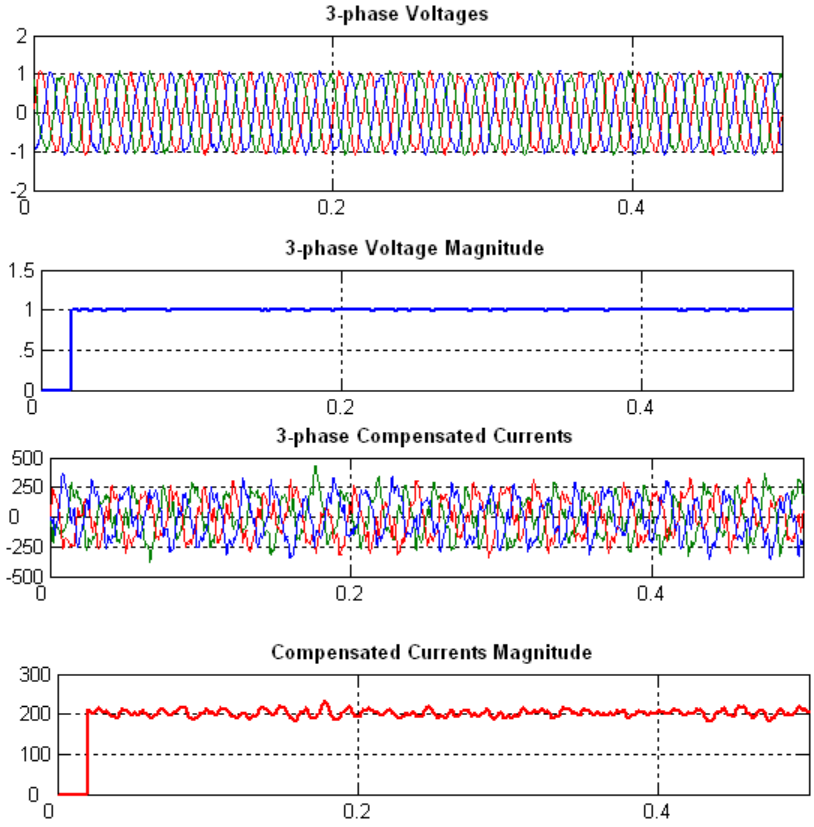


**Figure 4.10: D-STATCOM control with PI controller for single-phase to ground fault (phase a)**

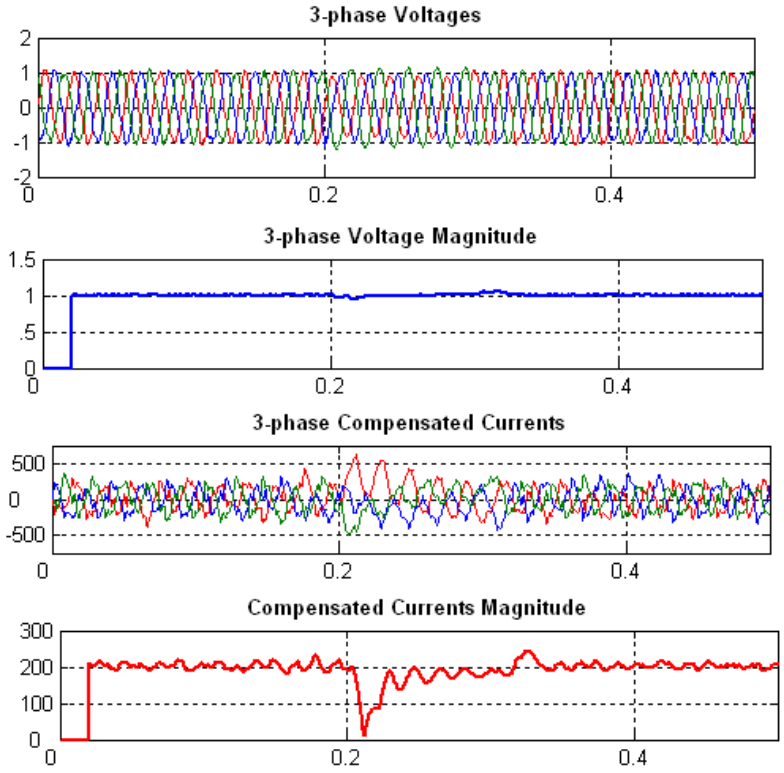


**(a)**

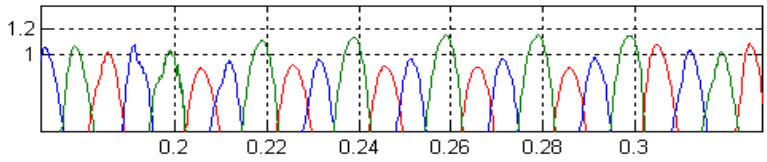


**(b)**

**Figure 4.11: D-STATCOM control with PI controller for double-phase to ground fault (phases a and b). (a) Full view. (b) Zoomed view for swelled phase (phase c) during sag**

Table 4.2: Results of System Simulation with PI control, System 1

| Key Factors | value |
|---|---|
| Voltage during Sag (pu) | 0.93 |
| Voltage during Swell (pu) | 1.0 |
| THD (%) | 1.05 |
| *p.f* | 0.975 |

### 4.2.2 System 2; Max. Load

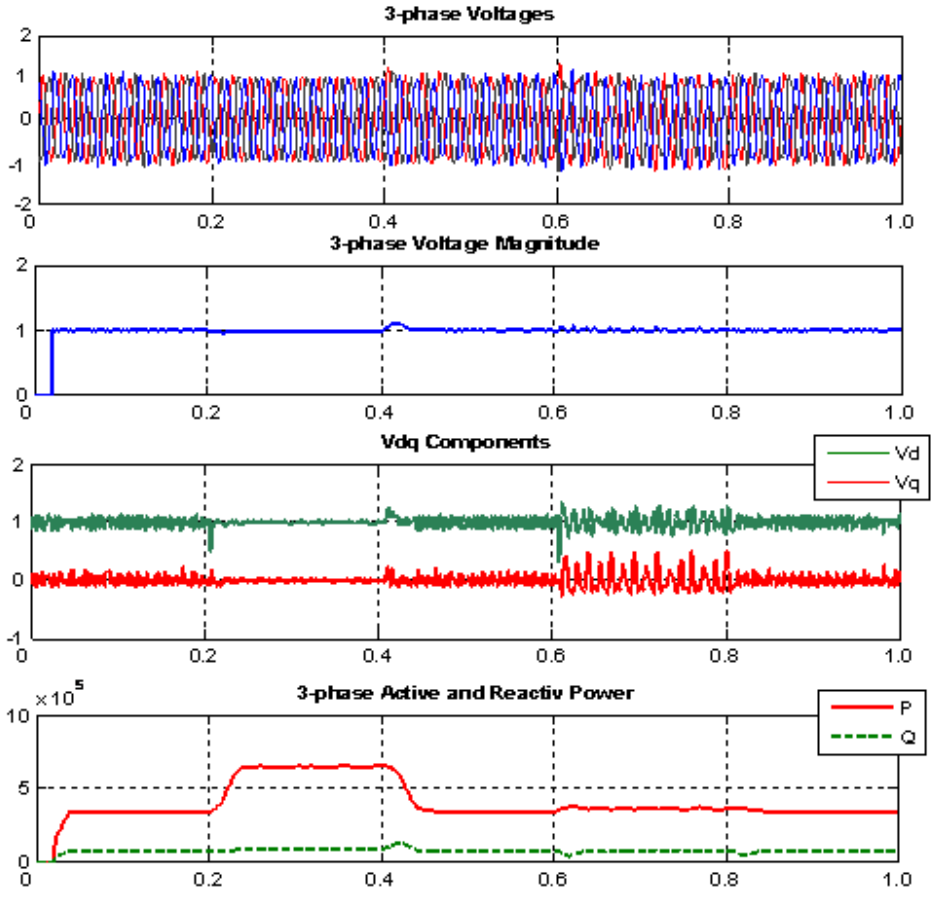


Figure 4.12: Simulation results of D-STATCOM, PI control for system 2

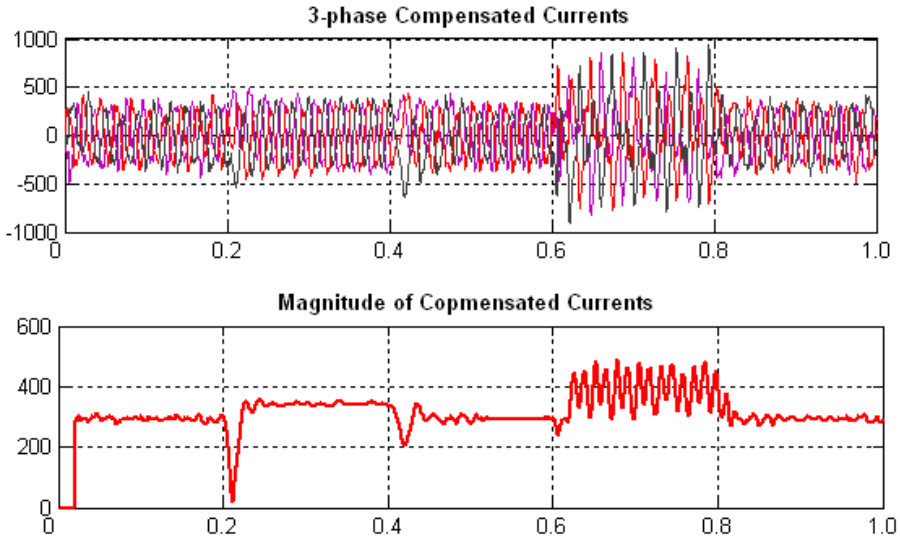


**Figure 4.13: Compensated currents with PI controller, system 2**

The voltage sag was compensated to 0.966 pu value (only 3.4% sag), and the THD was mitigated to 1.15%. The different compensated currents between the cases of system 1 and system 2; Figures 4.7 and 4.13 respectively, show the dynamically behavior of the D-STATCOM control to face different problems with different sizes. *p.f* was mitigated again to 0.978 value. Small overshoot can be observed for small time duration during start and end of sag compensation with 5% and 10%, respectively.

**Table 4.3: Results of System Simulation with PI control, System 2**

| Key Factors | value |
|---|---|
| Voltage during Sag (pu) | 0.966 |
| Voltage during Swell (pu) | 1.0 |
| THD (%) | 1.15 |
| *p.f* | 0.978 |

### 4.2.3 System 3; Min. Load

As shown in Figure 4.14, the voltage sag was completely compensated to 1.0 pu value, but the swell was not compensated with resultant 11.38% swell. This is swell result is an expected result due to the large reactive power injected to the system with low power consumption by the load. Applying more reality capacitive load condition; 100 KVA, yield the results of Figure 4.15; 1.0 pu voltage during sag and 1.015 during swell. *p.f* was mitigated to 0.90 value which is within the acceptable limit. Small overshoot can be observed also for small time duration during start of sag and start of swell compensation with 8.0% and 8.0%, respectively. THD was mitigated to 3.15% value.

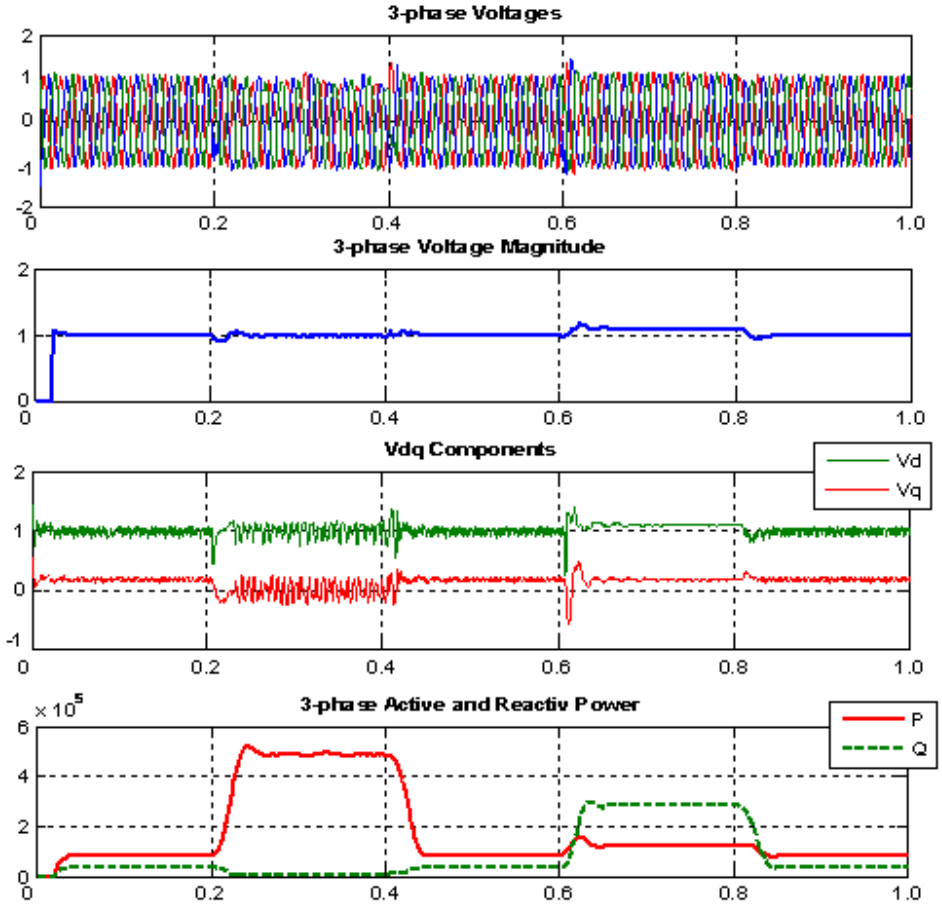


**Figure 4.14: Simulation results of D-STATCOM, PI control for system 3, (200KVAR capacitive load)**

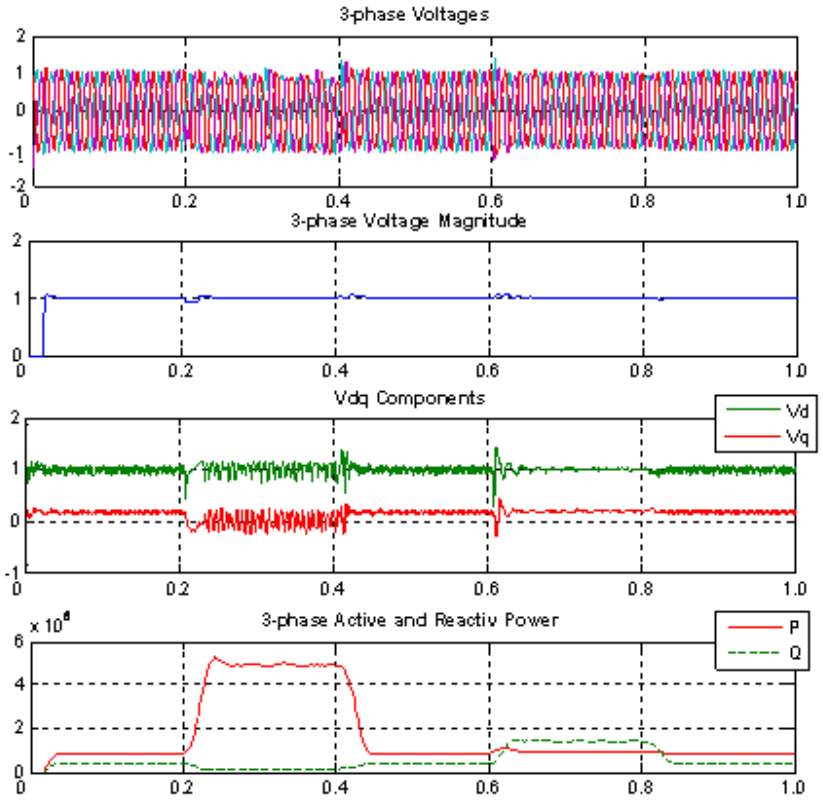


**Figure 4.15: Simulation results of D-STATCOM, PI control for system 3, (100KVAR capacitive load)**

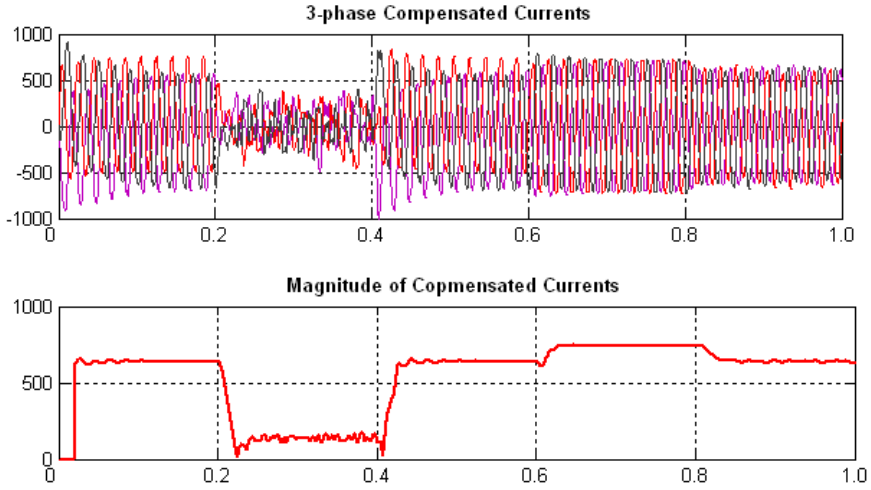


**Figure 4.16: Compensated currents, PI controller, system 3**

**Table 4.4: Results of System Simulation with PI control, System 3**

| Key Factors | value |
|---|---|
| Voltage during Sag (pu) | 1.0 |
| Voltage during Swell (pu) | 1.015 |
| THD (%) | 3.15 |
| *p.f* | 0.90 |

## 4.3 Simulation of PI/LQR Controller

As mentioned previously, the most important two variables (states) of the D-STATCOM system are: the voltage at PCC; $v_c$, and the load current $i_L$, so the LQR gain of these states are used to mitigate the PI control performance of the two states according to the LQR applied to the concept of system error scheme of equation (3.11). The two states; $v_c$ and $i_L$, are compared with corresponding references values, and then processed by the similar PI controller of Section 4.2 with the proposed control strategy of controlling the *d* an *q* components of the both, and then followed by the corresponding LQR gain values.

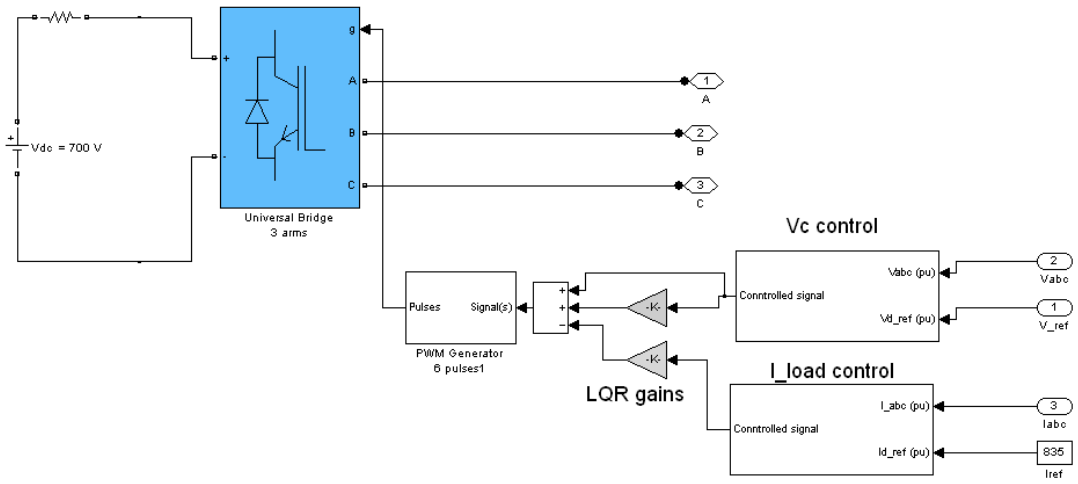


**Figure 4.17: Feedback PI/LQR control scheme for D-STATCOM system**

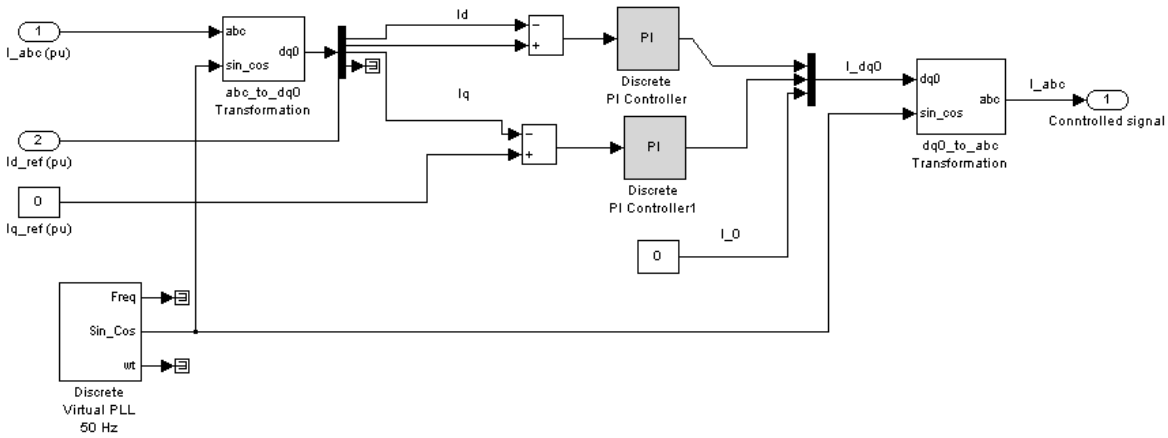


**Figure 4.18: PI control scheme for *dq* components of $i_L$**

As known, the voltage reference values is 1.0 pu for the three system conditions, while the current reference values are taken from the load data listed in Table 3.1 for the three system conditions as; 593 A, 905 A and 110 A respectively.

### 4.3.1 System 1; Rated Load

As shown in Figure 4.19, the voltage sag was compensated to 0.935 pu value (only 6.5% sag) which is approximately the same sag result with PI control scheme, but the THD was well mitigated to 0.57%. As expected, the swell compensation was achieved without oscillation that occurred with alone PI controller. *p.f* was mitigated to 0.97 value. Small overshoot can be observed for small time duration during sag start, sag end, swell start and swell end compensations with 13.0%, 10.0%, 9.0%, and 6.0%, respectively.

Single and double–phase to ground faults were tested and the results was similar to results of PI controller case; Figures 4.10 and 4.11.

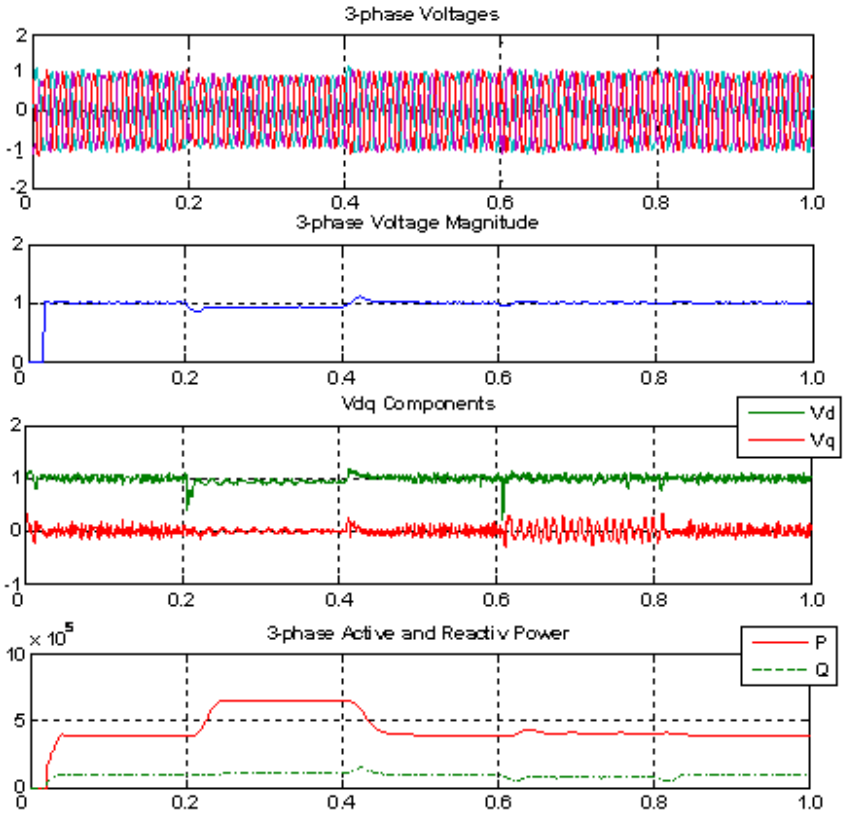


**Figure 4.19: Simulation results of D-STATCOM, PI/ LQR control for system 1**

**Table 4.5: Results of System Simulation with PI/ LQR control, System 1**

| Key Factors | value |
|---|---|
| Voltage during Sag (pu) | 0.935 |
| Voltage during Swell (pu) | 1.0 |
| THD (%) | 0.57 |
| *p.f* | 0.97 |

### 4.3.2 System 2; Max. Load

As shown in Figure 4.20, the voltage sag was compensated to 0.96 pu value (only 4.0% sag), THD was mitigated to 1.0%, and *p.f* was mitigated to 0.973 value. Small overshoot

can be observed for small time duration during start and end of sag compensation with 6.0% and 11.0%, respectively.

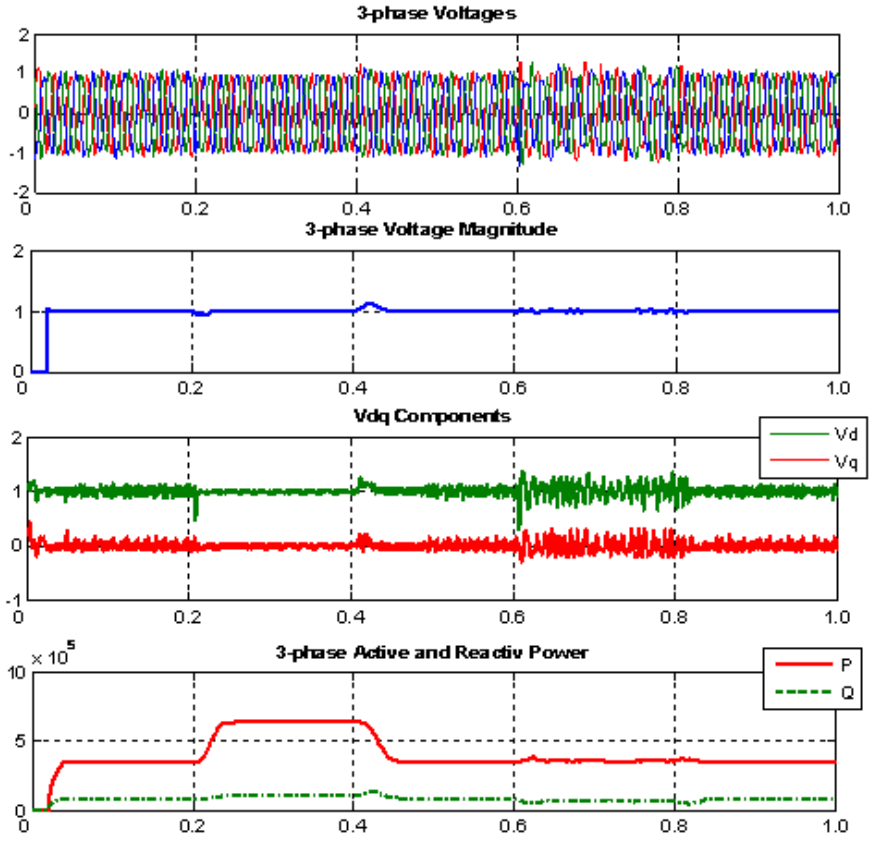


**Figure 4.20: Simulation results of D-STATCOM, PI/ LQR control for system 2**

**Table 4.6: Results of System Simulation with PI/ LQR control, System 2**

| Key Factors | value |
|---|---|
| Voltage during Sag (pu) | 0.96 |
| Voltage during Swell (pu) | 1.0 |
| THD (%) | 1.0 |
| *p.f* | 0.973 |

### 4.3.3 System 3; Min. Load

Similar to PI controller, PI/LQR controller will be tested with 100 KVAR capacitive load as a swell condition. As shown in Figure 4.21, the voltage sag and swell were compensated to 1.0 pu value, THD was mitigated to 2.92%., and *p.f* was well mitigated to 0.937 value. Small overshoots can be observed for small time duration during start and end of sag compensation with 8.0% and 10.0%, respectively.

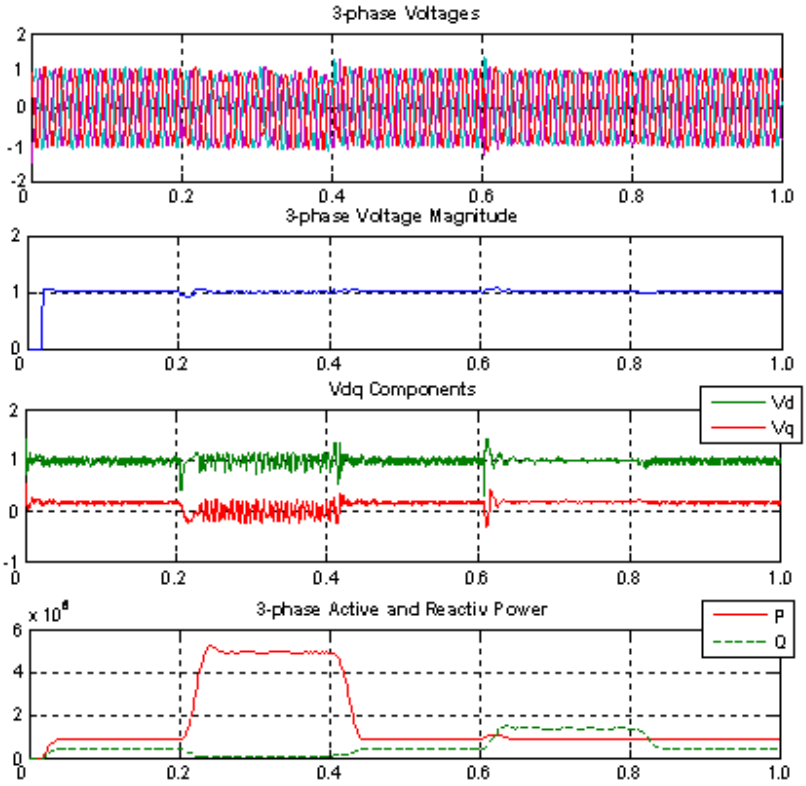


**Figure 4.21: Simulation results of D-STATCOM, PI/ LQR control for system 3 (100KVAR capacitive load)**

**Table 4.7: Results of System Simulation with PI/ LQR control, System 3**

| Key Factors | value |
|---|---|
| Voltage during Sag (pu) | 1.0 |
| Voltage during Swell (pu) | 1.0 |
| THD (%) | 2.92 |
| *p.f* | 0.937 |

## 4.4 Simulation of $H_2$ and $H_\infty$ Controllers

$H_2$ and $H_\infty$ controllers guarantee the system robustness by good selection of the weighting functions. This was tested and ensured by the step response in sections 3.5.2.3 and 3.5.2.4. Thus, it is expected that the simulation of D-STATCOM system with $H_2$ and $H_\infty$ controllers will result with better performance than the later ones. Using the same system parameters of the D-STATCOM system with PI and PI/LQR controllers; filter and DC storage device sizes, yield with improperly and slow response as shown in Figure 4.22.

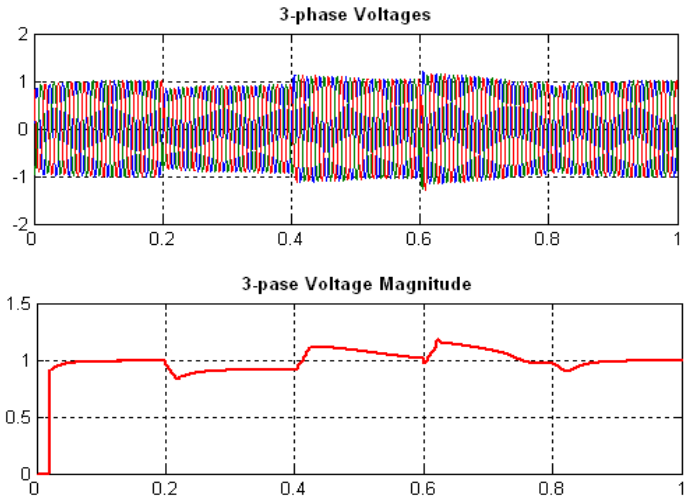


**Figure 4.22: Simulation results of D-STATCOM, $H_2$ and $H_\infty$ controllers (700V DC)**

It was observed that there is a possibility of increasing the DC storage device with better results and well mitigated THD. Thus, a 900V DC storage device is used. Harmonic filters added to the D-STATCOM system with $H_2$ and $H_\infty$ controllers was tuned to eliminate 5th, 7th, 48th and 52nd harmonic orders, which is the best harmonic tuning trials.

### 4.4.1 System 1; Rated Load

As shown in Figure 4.23, the voltage sag and swell was fully recovered to 1.0 pu value, *p.f* was mitigated to 0.991 value, and THD was mitigated to the values showed in Tables 4.8 and 4.9. The voltage signal shape is very smooth and well mitigated, and that reflects the effectiveness of $H_2$ and $H_\infty$ controllers. Small overshoots can be observed for small time duration during sag start, sag end, swell start and swell end compensations with 5.0% 5.0%, 7.0%, and 3.0%, respectively.

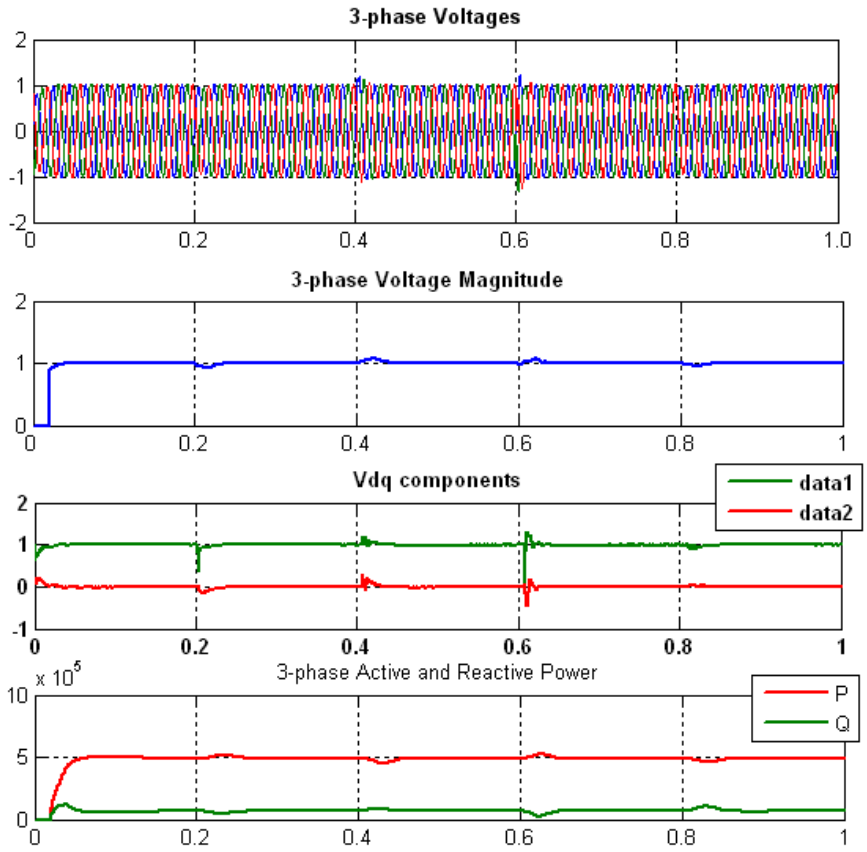


**Figure 4.23: Simulation results of D-STATCOM, $H_2$ and $H_\infty$ controllers for system 1 (900V DC)**

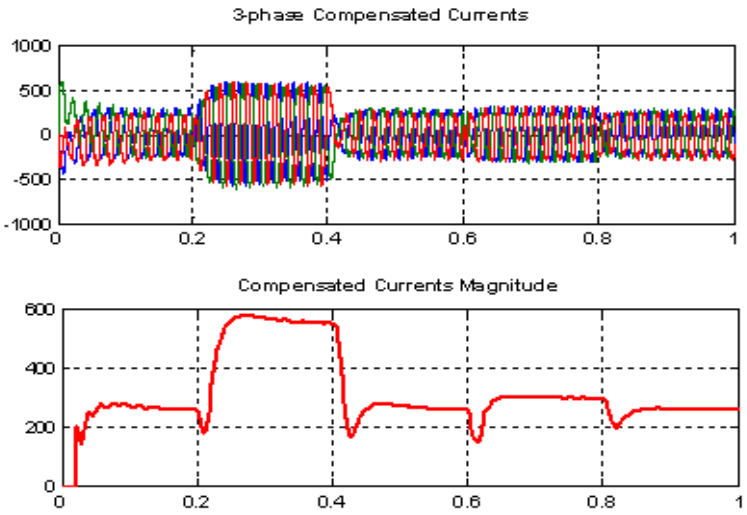


**Figure 4.24: Compensated currents with $H_2$ and $H_\infty$ controllers, system 1 (900V DC)**

**Table 4.8: Results of System Simulation with $H_2$ control, System 1**

| Key Factors | value |
|---|---|
| Voltage during Sag (pu) | 1.0 |
| Voltage during Swell (pu) | 1.0 |
| THD (%) | 0.55 |
| *p.f* | 0.991 |

**Table 4.9: Results of System Simulation with $H_\infty$ control, System 1**

| Key Factors | value |
|---|---|
| Voltage during Sag (pu) | 1.0 |
| Voltage during Swell (pu) | 1.0 |
| THD (%) | 0.54 |
| *p.f* | 0.992 |

Single and double–phase to ground faults are tested also and the results is presented in Figures 4.25 and 4.26 for single-phase and double–phase faults, respectively.

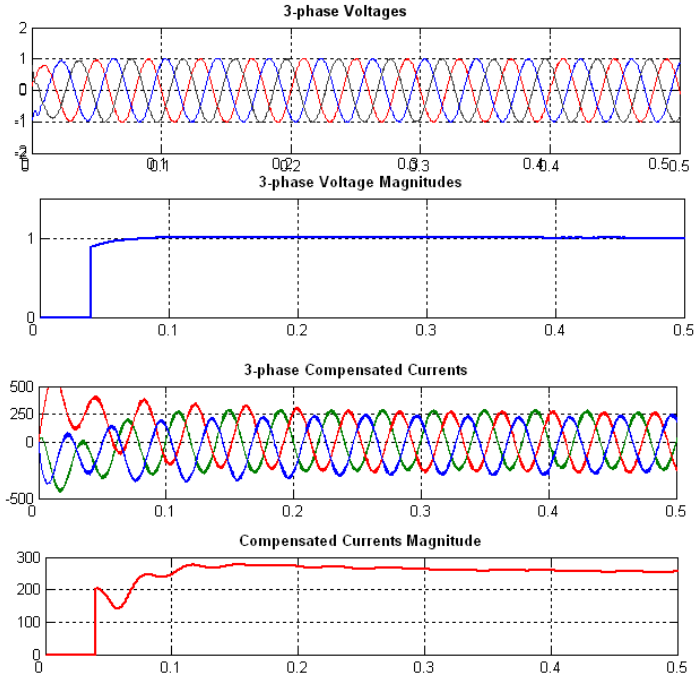


**Figure 4.25: D-STATCOM control with $H_2$ and $H_\infty$ controllers for single-phase to ground fault (phase a)**

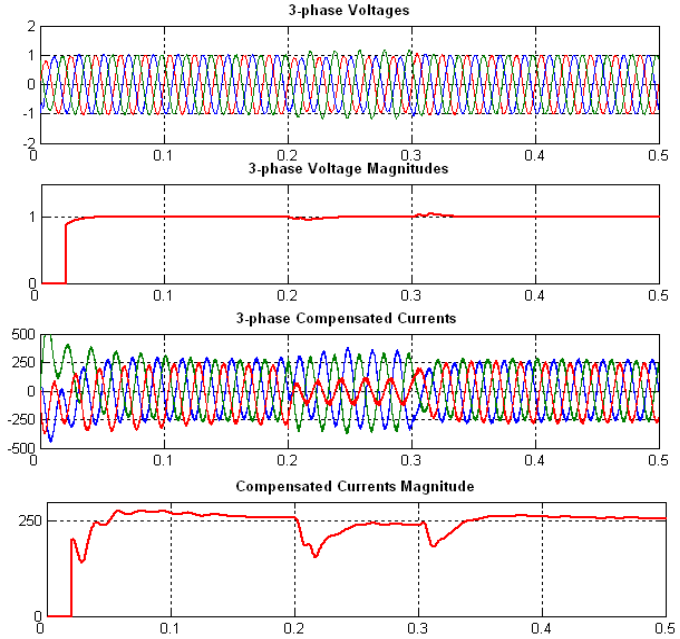


**Figure 4.26: D-STATCOM control with $H_2$ and $H_\infty$ controllers for double-phase to ground fault (phases a and b)**

### 4.4.2 System 2; Max. Load, and System 3; Min. Load

Similar good results can be showed for both system 2 and system 3 using $H_2$ and $H_\infty$ controllers, which can be summarized in Table 4.10.

Unlike PI and PI/LQR controllers, $H_2$ and $H_\infty$ controllers have a capability of compensating more size of swell condition. Applying 200KVA capacitive load yield the results shown in Figure 4.27.

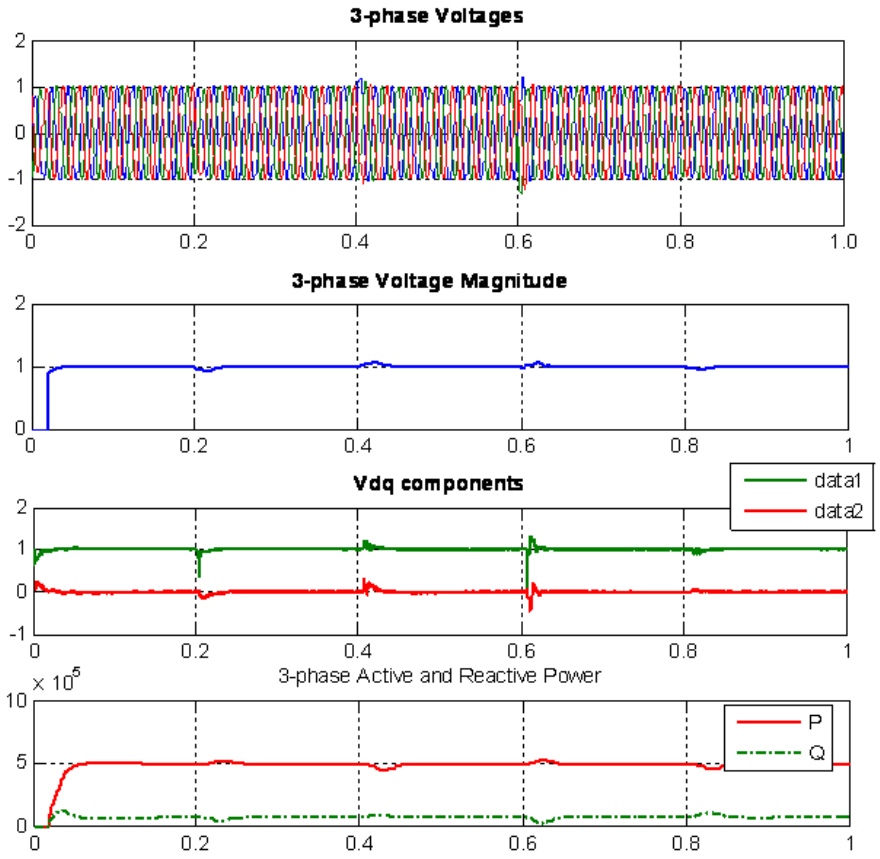


**Figure 4.27: Simulation results of D-STATCOM, $H_2$ and $H_\infty$ controllers for systems 2 and 3**

## 4.5 Results and Conclusion

The results of all simulations for the proposed control strategy for D-STATCOM system using optimal control methods; LQR, $H_2$ and $H_\infty$ controllers, for the three load conditions;

rated, maximum and minimum load, can be summarized in Table 4.10. The *Max. Overshoot* listed in the table is the maximum overshoot of the sag start, sag end, swell start and swell end cases occurred for the voltage signal, which can be considered as one of the performance factors of the controller.

**Table 4.10: Summery of Simulation Results**

| Performance | Controller | | | | | | | | | | | |
|---|---|---|---|---|---|---|---|---|---|---|---|---|
| | PI | | | PI /LQR | | | $H_2$ | | | $H_\infty$ | | |
| | Rated Load | Max. Load | Min. Load | Rated Load | Max. Load | Min. Load | Rated Load | Max. Load | Min. Load | Rated Load | Max. Load | Min. Load |
| **Voltage during Sag (pu)** | **0.93** | **0.966** | **1.0** | **0.935** | **0.96** | **1.0** | **1.0** | **1.0** | **1.0** | **1.0** | **1.0** | **1.0** |
| **Voltage during Swell (pu)** | **1.0** | **1.0** | **1.015** | **1.0** | **1.0** | **1.0** | **1.0** | **1.0** | **1.0** | **1.0** | **1.0** | **1.0** |
| **THD (%)** | **1.05** | **1.15** | **3.15** | **0.57** | **1.0** | **2.92** | **0.55** | **0.57** | **1.28** | **0.54** | **0.58** | **1.40** |
| ***p.f*** | **0.975** | **0.978** | **0.90** | **0.97** | **0.973** | **0.937** | **0.991** | **0.99** | **0.99** | **0.992** | **0.99** | **0.99** |
| **Max. Overshoot (%)** | **10.0** | **10.0** | **8.0** | **13.0** | **11.0** | **10.0** | **7.0** | **5.0** | **10.0** | **6.3** | **5.0** | **10.0** |

The summarized results of Table 4.10 can be represented by the statistical Figures 4.28 (a)-(e) for each performance factor.

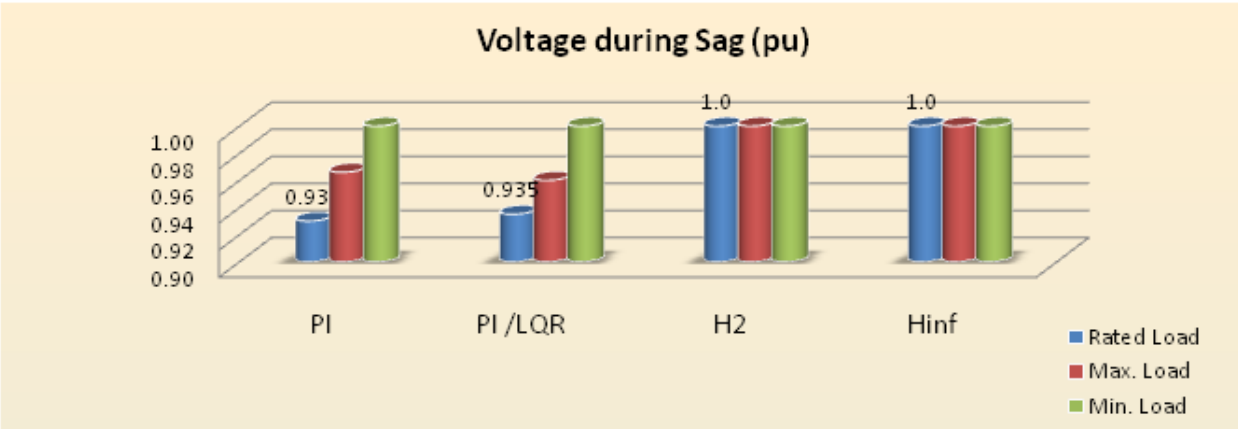


(a)

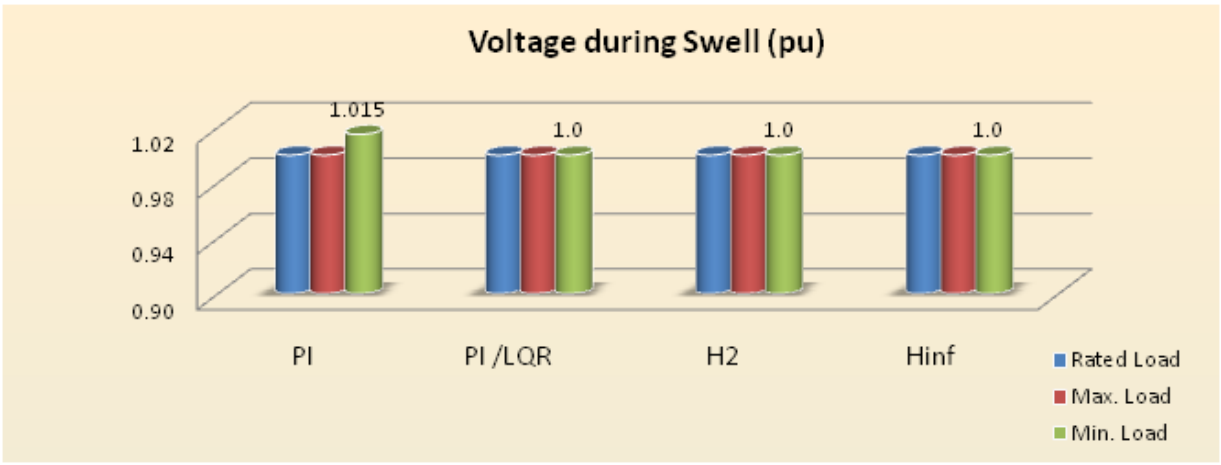
Voltage during Swell (pu)
1.02
0.98
0.94
0.90
1.015
1.0
1.0
1.0
PI
PI /LQR
H2
Hinf
Rated Load
Max. Load
Min. Load

(b)

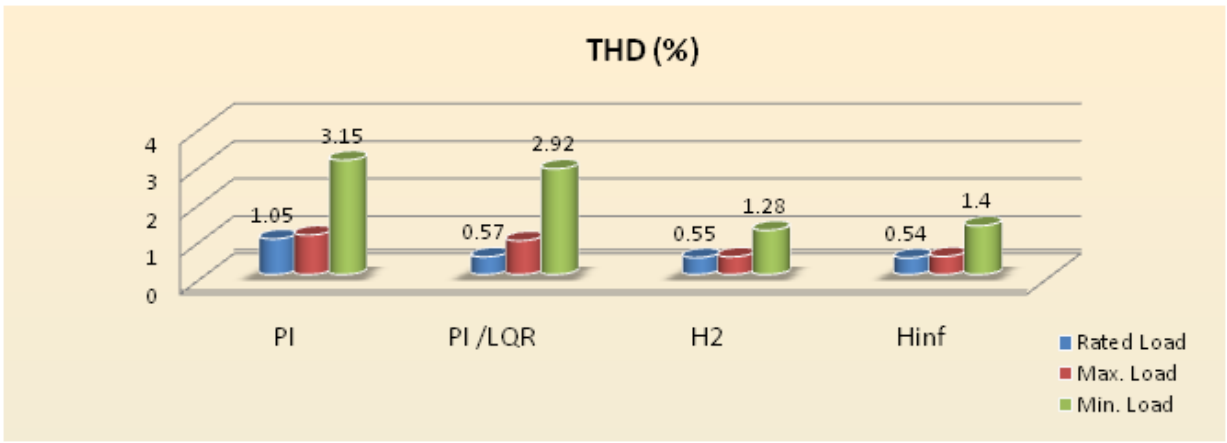
THD (%)
4
3
2
1
0
1.05
3.15
0.57
2.92
0.55
1.28
0.54
1.4
PI
PI /LQR
H2
Hinf
Rated Load
Max. Load
Min. Load

(c)

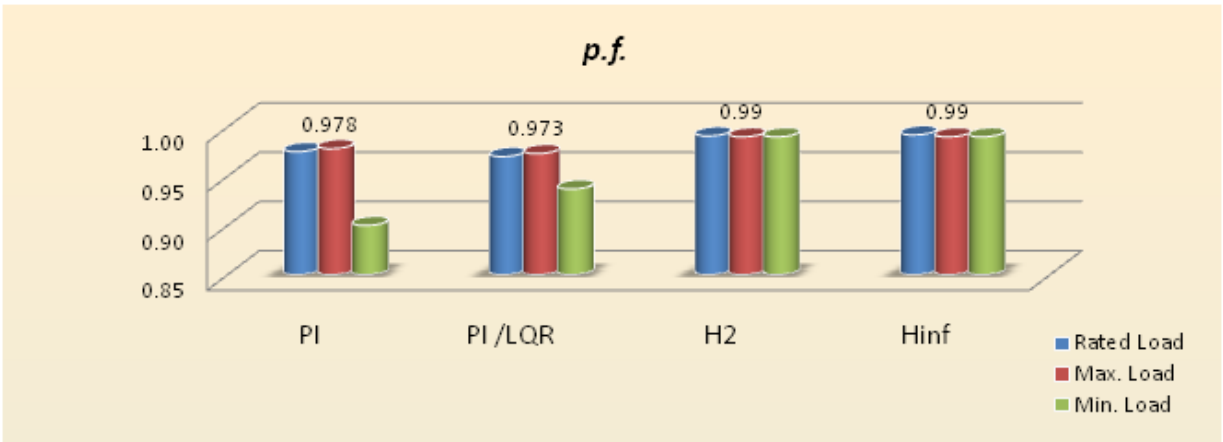
p.f.
1.00
0.95
0.90
0.85
0.978
0.973
0.99
0.99
PI
PI /LQR
H2
Hinf
Rated Load
Max. Load
Min. Load

(d)

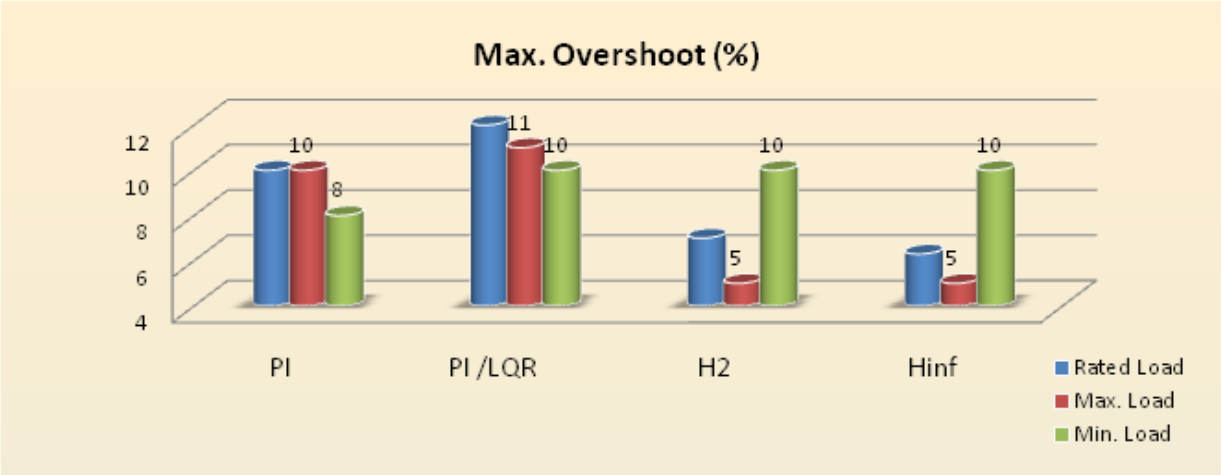


(e)

**Figure 4.28: Summery of simulation results**
**(a) Voltage during Sag**
**(b) Voltage during Swell**
**(c) THD**
**(d) *p.f***
**(e) Max. Overshoot**

In general, the proposed control strategy for D-STATCOM gave good performance for the four controllers; PI, PI/LQR, $H_2$ and $H_\infty$ for all system load conditions and various sag/ swell problems including three-phase, double-phase, single-phase faults and high capacitive load conditions. The load variations has no effect on the success of the four controllers involved in the proposed control strategy since all results are within the IEEE standards.

The PI controller had good performance with acceptable voltage level and THD values. This was the case also for PI/LQR controller, but with special contribution of mitigating the oscillation of voltage waveform during the swell compensation occurred with PI controller alone. Compared with $H_2$ and $H_\infty$ controllers, the disadvantages of PI and PI/LQR controllers are: the limited size of the used DC storage device which can't be exceeded more than 700V DC value, such that increasing DC voltage source will result with more and unmitigated THD. Thus the size of the DC storage device is constrained for some limitations and the trade off must be made between the recovered voltage level and the resultant THD. The other disadvantage is its limitation of compensating the swell situation

during minimum load condition, and the slightly reduction of the power factor during this case (0.90 value) but within the acceptable limit. These disadvantages are not the case of $H_2$ and $H_\infty$ controllers which have the capability of using more than 700V DC value in order to compensates more sag size, compensating more swell size situations and better power factor mitigation.

Harmonic filters with good tuning play an important role to mitigate THD to the optimum levels, but the D-STATCOM itself perform a good THD mitigation as shown in the simulation result of the D-STATCOM control without harmonic filters.

$H_2$ and $H_\infty$ controllers had perfect performance with fully recovered voltage level (1.0 pu, no oscillation), lowest THD values (0.55% and 0.54% for rated load), lowest overshoot cases (7.0% and 6.3% for rated load), max. $p.f$ (0.992) and smoothest voltage wave form. The main contribution of the $H_2$ and $H_\infty$ controllers are: the approximately fully elimination of THD, its ability to overcome system noise and disturbances, and its ability to use more DC storage device sizes in order to overcome more depth voltage sags.

As shown in Figures 4.23, and 4.27, the active and reactive power consumption in the case of $H_2$ and $H_\infty$ controllers has sustained values during various power problems and its compensations, which provide fixed system power factor compared with the other controllers.

# 5 CHAPTER 5: CONCLUSION AND FUTURE WORK

## 5.1 Conclusion

The objective of this thesis is to design an optimal based control strategy for D-STATCOM as a power quality solution, improve the performance of the D-STATCOM within this control strategy, and verify its work and improvement by simulation on one of Gaza low voltage (400V) networks for various load conditions as a case study. The analysis was composed of two parts; one is theoretical analysis using step response of the proposed control strategy, and the other is designing four controllers of the D-STATCOM; PI, PI/LQR, $H_2$ and $H_\infty$ controllers, and simulating its performance for compensating the main power quality problems; voltage sag, voltage swell and harmonic distortion.

Being a shunt device, the D-STATCOM is considered as a current source to contribute to the compensation of the voltage sag/ swell. The step response analysis and the design of LQR, $H_2$ and $H_\infty$ controllers require the state space model of the system with D-STATCOM connected, which has been derived.

The proposed control strategy depends on controlling the *d* and *q* transformed components of the 3-phase *abc* voltage signals using PI, PI/LQR, $H_2$ and $H_\infty$ controllers. Phase-Locked Loop (PLL) technique is used for synchronization purpose with fixed 50 Hz, $0^\circ$ phase shift information to avoid the additional control loops and to ensure ideal synchronization between the injected compensation signal and the main signal. Constant DC link voltage is the case in the proposed control strategy such that both active and reactive power can be injected to the power system by D-STATCOM with faster response comparing with other DC storage schemes. This thesis mainly focused on the optimal control for the D-STATCOM, which were not yet fully discovered in the past, and that have made this research area very attractive. Optimal control knowledge is a very suitable base for D-STATCOM control and power quality solutions due to its role to provide the best possible performance with respect to given measure of performance (cost function) and to give the best possible system for voltage sag/ swell compensation and THD elimination, in addition to disturbance and noise rejection.

Comparing with the other control strategies of D-STATCOM in the literature, the proposed control strategy is lower cost, more simple, and more fixable due to the facts of:

- It has only one control loop to control only the voltage at the load point (PCC),
- Only voltage measurement is required to achieve the control process,
- The using of *dq* transformation, to control only *d* and *q* components, and
- Ideal synchronization using virtual PLL scheme.

As shown in the simulation results, the constant DC link voltage source provide a useful active and reactive power exchange between the D-STATCOM and the power system according to the compensation needs. This is very useful specially for voltage sag compensation and power factor mitigation. It was observed also, that the D-STATCOM capacity for power compensation and voltage regulation depends mainly on two factors: the rating of the DC storage device and the characteristics of the filter between the device and the main system. The simulation results showed that the controller response time is very fast (less than 50 ms as the worst case).

Applying $H_2$ and $H_\infty$ as an optimal and modern controllers for D-STATCOM provided perfect results; fully recovered voltage level (1.0 pu, no oscillation), lowest THD values (0.54%), max. *p.f* (0.992), lowest overshoot, fastest response (0.02 sec) and smoothest voltage wave form. Hence, the main thesis problem was covered and the improvement of D-STATCOM performance with optimal control was investigated. This is the main contribution of the thesis with the weakness of researches on optimal control of D-STATCOM. These are an expected results due to the nature of $H_2$ and $H_\infty$ controllers by considering the system disturbances and noise, and guarantee the system robustness as showed in the simulation results. It is clear that good selection of the weighting functions for $H_2$ and $H_\infty$ controllers with the suitable size of DC storage device is the key factor for $H_2$ and $H_\infty$ optimality.

By varying the system parameters, the proposed control strategy is proved to be able to compensate the power quality problems at 400V networks of Gaza utility for various load

conditions. Therefore, it can be concluded that the D-STATCOM with the optimal based control strategy is a practical and realistic solution for power quality problems of Gaza power utility, and it can replace the *manual tap changer* used in the transformers to overcome the voltage variations during faults and load variations.

In addition to its role to compensate the sag, swell voltages and THD, D-STATCOM has very good behavior in order to improve the power factor ($p.f$) for excellent levels.

Finally, it can be concluded also that $H_2$ and $H_\infty$ controllers have the *Optimum Performance* for sag/swell compensation tasks, and THD and power factor mitigation.

## 5.2 Future Work

Although this thesis has covered the optimal control of D-STATCOM, additional work is required for future research.

It is interesting to extend the researches for the uncertainty of the system parameters in order to improve the controllers design to consider uncertain control design. This can be illustrated by the various load conditions of the electrical utility and the variations of power quality problems.

As mentioned in the conclusion, the rating of the DC storage device is an important factor for D-STATCOM capacity for power compensation and voltage regulation. The required energy can be stored in Dry batteries, Transportable Battery Energy Storage System (TBESS), Ultra-Capacitor energy storage, etc. Thus, it may be one of the topics to be covered by researchers to determine optimum and most economic DC storage device for D-STATCOM control.

In the case of Gaza strip power utility, the present research cover the low voltage networks. It is interesting also to model the medium and high voltage networks of Gaza strip and apply the STATCOM control to overcome power quality problems allocated within the utility.

# REFERENCES


[1] EPRI PEAC Corporation, 2000. Power Quality Solutions for Industrial Customers. *California Energy Commission*.

[2] Roger C. Dugan, Mark F. McGranaghan and H. Wayne Beaty, 1996. *Electrical Power Systems Quality*. 2nd edition, Mc Graw-Hill.

[3] M. Mohammadi and M. Nasab, 2011. Voltage Sag Mitigation with D-STATCOM In Distribution Systems, *Australian Journal of Basic and Applied Sciences*, vol. 5, no. 5, pp.201-207.

[4] Wei-Neng Chang & Kuan-Dih Yeh, 2009. Design And Implementation of DSTATCOM for Fast Load Compensation of Unbalanced Loads. *Journal of Marine Science and Technology*, vol. 17, no. 4, pp.257-263,

[5] IEEE Standards Board, 1995. *IEEE Recommended Practice for Monitoring Electric Power Quality* (IEEE Std. 1159-1995). IEEE Inc., New York.

[6] Frantisek Kinces, 2004. *Voltage Sag Indices and Statistics*. M.Sc. Chalmers University of Technology.

[7] T. Devaraju, V.C. Reddy and M. Kumar, 2010. Modeling and Simulation of Custom Power Devices to Mitigate Power Quality Problems. *International Journal of Engineering Science and Technology*, vol. 2, no. 6.

[8] H. Masdi, N. Mariun, S.M. Bashi, A. Mohamed and S. Yusuf, 2009. Construction of a Prototype D-Statcom for Voltage Sag Mitigation. *European Journal of Scientific Research*, vol. 30, no.1, pp.112-127.

[9] Richard P.Bingham, 1998. Sags and Swells. *Dranetz-BMI.*

[10] Johan Lundiqust, 2001. *On Harmonic Distortion in Power Systems*. Thesis for the Degree of Licentate of Engineering, Chalmers University of Technology.

[11] IEEE Standards Board, 1993. *IEEE Recommended Practices and Requirements for Harmonic Control in Electric Power Systems* (IEEE Std. 519-1992), IEEE Inc., New York.

[12] S. Gupta, H.P. Tiwari and R. Pachar, 2010. Study of Major Issues and Their Impact on DVR System Performance. *International Journal of Computer and Electrical Engineering*, vol. 2, no. 1, pp. 105-110,

[13] M.V. Perera, 2007. *Control of A Dynamic Voltage Restorer To Compensate Single Phase Voltage Sags*. M.Sc. KTH University.

[14] Alper Çentin, 2007. *Design And Implementation of A Voltage Source Converter Based STATCOM For Reactive Power Compensation And Harmonic Filtering*. Ph. D. Middle East Technical University.

[15] Suchismita A. Chatterjee and K. D. Joshi, 2010. A Comparison of Conventional, Direct-Output-Voltage and Fuzzy-PI Control Strategies for D-STATCOM. *Modern Electric Power Systems 2010,* paper P20.

[16] Liqun Xing, 2003. *A Comparison of Pole Assignment & LQR Design Methods for Multivariable Control for STATCOM*. M.Sc. The Florida State University.

[17] Cai Rong, , 2004. *Analysis of STATCOM for Voltage Dip Mitigation*. M.Sc. Chalmers University of technology.

[18] B. Singh and R. Saha, 2007. Modeling of 18-Pulse STATCOM for Power System Applications. *Journal of Power Electronics*, vol. 7, no. 2, pp.146-158.

[19] X.Y. Zhou, H.F Wang, R.K Aggarwal and P.Beaumont, 2005. The Impact of STATCOM On Distance Relay. *15th Systems Computation Conference*, Liege, 22-26 August 2005.

[20] N. Mariun, S. Aizam, H. Hizam, and N. Abd-Wahab, 2005. Design of the Pole Placement Controller for D-STATCOM in Mitigating Three Phase Fault. *5th WSEAS Conference on Power Systems and Electromagnetic Compatibility*. Greece, 23-25 August 2005.

[21] Amir H. Norouzi and A. M. Sharaf, 2005. Two Control Schemes to Enhance the Dynamic Performance of the STATCOM and SSSC. *IEEE Transactions on Power Delivery*, vol. 20, no. 1, pp.435-442.

[22] S.V Kumar and S. Nagaraju, 2007. Simulation of D-STATCOM And DVR In Power Systems. *ARPN Journal of Engineering and Applied Sciences*, vol. 2, no. 3, pp.7-13.

[23] K. Srinivas, B. Singh, A. Chandra and Kamal Al-Haddad, 2008. New Control Strategy of Two-level 12-pulse VSCs Based STATCOM Using Hybrid Fuzzy-PI Controller. *Indian Institute of Technology*.

[24] A. Ajami and N. Taheri, 2011. A Hybrid Fuzzy/LQR Based Oscillation Damping Controller Using 3-level STATCOM. *International Journal of Computer and Electrical Engineering*, vol. 3, no. 2, pp.184-189.

[25] Gaza Electricity Distribution Company (GEDCo), *Interview;* Eng. Mohammad El-Shanti. 13 December 2010*,* Maintenance department of GEDCo.

[26] Siriroj Sirisukprasert, 2004. *The Modeling and Control of A Cascaded-Multilevel Converter-Based STATCOM*, Ph. D. Faculty of Virginia Polytechnic Institute and State University.

[27] Ashfaq Ahmed, 1999. *Power Electronics For Technology*. Prentice Hall Inc.

[28] Hazim Bilgin, 2007. *Design And Implementation of A Current Source Converter Based STATCOM For Reactive Power Compensation And Harmonic Filtering*. Ph. D. Middle East Technical University.

[29] A. Shukla, A. Ghosh, and A. Joshi, 2007. State Feedback Control of Multilevel Inverters for DSTATCOM Applications. *IEEE Transactions on Power Delivery*, vol. 22, no. 4, pp.2409-2419.

[30] A. F . Huweg, S. M. Bashi, and N. Mariun, 2005. Application Of Inverter Based Shunt Device For Voltage Sag Mitigation Due To Start Of Induction Motor Load. *18th International Conference on Electricity Distribution*. Turin, Malaysia, 06-09 June 2005.

[31] S. Goyal, A. Ghosh, and G. Ledwich, 2008. A Hybrid Discontinuous Voltage Controller for DSTATCOM Applications. *Proceedings IEEE Power Engineering Society General Meeting 2008*.

[32] G. Ledwich and A. Ghosh, 2002. A flexible DSTATCOM Operating In Voltage or Current Control Mode. *IEEE Proc.-Gener. Trunsm. Disrrih.*, vol. 149, no. 2, pp.215-224.

[33] K.Chandrasekaran, P.A. Vengkatachalam, Mohd Karsiti and K.S.Rama Rao, 2009. Mitigation of Power Quality Disturbances. *Journal of Theoretical and Applied Information Technology*, pp.105-116.

[34] Gray, P. R. and Meyer. R. G., 1992. *Analysis and Design of Integrated Circuits*, 3rd edition, Wiley Inc.

[35] B. A. Anderson and John B. Moore, 1989. *Optimal Control – Linear Quadratic Methods*, Prentice-Hall Inc.

[36] Jeffrey B. Burl, 1999. *Linear Optimal Control:* $H_2$ and $H_\infty$ *methods*, Addison Wesley Longman, Inc.

[37] J. Gadewadikar, 2007. *H-infinity Output-Feedback Control: Application To Unmanned Aerial Vehicle.* Ph. D. University of Texas At Arlington.

[38] Hannu T. Toivonen, 1997. The H2-optimal control problem, *lecture notes*. Åbo Akademi University, Finland. Available at: <www.abo.fi/~htoivone/courses/robust> [Accessed 01 October 2011].

[39] Hannu T. Toivonen, 1997. The Hinf-optimal control problem, *lecture notes*. Åbo Akademi University, Finland. Available at: <www.abo.fi/~htoivone/courses/robust> [Accessed 03 October 2011].

[40] Gaza Electricity Distribution Company (GEDCo), *measured data;* Eng. Harb Agha. 04-05 April 2011, Maintenance department of GEDCo.

[41] Hatem El-Aydi, 2008. Design of $H_2$ and $H_\infty$ project, *EELE 6302 Optimal and Quadratic Control course.* Islamic University of Gaza.

# ANNEX A: Low voltage network of "Southern of Al-Zaitoon Neighborhood" - Gaza

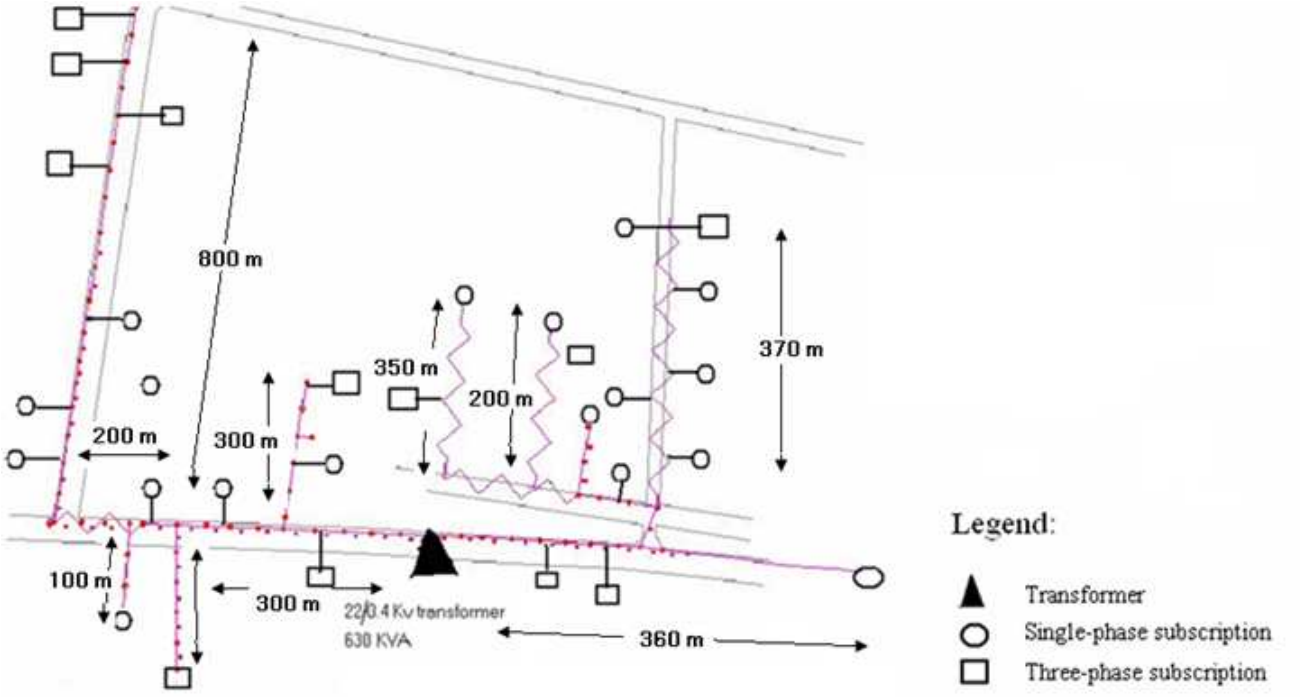


**Figure A.1: Plan of Southern of Al-Zaitoon Neighborhood low voltage network-Gaza [25]**

**Internal parameters of 630 KVA transformer [25]:**

$$R_s = \frac{V_{base}^2}{\text{Rated } KVA} \tag{A.1}$$

$$L_s = \frac{V_{base}^2}{\text{Rated } KVA} \cdot \frac{1}{2\pi f} \tag{A.2}$$

$V_{base}$ = 400 V, and the rated $KVA$ = 630 KVA , hence,

$R_s = 0.254\ \Omega$

$L_s = 0.808$ mH

**Rated load of the Network** = 410 KVA, 593 A

**Max. capacity of the transformer** = 625 KVA, 905 A

**Resistance *R* and inductive reactance *L* values for distributed lines per kilometer:**

For each line,

$$R = \text{Dc resistance } (\Omega/\text{km}) \times \text{ Length (m)} / 1000 \quad \text{(A.3)}$$

$$X = \text{inductive reactance at 50Hz } (\Omega/\text{km}) \times \text{ Length (m)} / 1000 \quad \text{(A.4)}$$

DC resistance and inductive reactance can be found from the following data sheet of the LV XPLE type Cables:

# LV XLPE Insulated Aerial Bundled Cables 2/3/4 Core Aluminium

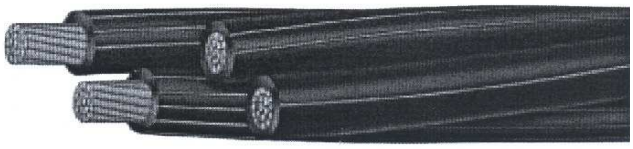

0.6/1kV XLPE (X-90) insulated, aerial bundled cables (service and mains cables) to AS/NZS 3560.
Hard drawn aluminium conductors.

## Physical Data

| Nominal conductor area mm² | Nominal conductor diameter mm | Average insulation thickness mm | Nominal diameter over insulation mm | Nominal diameter over laid-up cores mm | Approximate mass kg/km | Product code |
|---|---|---|---|---|---|---|
| **2 Core** | | | | | | |
| 16 | 4.7 | 1.3 | 7.4 | 14.8 | 130 | XDAB15AA002 |
| 25 | 5.9 | 1.3 | 8.6 | 17.2 | 190 | XDAB17AA002 |
| 35 | 6.9 | 1.3 | 9.6 | 19.3 | 250 | XDAB18AA002 |
| 50 | 8.1 | 1.5 | 11.2 | 22.3 | 340 | XDAB19AA002 |
| 95 | 11.4 | 1.7 | 14.9 | 29.8 | 640 | XDAB22AA002 |
| **3 Core** | | | | | | |
| 25 | 5.9 | 1.3 | 8.6 | 18.5 | 290 | XDAB17AA003 |
| 35 | 6.9 | 1.3 | 9.6 | 20.8 | 370 | XDAB18AA003 |
| 50 | 8.1 | 1.5 | 11.2 | 24.1 | 510 | XDAB19AA003 |
| **4 Core** | | | | | | |
| 16 | 4.7 | 1.3 | 7.4 | 17.8 | 270 | XDAB15AA004 |
| 25 | 5.9 | 1.3 | 8.6 | 20.8 | 390 | XDAB17AA004 |
| 35 | 6.9 | 1.3 | 9.6 | 23.2 | 500 | XDAB18AA004 |
| 50 | 8.1 | 1.5 | 11.2 | 27.0 | 670 | XDAB19AA004 |
| 70 | 9.7 | 1.5 | 12.8 | 30.8 | 930 | XDAB20AA004 |
| 95 | 11.4 | 1.7 | 14.9 | 36.0 | 1280 | XDAB22AA004 |
| 120 | 12.8 | 1.7 | 16.3 | 39.3 | 1570 | XDAB23AA004 |
| 150 | 14.2 | 1.7 | 17.7 | 42.8 | 1890 | XDAB24AA004 |

## Performance Data

| Nominal conductor area | DC resist. at 20°C | AC resist. at 50Hz 80°C | Inductive reactance at 50Hz | Voltage drop at 50Hz 80°C | Continuous current rating, A | | | Fault current rating kA for | Minimum bending radius (installed) mm | | Min. breaking load of cable | Rec. tension Highest everyday tension | Max working tension | Modulus of elasticity | Coeff. of linear expansion |
|---|---|---|---|---|---|---|---|---|---|---|---|---|---|---|---|
| | | | | | Still air | 1m/s wind | 2m/s wind | 1s | Core | Cable | | | | | |
| mm² | Ω/km | Ω/km | Ω/km | mV/A.m | | | | | | | kN | kN | kN | GPa | x10⁻⁶/°C |
| **2 Core** | | | | | | | | | | | | | | | |
| 16 | 1.91 | 2.37 | 0.094 | 4.75 | 49 | 78 | 91 | 1.4 | 30 | 90 | 4.4 | 0.79 | 1.23 | 59 | 23.0 |
| 25 | 1.20 | 1.49 | 0.089 | 2.99 | 64 | 105 | 120 | 2.2 | 35 | 100 | 7.0 | 1.26 | 1.96 | 59 | 23.0 |
| 35 | 0.868 | 1.08 | 0.086 | 2.16 | 78 | 125 | 145 | 3.1 | 60 | 120 | 9.8 | 1.76 | 2.74 | 59 | 23.0 |
| 50 | 0.641 | 0.796 | 0.086 | 1.60 | 94 | 150 | 180 | 4.1 | 65 | 130 | 14.0 | 2.52 | 3.92 | 59 | 23.0 |
| 95 | 0.320 | 0.398 | 0.080 | 0.812 | 140 | 230 | 275 | 8.3 | 90 | 270 | 26.6 | 4.79 | 7.45 | 56 | 23.0 |
| **3 Core** | | | | | | | | | | | | | | | |
| 25 | 1.20 | 1.49 | 0.089 | 2.99 | 59 | 97 | 115 | 2.2 | 35 | 110 | 10.5 | 1.89 | 2.94 | 59 | 23.0 |
| 35 | 0.868 | 1.08 | 0.086 | 2.16 | 72 | 120 | 135 | 3.1 | 60 | 120 | 14.7 | 2.65 | 4.12 | 59 | 23.0 |
| 50 | 0.641 | 0.796 | 0.086 | 1.60 | 88 | 140 | 165 | 4.1 | 65 | 140 | 21.0 | 3.78 | 5.88 | 59 | 23.0 |
| **4 Core** | | | | | | | | | | | | | | | |
| 16 | 1.91 | 2.37 | 0.10 | 4.11 | 44 | 74 | 86 | 1.4 | 30 | 110 | 8.8 | 1.58 | 2.46 | 59 | 23.0 |
| 25 | 1.20 | 1.49 | 0.097 | 2.59 | 59 | 97 | 115 | 2.2 | 35 | 120 | 14.0 | 2.52 | 3.92 | 59 | 23.0 |
| 35 | 0.868 | 1.08 | 0.094 | 1.87 | 72 | 120 | 135 | 3.1 | 60 | 140 | 19.6 | 3.53 | 5.49 | 59 | 23.0 |
| 50 | 0.641 | 0.796 | 0.093 | 1.39 | 88 | 140 | 165 | 4.1 | 65 | 160 | 28.0 | 5.04 | 7.84 | 59 | 23.0 |
| 70 | 0.443 | 0.551 | 0.088 | 0.966 | 110 | 175 | 205 | 6.0 | 75 | 280 | 39.2 | 7.06 | 11.0 | 56 | 23.0 |
| 95 | 0.320 | 0.398 | 0.087 | 0.706 | 135 | 215 | 255 | 8.3 | 90 | 320 | 53.2 | 9.58 | 14.9 | 56 | 23.0 |
| 120 | 0.253 | 0.315 | 0.085 | 0.566 | 155 | 250 | 300 | 10.5 | 100 | 350 | 67.2 | 12.1 | 18.8 | 56 | 23.0 |
| 150 | 0.206 | 0.257 | 0.084 | 0.468 | 180 | 280 | 345 | 12.9 | 110 | 390 | 84.0 | 15.1 | 23.5 | 56 | 23.0 |

**Note** Voltage drops are single-phase for 2 & 3 core cables and three-phase for 4 core cables. Continuous current ratings are based on an ambient temperature of 40°C, maximum conductor temperature of 80°C and solar radiation intensity of 1000W/m². Ratings for 2 & 3 core cables are based on all cores fully loaded. Ratings for 4 core cables are based on a lightly loaded neutral. Fault current ratings are based on initial and final conductor temperatures of 80°C and 210°C respectively.

An improved performance grade of XLPE (X-FP-90) designed to provide improved circuit integrity when subjected to the heat radiation effects of a bush fire or overload conditions is available as an option.



AERIAL

# ANNEX B: MATLAB Code

## B.1 System State-Space Model

```
Rs = 0.0254;              % source resistance
Ls = 0.808e-3;            % source reactance
Rl = 0.357;               % load resistance: varied according to
                           load condition
Ll = 0.484e-3;            % load reactance: varied according to
                           load condition
Rc = 0.010;               % filter resistance
Lc = 2.5e-3;              % filter reactance
C  = 60e-6;               % filter capacitance


a = [-1*Rs/Ls     0        0      -1/Ls;
          0    -1*Rc/Lc    0      -1/Lc;
          0        0    -1*Rl/Ll    1/Ll;
          1/C     1/C     -1/C        0   ];

b = [1/Ls; 0; 0 ;0];

c = [ 0   0   0   1];

d= [0];
```

## B.2 Design of LQR Controller

```
 Q=[0    0    0    0;
   0    0    0    0;
   0    0  2000   0;
   0    0    0  100];


R=[100];

[K1,S,e] = LQR(a,b,Q,R)       % K - Gain Matrix (Kalman gain), e -
                              closed-loop  eigenvalues
```

## B.3 Design of $H_2$ Controller

```
format short

% performance  function W1
num1=[0.03 0.05 0];
den1=[0.05 15  10];
% inout weighting function W2
num2=[5 10];
den2=[10 10];
% robust weighting function W3
num3=[1];
den3=[1];

sys = ss(a,b,c,d);

% Construct the wieghting functions
[aw1,bw1,cw1,dw1] = tf2ss(den1,num1); sysw1 = ss(aw1,bw1,cw1,dw1);
[aw2,bw2,cw2,dw2] = tf2ss(num2,den2); sysw2 = ss(aw2,bw2,cw2,dw2);
[aw3,bw3,cw3,dw3] = tf2ss(den3,num3); sysw3 = ss(aw3,bw3,cw3,dw3);

sys_=augss(sys,sysw1,sysw2,sysw3,0);    % augss  --- state space
                                        plant augmentation with
                                        weighting function

[A,B1,B2,C1,C2,D11,D12,D21,D22]=branch(sys_);

[ss_cp,ss_cl]=h2lqg(sys_);      % --  H_2 optimal controller design

[ae,be,ce,de]=ssdata(ss_cp);

p=[A B1 B2;C1 D11 D12;C2 D21 D22];
```

## B.4 Design of $H_\infty$ Controller

```
format short

% performance weighting function W1
num1=[0.03 0.05 ];
den1=[0.05 15 ];
% inout weighting function W2
num2=[5 10];
den2=[10 10];
% robust weighting function W3
num3=[1.0];
den3=[1.0];

sys = ss(a,b,c,d);

% Construct the wieghting functions
[aw1,bw1,cw1,dw1] = tf2ss(den1,num1); sysw1 = ss(aw1,bw1,cw1,dw1);
[aw2,bw2,cw2,dw2] = tf2ss(num2,den2); sysw2 = ss(aw2,bw2,cw2,dw2);
[aw3,bw3,cw3,dw3] = tf2ss(den3,num3); sysw3 = ss(aw3,bw3,cw3,dw3);

s=zpk('s');

sys_=augtf(sys,sysw1,sysw2,sysw3)    % augss     --- state space
                                     plant augmentation with
                                     weighting function

[A,B1,B2,C1,C2,D11,D12,D21,D22]=branch(sys_);

[K,CL,GAM]=hinfsyn(sys_);      % -- H_inf optimal controller design

[ae,be,ce,de]=ssdata(K)

p=[A B1 B2;C1 D11 D12;C2 D21 D22];
```